



# An oblique subduction model for closure of the Proto-Tethys and Palaeo-Tethys oceans and creation of the Central China Orogenic Belt

Mark B. Allen<sup>a,\*</sup>, Shuguang Song<sup>b</sup>, Chao Wang<sup>c</sup>, Renyu Zeng<sup>d</sup>, Tao Wen<sup>b</sup>

<sup>a</sup> Department of Earth Sciences, Durham University, Durham DH1 3LE, UK

<sup>b</sup> MOE Key Laboratory of Orogenic Belts and Crustal Evolution, School of Earth and Space Sciences, Peking University, Beijing 100871, China

<sup>c</sup> Department of Earth Sciences, The University of Hong Kong, Pokfulam Road, Hong Kong, China

<sup>d</sup> State Key Laboratory of Nuclear Resources and Environment, East China University of Technology, Nanchang, 330013, Jiangxi, China

## ARTICLE INFO

### Keywords:

Central China Orogenic Belt  
Kunlun  
Qaidam  
Qilian  
Qinling  
Proto-Tethys  
Palaeo-Tethys  
Orogeny  
Subduction  
collision

## ABSTRACT

Subduction and closure of the Proto-Tethys and Palaeo-Tethys oceans were important events in the assembly of Eurasia, and created the Central China Orogenic Belt (CCOB). This paper presents a new tectonic model for the CCOB in which we propose that elongate Precambrian basement blocks within the CCOB were originally part of a single ribbon continent, here named K-Qubed after the Kunlun-Qaidam-Qilian-Qinling regions. K-Qubed separated from the South China Block in the Neoproterozoic. Dextral-oblique subduction of the Proto-Tethys Ocean took place southwards (present co-ordinates) under K-Qubed in latest Precambrian - Cambrian times (ca. 550–500 Ma). Subduction-accretion complexes were generated alongside the basement, while arc magmatism overprinted both basement and accretionary crust. Initial collision of the northern side of the ribbon continent and the North China and Tarim blocks occurred at ca. 500 Ma. High-pressure and ultrahigh-pressure metamorphism resulted by ca. 490 Ma, in the North Qilian, South Altun/North Qaidam and North Qinling regions. Collision triggered a flip in subduction polarity, and caused a subduction-accretion complex and magmatic arc to build out southwards from K-Qubed, as Palaeo-Tethys was consumed northwards in the Ordovician. Magmatic timings were similar between different tectonic units; twin peaks in magmatism at ca. 500–490 Ma and ca. 440–430 Ma occurred in several terranes. Oblique subduction caused strain partitioning, in turn causing slivering and across-strike repetition of basement and accretionary crust. Tectonic units in the Qilian Shan and Kunlun can be partly correlated with equivalents in the Qinling Orogen. We suggest a match between the North Qilian Orogenic Belt and the Erlangping Unit, between the Central Qilian Block and the North Qinling Belt, between the South Qilian Accretionary Belt and the Shangdan Suture Zone. Basement terranes of the Qaidam region and the East Kunlun Orogen have no obvious lateral equivalents in the Qinling, and are truncated at the eastern margins by the West Qinling Belt. There are similar ages for peak metamorphism at ca. 440–420 Ma in an eclogite belt in the North Qaidam Ultra High-pressure Metamorphic Belt (NQUB) and eclogite localities in the East Kunlun Orogen. We interpret this metamorphism to be result of slab break-off beneath the K-Qubed continent, with metamorphic rocks repeated across-strike by dextral shear. The component of Precambrian crust in the Kunlun diminishes westwards into the West Kunlun, where Early Palaeozoic accretion of crust was more continuous. A magmatic gap throughout the CCOB between ca. 370 and ca. 290 Ma was possibly related to extremely oblique and/or slow plate convergence, or represents a time through which subduction stopped. Renewed northwards subduction of the Palaeo-Tethyan Ocean took place under the south side of the Kunlun and Qinling in the Permian, completed by Triassic collisions of the Qiangtang and South China blocks with the southern side of the CCOB. This model for the CCOB is an alternative to collisional and accretionary end members for orogeny, whereby oblique subduction and collision of a ribbon continent produces interleaving of basement and more juvenile terranes. Closure of Proto-Tethys did not involve multiple, separate and synchronous subduction zones, or repetition of a subduction zone by oroclinal bending, as previously proposed.

\* Corresponding author.

E-mail address: [m.b.allen@durham.ac.uk](mailto:m.b.allen@durham.ac.uk) (M.B. Allen).

<https://doi.org/10.1016/j.earscirev.2023.104385>

Received 27 September 2022; Received in revised form 13 February 2023; Accepted 12 March 2023

Available online 16 March 2023

0012-8252/© 2023 The Authors. Published by Elsevier B.V. This is an open access article under the CC BY license (<http://creativecommons.org/licenses/by/4.0/>).

## 1. Introduction

The continental crust of Eurasia has grown by a series of orogenies through the Phanerozoic (e.g., Şengör and Natal'in, 1996; Yin and Nie, 1996; Metcalfe, 2021). The Central China Orogenic Belt (CCOB) (Fig. 1) is defined as the broad zones of magmatism and deformation that resulted from multiple Palaeozoic collisions and subduction zones to the south of the Tarim and North China blocks and north of the Qiangtang and South China blocks (Lo et al., 2006; Dong et al., 2021). The term covers several individual belts within modern mountain ranges such as the Kunlun, Qilian and Qinling, which extend for >4000 km through the interior of China (Fig. 2). Collectively, the geology of these belts records the subduction and closure of the Proto-Tethys and Palaeo-Tethys oceans, but the extents, timings and processes involved are all debated, and the very extents and definitions of Proto-Tethys and Palaeo-Tethys are not well understood.

This paper presents a new model for the closure of Proto-Tethys and Palaeo-Tethys and assembly of crust in the CCOB. We synthesise geochronological, geochemical and structural data, and correlate tectonic units presently exposed across the Kunlun, Qilian and Qinling ranges and adjacent continental blocks. Our model emphasises the lateral continuity of several tectonic units between the Qinling and Qilian, and we propose that basement units along the CCOB originated as a ribbon continent along the northern margin of the South China Block. We name this composite continent K-Qubed, after the Kunlun, Qaidam, Qilian and Qinling regions where it is now distributed. Orogens are commonly described as one of two end members – collisional and accretionary (Fig. 3). The CCOB has hybrid elements, with the interleaving of older basement and more accretionary and/or juvenile crust (Fig. 3). A key aim of this paper is to understand the process that caused this juxtaposition. There are terranes in the CCOB where there is abundant Precambrian basement that pre-dates the Proto-Tethys orogenic cycle. There are also terranes where a majority of the crust (igneous, sedimentary or metamorphic) formed or consolidated in the Early Palaeozoic. It is this latter kind of crust that we refer to as accretionary in this paper. Such crust needs not be juvenile in the sense of recently extracted from the mantle, only that it carries no corporeal record of the older history.

There is now a huge volume of data on individual areas, especially petrology and geochronology data for igneous and metamorphic complexes. Structural studies are rarer. There are a few studies that make specific correlations between the tectonic units of the west and east parts of the CCOB, despite a general recognition that there is a connection between these areas. Several studies have synthesised one or other of the ranges involved, and the structure and evolution of that particular region (e.g., Meng and Zhang, 2000; Gehrels et al., 2003a; Xiao et al., 2009a; Dong et al., 2011a, 2011b; Song et al., 2013; Song et al., 2014a; Dong and Santosh, 2016; Dong et al., 2018; Zuza et al., 2018; Wu et al., 2019a; Wu et al., 2021; Yu et al., 2020; Yu et al., 2021; Li et al., 2022b).

Other papers have attempted a regional synthesis of the entire CCOB or even larger areas, including Şengör and Natal'in (1996), Yin and Nie (1996), Bian et al. (2001), Metcalfe (2013, 2021), Zuza and Yin (2017), Li et al. (2018a), Dong et al. (2021) and Wu et al. (2022a).

The next section of this paper reviews the geology of each tectonic unit in the CCOB, focussing on the petrology and geochronology of the late Precambrian and early Palaeozoic lithologies, and stating the interpretations of the origins of rock suites made by previous authors. Units are described from north to south from the northern side of the Qilian Shan through to the Kunlun, and then north to south through the Qinling. Regions are summarised in tectonic maps (e.g., Fig. 5), and a space-time chart for the main tectonic units (Fig. 6). Fig. 7 shows kernel density estimation (KDE) plots, for published zircon ages of latest Neoproterozoic and Phanerozoic igneous rocks, displayed by tectonic units. Over 1000 rock ages are represented. We do not attempt a detailed description of the geochemistry of igneous rocks from across the entire CCOB, but we focus on the North Qaidam Ultra High-pressure Metamorphic Belt (NQUB) because of our previous work on this specific area. Section 3 presents a correlation between different tectonic units, along the strike of the entire CCOB. In section 4 we summarise data for the sense of shear during early Palaeozoic deformation, especially strike-slip motion, and explain the importance of dextral strike-slip deformation in distributing the components of the K-Qubed continent along the south side of the North China and Tarim blocks. All data are combined to develop a model for the evolution of the entire CCOB over time (section 5), and place the CCOB in the context of the evolution of the northern margin of Gondwana (Fig. 4).

## 2. Tectonic units

### 2.1. Alashan Block

The Alashan (also Alxa or Alax) Block is a triangular region at the western side of the North China Block. Patchy exposure makes its margins poorly-defined. The eastern margin with the rest of the North China Block lies along the Helan Shan (Fig. 5). The southern margin is with the North Qilian Orogenic Belt (Figs. 5 and 6). The northwest boundary of the Alashan consists of the Engger Us and Quagan Qulu ophiolitic belts (Zheng et al., 2014). These ophiolites record Carboniferous closure of an ocean and back-arc ocean, as the Alashan collided with arcs to the northwest during the Altaid orogeny (Central Asia Orogenic Belt) and the closure of the Palaeo-Asian Ocean (Liu et al., 2018a). The southern boundary of the Alashan lies along the south side of the Longshoushan, at the northern side of the Mesozoic-Cenozoic basins along the Hexi Corridor (Wu et al., 2022b).

Multiple Neoproterozoic and Palaeoproterozoic episodes of magmatism and metamorphism have been detected in the basement of the Alashan Block. Combinations of magmatism and metamorphism are dated to ca. 2.5 Ga and ca. 1.85 Ga in the Beidashan region in the west of

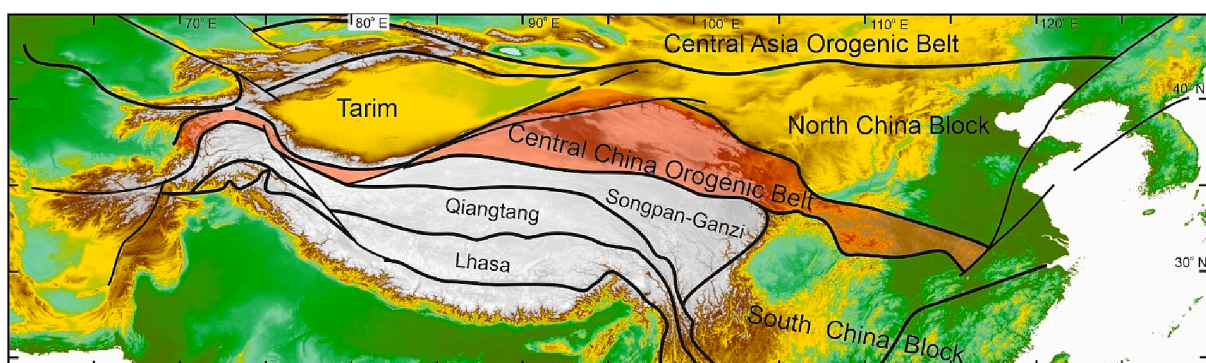


Fig. 1. Simplified tectonic map showing the regional context of the Central China Orogenic Belt.

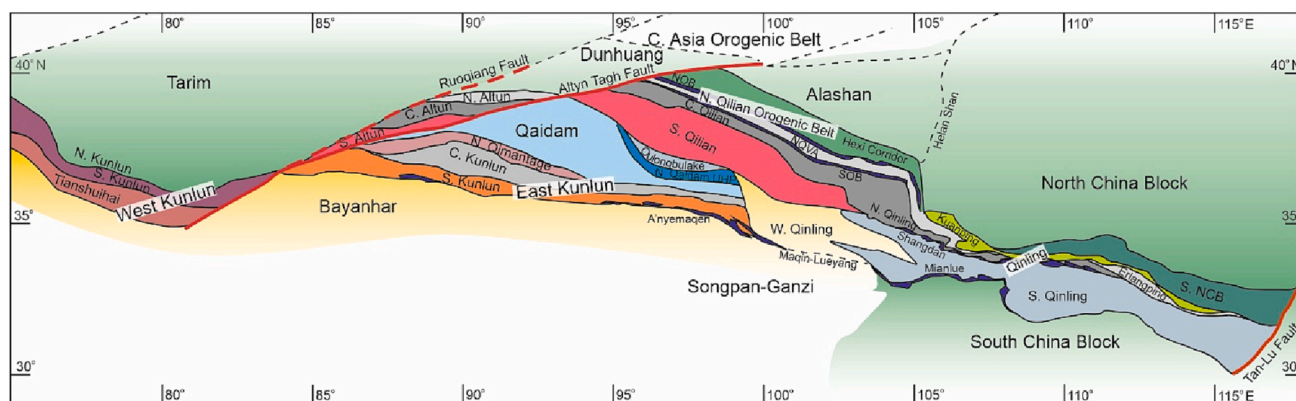


Fig. 2. Summary tectonic map of the Central China Orogenic Belt, showing units described and correlated in this study.

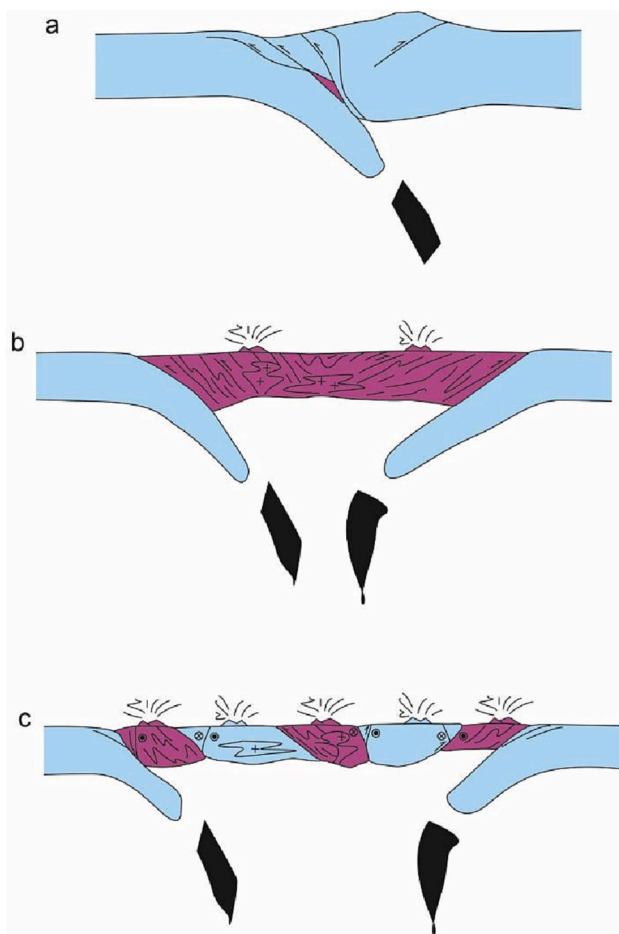


Fig. 3. Schematic cross-sections through different styles of orogenic belts. (a) Classical collisional orogen. (b) Accretionary orogen, with wide zone of juvenile crust (purple) between older continental nuclei (blue). (c) Hybrid style of orogen proposed in this study, with interleaved slices of basement and accretionary crust.

the Alashan (Zhang et al., 2013a). Granitoids in the centre of the region have Neoproterozoic ages, of 930 and 910 Ma (Dan et al., 2014). There is a long-running debate over the relationship of the Alashan to the rest of the North China Block, with various models and ages proposed for their connection. These range in age from Ordovician to post-Palaeozoic (Yuan and Yang, 2015a, 2015b; Dan et al., 2016; Zhang et al., 2016). Song et al. (2017a) used detrital zircon ages from pre-Sinian strata to infer that the Precambrian basement of the Alashan shares more

similarities with the South China Block than the North China Block.

The southern part of the Alashan, including the Longshoushan and Beidashan areas, exposes Palaeozoic intrusions dated between ca. 480 and 400 Ma (Fig. 7a), which is an older age range than the Hexi Corridor immediately to the south (Zhou et al., 2016a; Zeng et al., 2021; Zhang et al., 2021). The interior of the Alashan also contains Carboniferous-early Mesozoic plutons (Fig. 5), believed to relate to the late stages of closure of the Palaeo-Asian Ocean and the evolution of the Central Asian Orogenic Belt, north of the Tarim-Alashan-North China blocks (e.g., Liu et al., 2017a, 2017b, Liu et al., 2018a). Plutons of this age are not recorded from the Hexi Corridor or areas of the Qilian further south.

The Dunhuang region lies west of the Alashan, on the northwest side of the Altyn Tagh Fault (Fig. 5). Dunhuang is normally included with the Tarim Block to its west, but the early Palaeozoic records of magmatism and metamorphism (e.g., Wang et al., 2022; Gan et al., 2020) have similarities with the evolution of the Alashan as well.

## 2.2. North Qilian Orogenic Belt: overview

The North Qilian Orogenic Belt is the ~150 km wide zone of early Palaeozoic rocks between the Alashan in the north and the northern margin of the Central Qilian Block to the south (Fig. 5). It is commonly summarised as one tectonic zone on regional maps, but there is also a scheme that divides it into two paired belts, each with a strip dominated by magmatic rocks on the north side of an ophiolitic belt (e.g., Fu et al., 2019). The northern magmatic belt mainly underlies Mesozoic-Cenozoic strata to the north of the Qilian Shan, which we here name the Hexi Corridor, after the geographic term for this region. From north to south the remaining three of these sub-units of the North Qilian Orogenic Belt are termed the Northern Ophiolite Belt, the North Qilian Volcanic Arc, and the Southern Ophiolite Belt (following Song et al., 2013). Recent identification and study of ophiolites across the northern Qilian Shan casts doubt on this scheme (e.g., Ma et al., 2020), because there are ophiolites within terrain normally described as the North Qilian Volcanic Arc, between the two main ophiolite belts. Regionally, there is a broad pattern of Ordovician arc-related magmatism dying out through the Silurian and giving way to marine turbidite deposition (flysch). Devonian non-marine clastics (molasse) lie unconformably over the older, more deformed, Palaeozoic sequences (e.g., Du et al., 2004; Xiao et al., 2009a). Structural vergence is variable across the whole region, but possibly more commonly to the south than the north (Şengör and Okurogullari, 1991; Allen et al., 2017).

## 2.3. Hexi Corridor

Plutons dated at ca. 460–405 Ma (Fig. 7b) crop out as inliers within the Hexi Corridor (Liu et al., 2017a; Zhang et al., 2017a; Wang et al., 2019), including granodiorites, monzogranites and diorites (Fig. 5). This

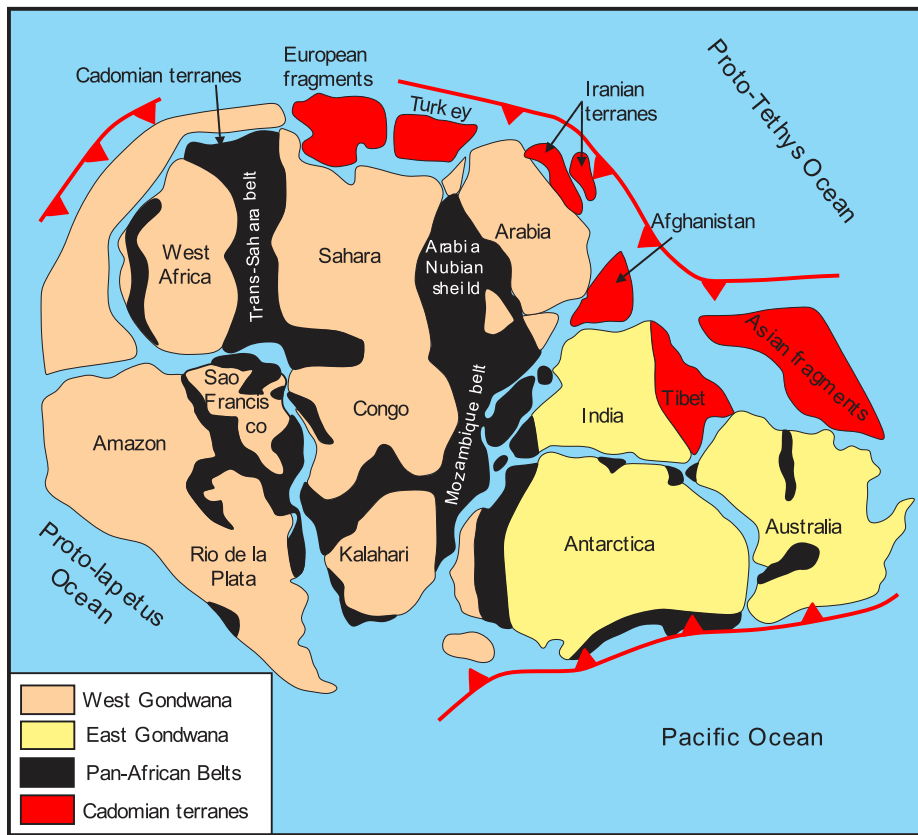


Fig. 4. Proto-Tethys in the context of Gondwana. From Nouri et al. (2021), based on Stern (1994), Meert (2003). Continental units within or at the margins of the CCOB are conventionally grouped as “Asian fragments”

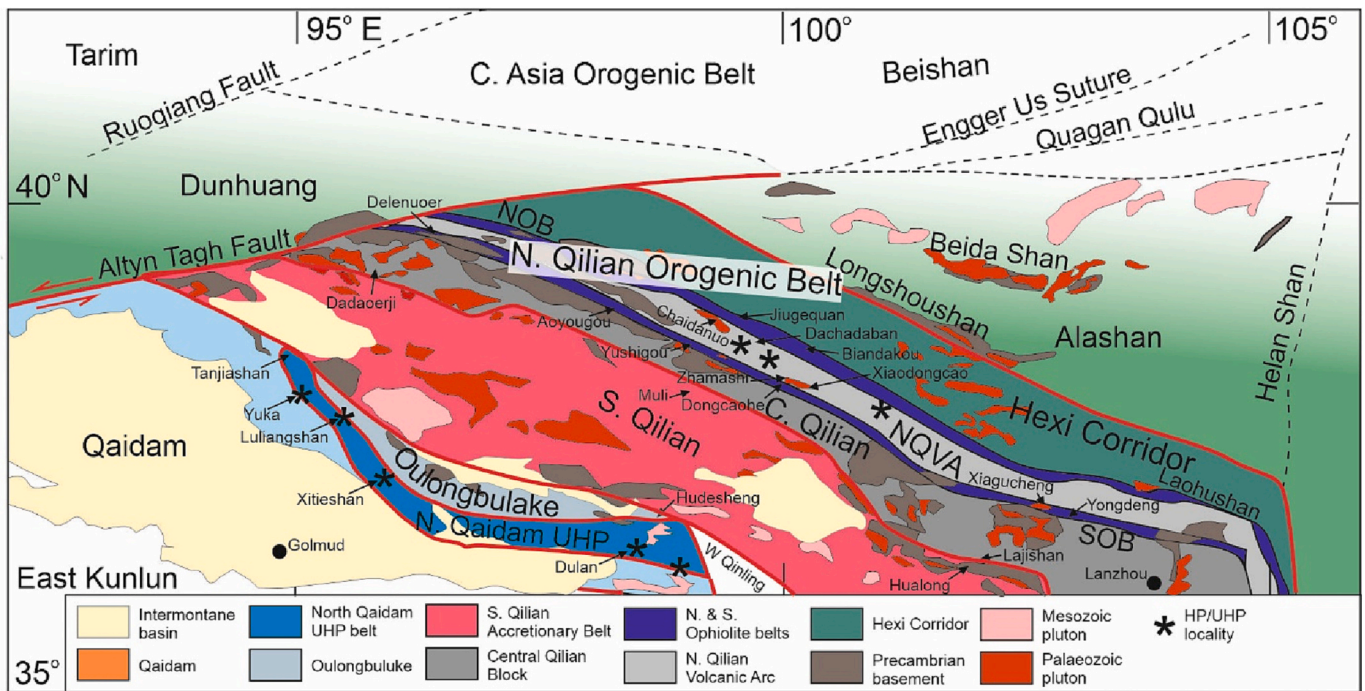


Fig. 5. Tectonic units of the Qilian Shan and adjacent regions, showing the main tectonic units, major plutons and locations of HP and/or UHP metamorphic rocks. From Song et al. (2013), Yang et al. (2019a, 2019b).

is a narrower age range than zones to the north and south (Fig. 7), but this may reflect the relatively small number of exposures and analyses from this area. Both older and younger examples of these granitoids

have high Sr/Y ratios, interpreted to indicate high pressure melting/fractionation conditions and thick crust (e.g., Zhang et al., 2017a). Granodiorites and younger A-type granites may have originated from

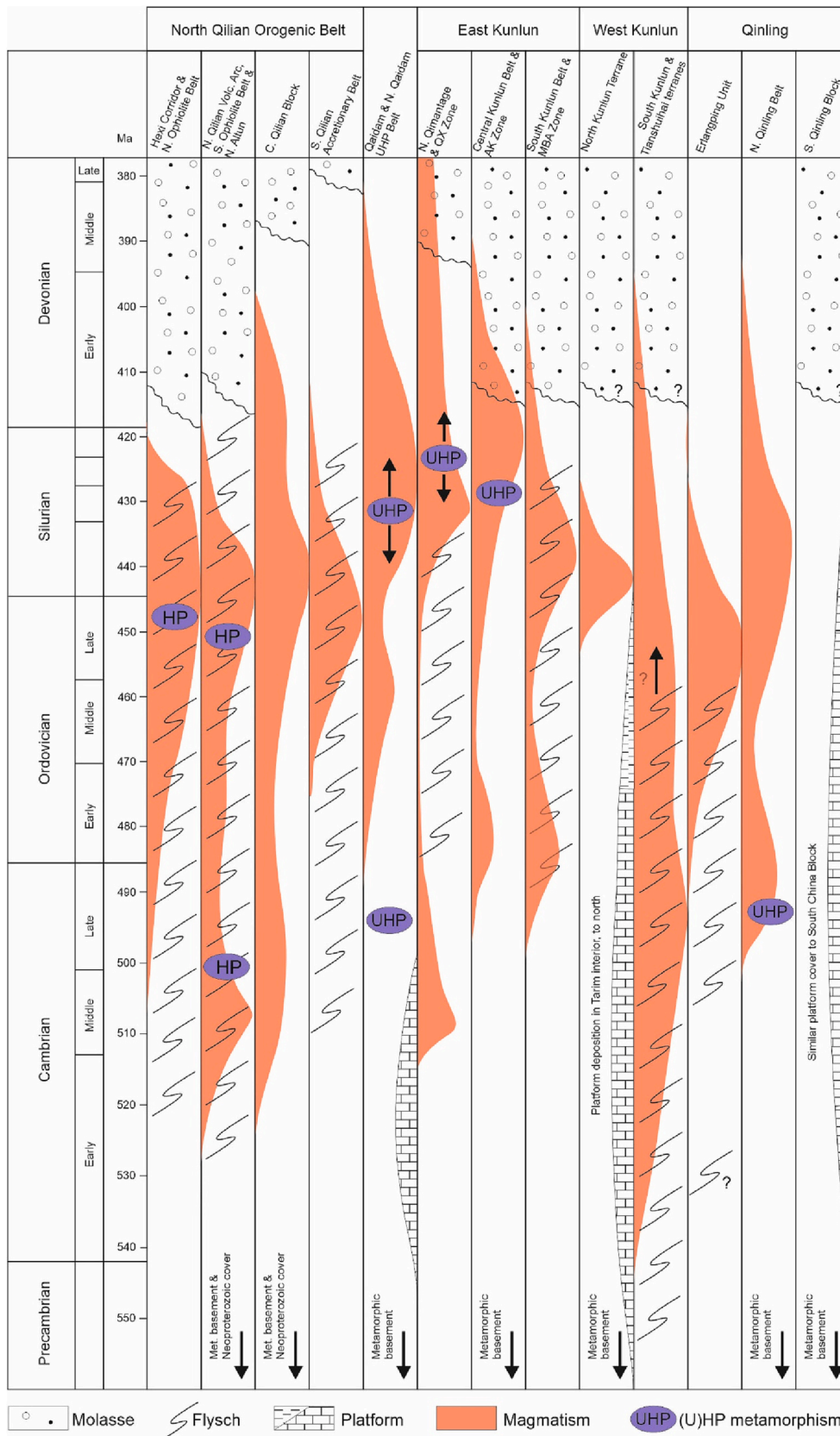
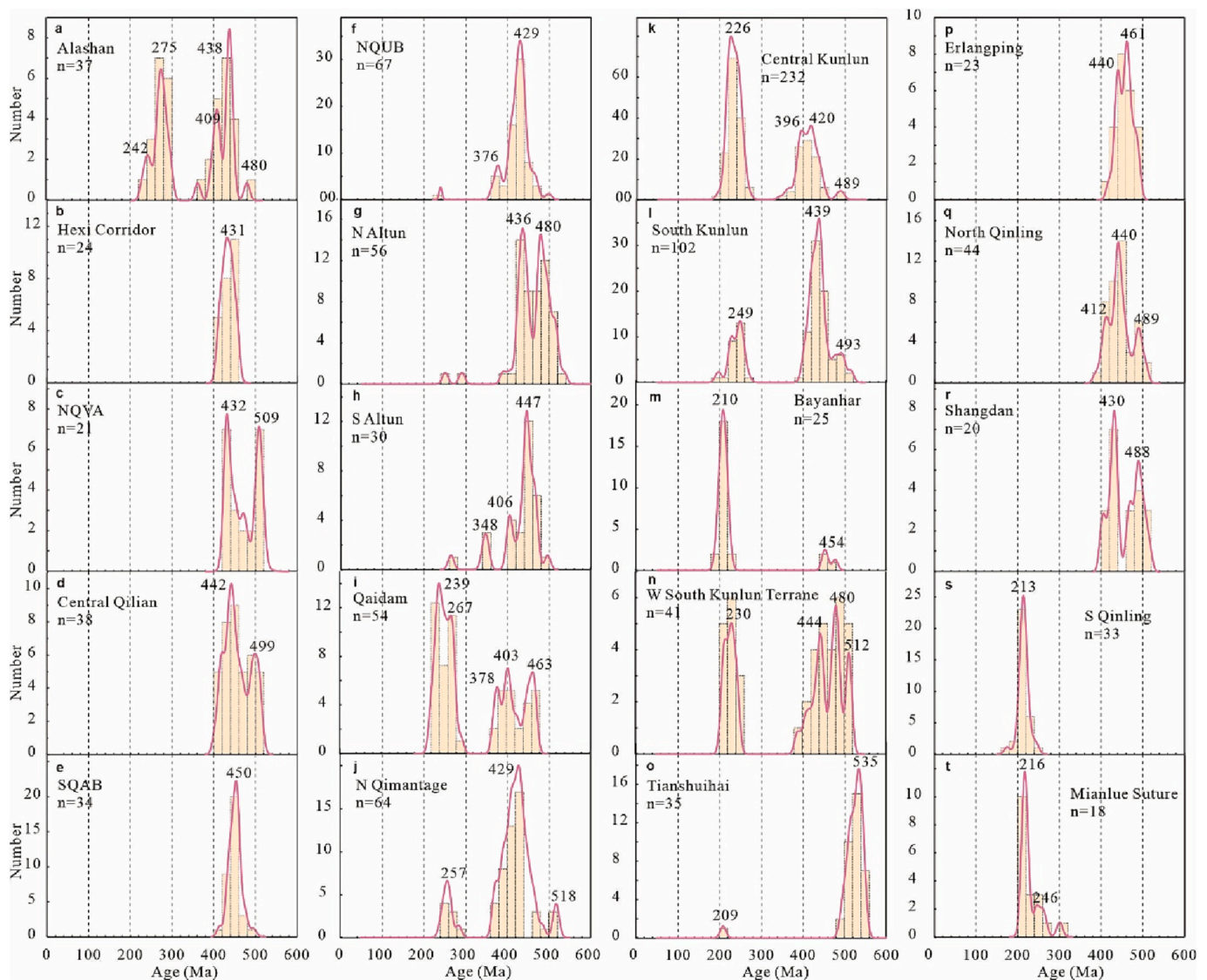


Fig. 6. Space-time chart for the evolution of tectonic units within the CCOB. QX Zone - Qimantage-Xiangride Zone (= North Kunlun Fault); AK Zone – Aqikekule-Kunzhong Fault (= Central Kunlun Fault); MBA Zone – Muztagh-Buqingshan-A’nyemaqen Zone (= South Kunlun Fault).



**Fig. 7.** Kernel density estimate (KDE) plots for Palaeozoic and Mesozoic magmatic ages in the COOB, by region. Ophiolitic rocks are not included. Data are in Supplementary materials Table S1. All dates are zircon U-Pb ages.

crustal melting, of lower crustal basaltic rocks and shallower felsic crust, respectively (Zhang et al., 2017a). Mesoproterozoic (ca. 1.6 Ga) Nd and Hf model ages and xenocrysts ranging from 2.7 to 1.3 Ga indicate Precambrian continental basement underlies this area (Zhang et al., 2017a), although there is a lack of exposed basement, in contrast to the Alashan on the north side of the Longshoushan Fault. Given the relative lack of exposure in the Hexi Corridor region, it is difficult to determine whether the plutonic rocks belong to an arc segment that was distinct from the Alashan and later docked with it – in which case the Longshoushan Fault represents a suture trace, despite the lack of ophiolitic lithologies along it. Alternatively, the plutonic complexes could represent magmatism developed at the southern side of the Alashan, with the Northern Ophiolite Belt marking the boundary (suture) between the Alashan and allochthonous belts further south. It is distinctive that the oldest recorded Palaeozoic magmatism in the Hexi Corridor, at ca. 460 Ma, is tens of millions of years younger than many of the belts to the south, but similar in age to the adjacent Alashan region to the north (Figs. 6 and 7). Lower and Middle Devonian continental clastics of the Xueshan Formation crop out sporadically (Hou et al., 2018).

#### 2.4. Northern Ophiolite Belt

Discontinuous ophiolites within the Northern Ophiolite Belt (Fig. 5) are dated to ca. 490–450 Ma (Song et al., 2013). Zircons from gabbros in two of these ophiolites in the northwest (Jiugequan and Biantukou; Fig. 5) give U-Pb ages in the range 508–470 Ma, with concentrations in the range 490–480 Ma (Song et al., 2013). The Laohushan ophiolite in the southeast (Fu et al., 2020b) is notably younger, and dated at 449 Ma (Fig. 5). A strip of low grade blueschists crops out in the west at Jiugequan (Song et al., 2009a), with Ar-Ar ages of ca. 415–413 Ma (Lin et al., 2010). The blueschist belt consists of lawsonite–pumpellyite–glaucofane schist, recording metamorphic conditions of  $T = \sim 250\text{--}350\text{ }^{\circ}\text{C}$  and  $P = 0.6\text{--}1.1\text{ GPa}$  (Song et al., 2009a). Protoliths of the lawsonite-bearing mafic blueschist resemble modern N-type MORB in their chemistry. Basaltic rocks have either N-type MORB chemistry or supra-subduction zone characteristics (Song et al., 2013). Boninite-protolith blueschists in the east at Laohushan underwent high pressure metamorphism at ca. 455 Ma (Fu et al., 2022).

Plutons intruded the Northern Ophiolite Belt. A reported age of 505 Ma from the Xiagucheng granite at the southeast end of the belt (Qin et al., 2014a) is older than current ages of the ophiolites (Song et al., 2013), and indicates Cambrian subduction in the region. Quartz diorites

at Laohushan (ca. 426 Ma) were generated from melting of accreted oceanic crust and sedimentary rocks, although hornblende xenoliths have Archaean Nd model ages indicating an older, continental protolith (Fu et al., 2019). Adakites derived from melting of thickened crust are present in the same area, dated at 450–430 Ma (Tseng et al., 2009; Yang et al., 2020a).

Middle Ordovician cherts are reported from the Northern Ophiolite Belt (Yan et al., 2021). Middle Ordovician-Silurian flysch and conglomerates overlie the Northern Ophiolite Belt, especially in the west. These rocks have been previously interpreted as forearc deposits, that passed upwards into syn-collisional, foreland basin deposits (Yang et al., 2009; Yan et al., 2010; Xu et al., 2010a). Environments become terrestrial and deposits become coarser up-section in each area; Devonian rocks are terrestrial clastic deposits (“molasse”; Xu et al., 2010a, 2010b; Hou et al., 2018) that post-dated the end of magmatism in the region.

## 2.5. North Qilian Volcanic Arc

There are Precambrian rocks exposed northwest of and along strike from the main North Qilian Volcanic Arc. This region exposes pre-Sinian basement of the Beidahe Group, underlying a mixed marine carbonate-clastic succession and basaltic lavas dated at 600–580 Ma (Xu et al., 2015). Cambrian strata within the same region are more volcanoclastic in composition, with bimodal volcanic rocks (Du et al., 2007).

High-pressure blueschists are exposed in three main discontinuous, fault-bound strips within the centre of the North Qilian Volcanic Arc (Song et al., 2007), structurally interleaved with Middle Ordovician cherts (Yan et al., 2021). Zircons from eclogites in these rocks are dated at  $463 \pm 6$  Ma to  $489 \pm 7$  Ma (Song et al., 2004; Zhang et al., 2007a; Song et al., 2013). White mica  $^{40}\text{Ar}/^{39}\text{Ar}$  ages range from 454 to 442 Ma (Liu et al., 2006a). Mineralogies include carpholite in metapelites and lawsonite in eclogites and blueschists (Wu et al., 1993; Song et al., 2007), with PT conditions for peak metamorphism of  $\sim 460$ – $550^\circ\text{C}$  and  $\sim 2.2$ – $2.6$  GPa. Detrital zircons from metasedimentary rocks within this high-pressure belt have age spectra consistent with derivation from the Alashan (i.e., from the north) rather than the Central Qilian Belt (Xiong et al., 2023).

These Precambrian basement and Palaeozoic blueschist exposures are subordinate to the volcanic and plutonic rocks that dominate this tectonic unit. The volcanic rocks and plutons extend to a younger age range than the ophiolites, from 520–425 Ma (Fig. 7c; e.g., Wang et al., 2005a; Tseng et al., 2009; Yan et al., 2010; Wu et al., 2011; Xia et al., 2012; Song et al., 2013; Chen et al., 2014; Yu et al., 2015a; Pan et al., 2020; Yang et al., 2020a). Two age peaks are present in the data (Fig. 7c), at 509 and 432 Ma. The character of the volcanic rocks changes from back-arc compositions in the north to arc compositions in the south (Xia et al., 2003), with the latter rocks having  $Y < 20$  ppm,  $\text{TiO}_2 < 0.60$  wt%,  $\text{Th}/\text{Yb} > 0.60$ . A boninite complex crops out in the middle of the arc belt at Dachadaban, with boninitic pillows lavas overlying tholeiitic gabbro and massive dolerite (Xiao et al., 2009a). Zircons from gabbros in the tholeiitic section have ages of  $517 \pm 4$  Ma and  $505 \pm 8$  Ma, and from the boninitic section,  $483 \pm 9$  Ma (Xia et al., 2012). This unit may be ophiolitic, which, alongside the blueschists to the southeast and other ophiolitic localities within the North Qilian Volcanic Arc, is problematic for the model of a four-fold division of the North Qilian Orogenic Belt.

Magmatism in the North Qilian Volcanic Arc was both long-lived (Figs. 6 and 7) and compositionally variable. Examples from the two ends of the age spectrum are: peraluminous monzogranite with a zircon U-Pb age of  $505 \pm 3$  Ma and Hf model ages of 1.5–1.9 Ga (Pan et al., 2020); trondhjemite with adakitic affinity, dated at  $438 \pm 3$  Ma and Nd model ages of 840–930 Ma (Chen et al., 2012a). The implication of these Proterozoic model ages, and Proterozoic outcrops in the northwest, is that there is Precambrian basement associated with the North Qilian Volcanic Arc. The Chaidanuo pluton is an S-type granite derived from crustal melting, and represents some of the oldest arc magmatism in the belt, at  $516 \pm 4$  Ma (Chen et al., 2014). In contrast, 506–481 Ma

trondhjemite from the east of the belt has  $\epsilon\text{Nd}(t) = +4.0$  to  $+4.3$ , with little evidence for continental crustal contributions (Chen et al., 2020a). Like other areas of the North Qilian Orogenic Belt, the North Qilian Volcanic Arc contains relatively young, high Sr/Y plutons, previously interpreted as the result of melting of thickened crust at ca. 435 Ma (Yang et al., 2020a). As well as felsic intrusions, there are mafic-ultramafic plutons, interpreted as Alaskan-type, including the Zhama-shi intrusion dated at  $513 \pm 5$  Ma (Tseng et al., 2009).

## 2.6. Southern Ophiolite Belt

The Southern Ophiolite Belt contains tectonised slices of serpentinite, gabbro and massive and pillow basalts in five main lenses along the length of the Qilian Shan (Fig. 5). From the northwest these are Delenuoer, Aoyougou, Yushigou, Dongcaohe and Yongdeng. Zircons from gabbros have U-Pb ages of ca. 550–472 Ma (Shi et al., 2004; Tseng et al., 2007; Song et al., 2013; Ma et al., 2020), with the oldest ages recorded from the Yushigou ophiolite. These ages are commonly older than the North Ophiolite Belt. The chemistry of basaltic rocks resembles N-type and E-type MORB, i.e., lacking the supra-subduction zone signatures of the Northern Ophiolite Belt (Tseng et al., 2007; Song et al., 2013, 2019a). Plutons with variable but subduction-related chemistry are recorded from this belt, dated to 517–498 Ma (Fu et al., 2020a). These ages overlap with, or are slightly younger than the ophiolite ages in the same region; the ages are at the older end of the CCOB range for magmatism.

## 2.7. Central Qilian Block

The Central Qilian Belt is offset by the Cenozoic Altyn Tagh Fault; it is present to the northwest of this fault as the Central Altun Belt. Metamorphic Precambrian basement of the Central Qilian Block (Fig. 5) is defined as the Tuolai Group; this is a composite unit, covering several different elements that are still being resolved (Liu et al., 2018b). The widespread outcrop of this basement has led to the Central Qilian Block being regarded as a Precambrian terrane within the CCOB (e.g., Song et al., 2013) (Fig. 6). Zircons from gneiss yielded youngest ages of ca. 1150 Ma, interpreted as the youngest ages for the rocks that formed the protolith (Liu et al., 2018b). Basement of the Central Qilian Block includes Proterozoic granitoids in two types (Wu et al., 2017): arc magmatism was focussed at ca. 960 Ma, and A-type and S-type plutons were intruded at ca. 820–800 Ma, possibly indicating continental rifting (Tung et al., 2013). Paragneisses of the Hualong Group were derived from protoliths with maximum depositional ages of ca. 900 Ma (Li et al., 2018b). Ophiolitic remnants among the basement units of the Central Qilian are Neoproterozoic in age (Smith, 2006). Overall age distributions of the Central Qilian basement resemble the South China Block (Tung et al., 2007, 2013).

The Dadaoerji ultramafic-mafic complex crops out in the west of the Central Qilian Block, and possibly represents the oldest Palaeozoic, subduction-related magmatism in the region, with zircon U-Pb ages of 524–517 Ma reported in Wang et al. (2017a). However, Song et al. (2019a) suggested that these rocks might be an ophiolitic complex, with affinities with the South Qilian Accretionary Belt to the south. Different studies place the boundary between the Central Qilian Block and the South Qilian Accretionary Belt in different locations (Gehrels et al., 2003b; Wang et al., 2017a).

A variety of granitoids with a range of subduction characteristics intruded the Central Qilian Block, with ages lying between 510 and 410 Ma in the west of the block (Fig. 7d; Gehrels et al., 2003a; Huang et al., 2014, 2015; Luo et al., 2015; Wang et al., 2017a). Fig. 7d has two age peaks, at 499 and 442 Ma. Rock types include granodiorite and monzogranite. Chen et al. (2020b) identified Nb-rich and A-type granites, dated from 509–492 Ma. Volcanic rocks also crop out in the northwest of the block, dated at  $475 \pm 11$  Ma (Zhao et al., 2020). These rocks have a variety of chemical signatures; shoshonites indicate high pressure

(1.8–2.0 GPa) melting at the base of thickened arc crust (Zhao et al., 2020).

Tung et al. (2016) dated intrusions in the east of the Central Qilian Block, 100–300 km WNW of Lanzhou, at 447–402 Ma for S-type plutons and 451–419 Ma for I-type plutons (see also Huang et al., 2015). These suites are interpreted as largely melting Precambrian meta-sedimentary and meta-igneous rocks, respectively (Tung et al., 2016). Proterozoic lithosphere was involved in the generation of shoshonitic plutons in the west of the Central Qilian (Wang et al., 2017a). Peak metamorphism (granulite-facies) was recorded at ca. 450 Ma along the northern margin of the Central Qilian (Peng et al., 2022).

## 2.8. South Qilian Accretionary Belt

The South Qilian Accretionary Belt (Fig. 5) contains Cambrian ophiolites (535–500 Ma) and Ordovician volcanic rocks/plutons with island arc affinities (470–440 Ma) (Song et al., 2017b; Zhang et al., 2017b; Yang et al., 2019a, 2019b; Yan et al., 2019a; Wen et al., 2022a; Wang et al., 2023). These ophiolites and volcanic rocks/plutons are mainly distributed on the north side of the belt, while a belt of Silurian turbidites crops out to the south (Yan et al., 2020). The Lajishan ophiolite crops out in the southeast of the belt, and was thrust north over the Central Qilian Block (Zhang et al., 2017b; Fu et al., 2018). Picritic and basaltic rocks in this ophiolite have a variety of chemistries, with signatures ranging from OIB-like, MORB and arc-like, dated to between 525 and 491 Ma (Zhang et al., 2017b; Fu et al., 2018; Tao et al., 2018; Zhao et al., 2019).

The Hualong Complex contains metasedimentary amphibolite-grade gneisses in the southeast of the belt, in fault contact with the Lajishan ophiolite to its north (Yan et al., 2015). It is not clear whether this unit represents a sliver of Precambrian basement within or at the base of the South Qilian Accretionary Belt, or a tectonic lens detached from the Qaidam Block to the south.

Palaeozoic plutons with subduction signatures within the Hualong Complex cover a distinctively wide age range, from 470–410 Ma (Yan et al., 2015). There are 470–450 Ma plutons with similar subduction characteristics, that intruded into arc and ophiolite rocks at Muli to the northwest (Yan et al., 2019a). Basalts have La/Nb ratios of 1.4 to 5 times N-MORB values, consistent with a subduction setting. Fig. 7e shows a similar peak in magmatism to zones to the north, at ca. 450 Ma, but the South Qilian Accretionary Belt lacks an earlier peak at ca. 500 Ma. Volcanic rocks in the southeast of the belt at Lajishan have a distinctively wide range of compositions, developed over a relatively short time range of 455–440 Ma. (Yang et al., 2019a). These include five lithological types: ankaramite, high-Mg basaltic andesite, high-Al andesite, boninite and sanukite (Yang et al., 2019a). Plutons in the same area have slightly older ages (474–460 Ma) and calc-alkaline chemistry typical of arc settings (Wang et al., 2023).

Subduction polarity beneath the South Qilian Accretionary Belt is debated, with both northwards- and southwards- dipping subduction proposed as responsible for causing arc magmatism, ophiolite obduction and formation of accretionary prisms (Song et al., 2017b; Yang et al., 2018; Fu et al., 2018; Yan et al., 2019a). Xiao et al. (2009a) depicted simultaneous subduction under both sides of the unit. Yang et al. (2018, 2019b) noted that Cambrian ophiolites with OIB affinities occur in the north of the South Qilian Accretionary Belt, with the island arc assemblages to the south. They developed a model where by collision of a plateau of this OIB-like crust with the Central Qilian Block jammed the subduction zone and rapidly generated a new subduction zone and arc to the south. Yan et al. (2019b) described non-marine clastics of latest Ordovician to Late Silurian ages, from the north side of the South Qilian Accretionary Belt, attributed to a foreland basin developed after ca. 450 Ma collision of a continental arc with the Central Qilian Block to the north.

## 2.9. Oulongbuluke Belt

The small Oulongbuluke (Quanji) Belt is sandwiched between the South Qilian Accretionary Belt to the north and the ultra high-pressure (UHP), >2.7 GPa, metamorphic rocks to the south (Fig. 5). The belt contains late Palaeoproterozoic (ca. 1.93 Ga) granulite-grade gneisses and migmatites (Chen et al., 2009; Wang et al., 2015; Yu et al., 2017a). Zircon U-Pb ages suggest these rocks formed as early as 2.47 Ga (Gong et al., 2012). These rocks are both older and at a higher metamorphic grade than is typical in the Qilian Shan/Qaidam regions. There is early Palaeozoic magmatism within the belt: the Hudesheng mafic-ultramafic intrusions are at the eastern side of the block, and are dated at 466 and 455 Ma from zircon U-Pb ages of gabbro and pyroxenite (Li et al., 2019a). These intrusions are interpreted as Alaskan-type complexes from a supra-subduction zone setting (Li et al., 2019a). These ages fall within the range of 483–450 Ma; the dates obtained on zircons from gneiss represent the time of the peak LP/HT metamorphism (Li et al., 2015a), associated with granitic magmatism in the same region (Lu et al., 2018).

## 2.10. North Qaidam Ultra High-pressure Metamorphic Belt (NQUB)

The NQUB is exposed south of the Qulongbuluke Belt (Fig. 5), in a series of discontinuous outcrops of eclogite surrounded by gneiss (Song et al., 2005, 2009b, 2012, 2014a). Both oceanic and continental protoliths are recorded (Song et al., 2006, 2019b; Yin et al., 2007; Zhang et al., 2006; Zhang et al., 2011; Zhang et al., 2017c). The oceanic protoliths are interpreted as relicts of Cambrian oceanic lithosphere, while the continental protoliths have chemical and isotopic signatures of flood basalts, dated at ca. 850–820 Ma (Song et al., 2006; Song et al., 2014a, 2014b; Xu et al., 2016). Zircons from the Luliangshan peridotite have a variety of ages from 484 – 349 Ma, interpreted as the full range from cumulate protolith formation to late-stage alteration rims (Song et al., 2005). Metamorphic zircon rims with a mean age of  $423 \pm 5$  Ma are taken to represent peak burial to depths of ~200 km. Similar ages and PT conditions are recorded in the Xitieshan and Dulan belts to the east (Song et al., 2003; Zhang et al., 2010), and the Yuka belt to the northwest (Ren et al., 2021). Zircons from eclogites from Dulan vary in age from 495 to 443 Ma (Yang et al., 2002), taken as the age range for peak UHP conditions. It is possible that two peaks for UHP metamorphism are recorded in the NQUB overall (Fig. 6): an initial event as old as ca. 495 Ma (e.g., Yang et al., 2002; Ren et al., 2021), and a younger event at ca. 440–420 Ma (Song et al., 2014a). The older events affected ophiolite protoliths (Song et al., 2006; Zhang et al., 2009a), while the younger event affected eclogites whose protoliths formed in a continental setting during the Neoproterozoic (Yu et al., 2019).

A long-lived history of magmatism accompanied the generation and exhumation of the UHP rocks, with an overlapping age range (446–372 Ma; Wu et al., 2007; Yu et al., 2013; Yu et al., 2019; Yang et al., 2020b). In contrast, there is little evidence of the older Palaeozoic magmatism at ca. 500–480 Ma, which occurred to the north (Fig. 7f). Much of this Silurian-Devonian magmatism was related to melting of different types of subducted crust, during exhumation (Yu et al., 2015b; Yang et al., 2020b; Xu et al., 2022). Individual zircons in granitoids have magmatic rims  $\leq 20$  Myr younger than metamorphic cores, interpreted as the interval between peak UHP metamorphism and melting during exhumation (Yang et al., 2020b). Exhumation to shallow levels was achieved by ca. 402 Ma, based on Ar-Ar ages of muscovite (Song et al., 2006) and biotite within an extensional detachment above the UHP rocks and below low-grade volcanic-metasedimentary rocks of the Tanjianshan Group (Zhang et al., 2019a). Therefore, felsic magmatic rocks are common across the NQUB, but commonly represent melting during the exhumation of the UHP rocks rather than generation in straightforward arc settings. Magmatism in the age range of 440–400 Ma is adakitic, with S-type granite (Song et al., 2014a, 2014b; see Yang et al., 2020b for a review of ages). Younger magmatism (400–360 Ma) is predominantly I-

type granite (Zhao et al., 2018b). Zhou et al. (2021) described basic-intermediate and ultrabasic dykes in the region, with ages at 392–375 Ma and 360 Ma respectively. Sources for these dykes changed from mantle lithosphere to asthenosphere over time. The eastern end of the NQUB includes Triassic plutons, related to more extensive magmatism found in the West Qinling Belt (Fig. 2), which lies to the east (Chen et al., 2012b).

Figs. 8 and 9 summarise the geochemistry of Palaeozoic magmatic rocks within the NQUB, adopting previous age divisions of > 440 Ma (“pre-collisional” in the scheme of Zhou et al., 2021, noting the < 440 Ma ages for peak metamorphism of continental protoliths), 440–400 Ma (“syn-collisional”) and < 400 Ma (“post-collisional”). The older rocks include basaltic types and some granodiorite; compositions are dominantly metaluminous (Fig. 8a,b). The 440–400 Ma division is more granitic, with more peraluminous rocks, a pronounced trend towards the  $\text{Na}_2\text{O}+\text{K}_2\text{O}$  end-member in the  $\text{Na}_2\text{O}+\text{K}_2\text{O}-\text{FeO}_t-\text{MgO}$  triangular plot, and a shift to sodic compositions in the Na-K-Ca triangular plot (Fig. 8c, d). The < 400 Ma division sees a reversion to more basaltic rocks and metaluminous compositions, with a similar spread of data in the  $\text{Na}_2\text{O}+\text{K}_2\text{O}-\text{FeO}_t-\text{MgO}$  and Na-K-Ca triangular plots as for > 440 Ma. The same age evolution can be seen in the trace element patterns of the Sr/Y v Y plot (Fig. 8e) and the rare earth element (REE) plots (Fig. 9a) and primitive mantle normalised diagrams (Fig. 9b): samples from > 440 Ma and < 400 Ma are similar to each other, e.g., lying predominantly outside of the typical adakite field in the Sr/Y v Y diagram. Samples aged 440–400 Ma include many data in the tonalite-trondhjemite-granodiorite (TTG)/adakite field.

Palaeoproterozoic ages from gneiss surrounding the eclogite in the Dulan unit are 2.4–2.3 Ga for magmatism and 1.9–1.8 Ga for metamorphism, which is similar to those of the Oulongbuluke Belt to the north and may indicate a correlation between the two regions (Lu et al., 2018).

Ophiolitic protoliths have been identified within the NQUB (e.g., Zhang et al., 2009a; Song et al., 2019a). It is not yet clear to what extent these fragments represent Neoproterozoic or early Palaeozoic oceanic lithosphere; ophiolitic eclogite outcrops are small and discontinuous. Zircon U–Pb SHRIMP dating of an eclogite yielded a Cambrian age of  $516 \pm 8$  Ma (Zhang et al., 2008), interpreted as the time of protolith formation. Island arc volcanic rocks were identified in the west of the belt by Shi et al. (2006), dated at 514 Ma, and now at greenschist facies. Volcanic rocks of the Tanjianshan Group represent continental back-arc magmatism above a north-dipping subduction zone, from ca. 460–440 Ma (Sun et al., 2019). Pyroxenite dykes within peridotites may be the mantle wedge expression of this subduction at ca. 470 Ma (Xiong et al., 2014a). These supra-subduction zone rocks are distributed on both sides of the UHP rocks. Although fragmentary, these data collectively indicate remnants of an early Palaeozoic north-dipping(?) subduction zone between the UHP rocks and the basement of the Oulongbuluke Belt to the north. The discontinuous nature of the outcrops means that no distinct belt is defined in Fig. 5.

### 2.11. North Altun Belt

The three subdivisions of the Altun region, to the north of the Altyn Tagh Fault, represent offset sections of the Qilian tectonic units to the south (Sobel and Arnaud, 1999; Fig. 2). The North Altun Belt is the equivalent of the North Qilian Orogenic Belt, but narrower and with fewer sub-divisions recorded. Both regions contain high-pressure metamorphic rocks with similar ages and PT conditions, and the original extent is restored by removing the ~375–475 km Cenozoic offset along the Altyn Tagh Fault (Cowgill et al., 2003; Gehrels et al., 2003a; Zhang et al., 2019a). High-Mg diorites in the North Altun belt are dated at 536 Ma (Ye et al., 2020), which are among the oldest subduction-related, Proto-Tethyan, magmatic rocks in the CCOB. Granitoids fall in the broad range 518–405 Ma (Fig. 7g; Zheng et al., 2019), and the KDE plot has twin peaks of similar ages to the North Qilian Volcanic Arc, at

480 Ma and 436 Ma (Fig. 7g). Granodiorites in the range 520–470 Ma have arc chemistries, and Nd and Hf signatures indicating melting of Proterozoic (ca. 1 Ga) crust (Zheng et al., 2019). Adakitic and S-type granites are somewhat younger, between 460 and 425 Ma. Granitoids with ages of 420 Ma and younger tend to have I-type chemistries (Zheng et al., 2019).

High-pressure low-temperature metamorphic rocks in the North Altun Belt occur as small lenses of eclogite and blueschist within a 40 km long slab of mica schist, itself interleaved within an ophiolitic mélange (Zhang et al., 2005). Peak metamorphic conditions were  $T = 430\text{--}540^\circ\text{C}$  and  $P = 2\text{--}2.3$  GPa. Phengite from eclogite produced a  $^{40}\text{Ar}/^{39}\text{Ar}$  age of  $512 \pm 3$  Ma; paragonite from blueschist gave a  $^{40}\text{Ar}/^{39}\text{Ar}$  plateau age of  $491 \pm 3$  Ma (Zhang et al., 2007b).

The western limit of the North Altun Belt, and therefore the North Qilian Orogenic Belt, is enigmatic, because exposure of the North Altun Belt dies out westwards under sedimentary cover of the Tarim Basin. The end is plausibly at the ENE-WSW trending Ruoqiang Fault (Figs. 2 and 5) in the southeast of the Tarim Block. To the north of this fault, the Tarim Basin contains Lower Palaeozoic carbonates and clastic sedimentary rocks, interpreted as deposits on a stable continental platform (Kang and Kang, 1996) with Precambrian basement (Guo et al., 2005; Xu et al., 2013). This Lower Palaeozoic platform sequence does not occur to the south of the Ruoqiang Fault, where Carboniferous and younger strata lie over crystalline basement. The basement is recorded as Precambrian in age (e.g., Yin and Nie, 1996).

### 2.12. Central Altun Belt

Proterozoic basement in the Central Altun Belt (Fig. 10) is interpreted as the offset equivalent of similar lithologies exposed in the Central Qilian Block (Wu et al., 2009b), although details are sparse. Metamorphic rocks are classified as the Mesoproterozoic Altyn Tagh Group and the Neoproterozoic Jinyanshan Group (Dong et al., 2021), although other subdivisions have been proposed (Peng et al., 2019).

### 2.13. South Altun Belt

The South Altun Belt (Fig. 10) lies along the northwest side of the Cenozoic Altyn Tagh Fault, and is the offset continuation of the NQUB, with similar overall UHP metamorphic assemblages and ages (Zhang et al., 2019a). There are some differences between the two regions, however. The age range for peak metamorphic conditions is 509–475 Ma (Liu et al., 2009), which overlaps the older range of UHP ages from the NQUB, but not the younger range of the NQUB at 440–420 Ma. The Jianggalesayi eclogite (Fig. 10) has chemical and isotopic signatures indicating that its protolith was E-type MORB (Liu et al., 2009), such as high Nb and Ta contents and positive  $\epsilon\text{Nd}$  values. Gneiss to the south of the Jianggalesayi eclogite has textures indicating Al–Fe-rich stishovite, meaning formation pressures as high as 12 GPa (Liu et al., 2007). The Munabulake ophiolite from the South Altun Belt is dated at  $518 \pm 2$  Ma, and interpreted as forming in a Mariana-type subduction initiation setting, based on the mineral and whole-rock chemistry (Yao et al., 2021).

Palaeozoic granitoids from the South Altun Belt have an unusually wide spread of zircon U–Pb ages, with as many as six different periods of emplacement between 513 Ma and 238 Ma (Wu et al., 2018; Liu et al., 2020; Xu et al., 2020). Peak magmatism was at ca. 450 Ma (Fig. 7h), ~20 Myr earlier than the NQUB to the east. Even discounting the youngest, Permian-Triassic, ages as belonging to the late Palaeozoic–Early Mesozoic subduction history of Palaeo-Tethys, the next youngest magmatism of 352–343 Ma is still unusually young for the region. Most of the early Palaeozoic plutons have subduction signatures, including high-K calc-alkaline series, I-type granitoids, but Devonian (419–404 Ma) intrusions have A-type chemistry (Xu et al., 2020).

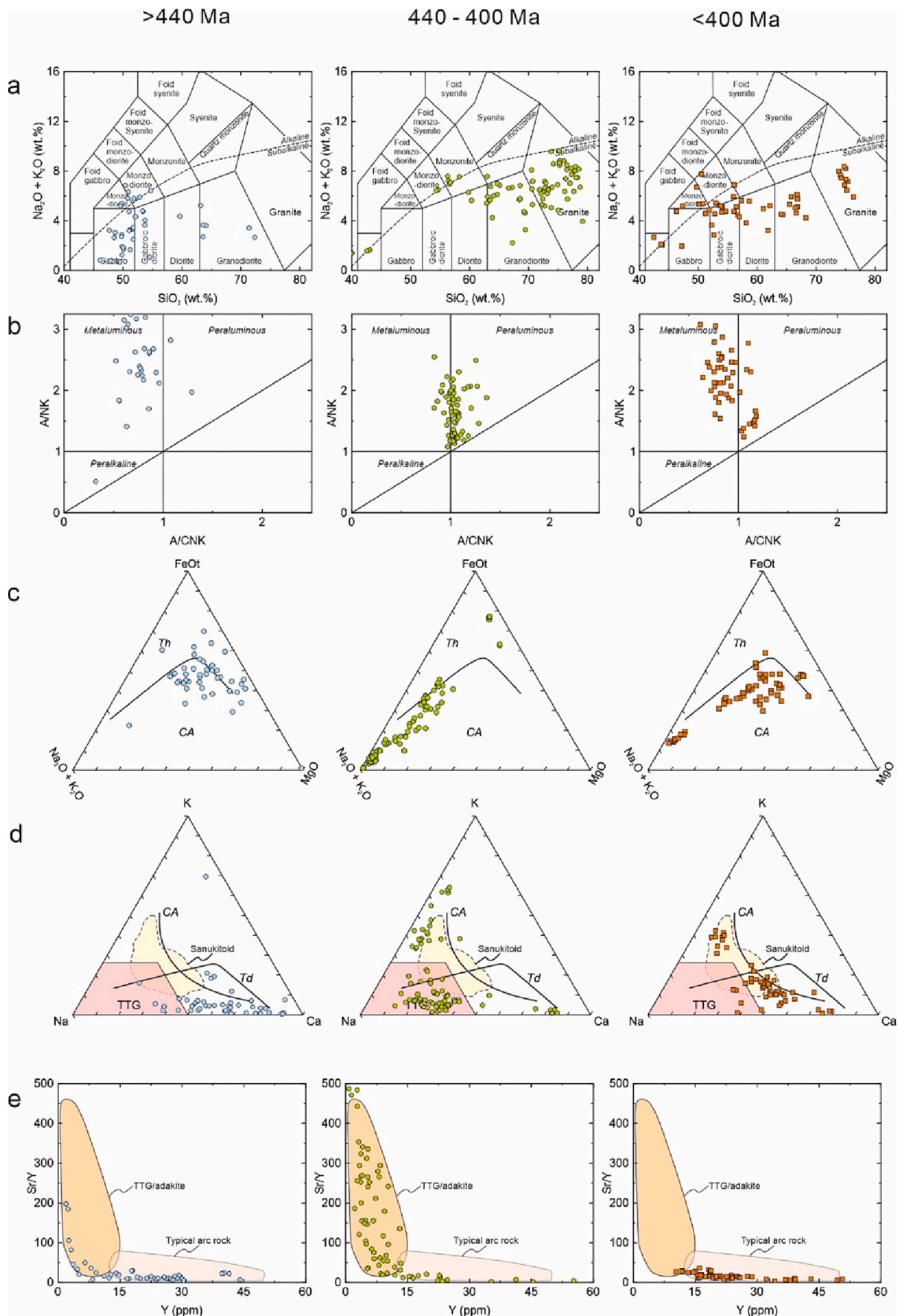


**Fig. 8.** Selected major and trace element characteristics of Palaeozoic magmatic rocks from the NQUB. Derived from: Shi et al., 2006; Zhu et al., 2010; Zhu et al., 2012a; Chen et al., 2012b; Song et al., 2014a; Wang et al., 2014a; Zhang et al., 2015a; Sun et al., 2019; Yang et al., 2020b; Zhou et al., 2021. Time divisions are based on the ca. 440 Ma UHP rocks in the region marking continental collision, following Zhou et al. (2021). Data are in Supplementary materials Table S2. See text for discussion.

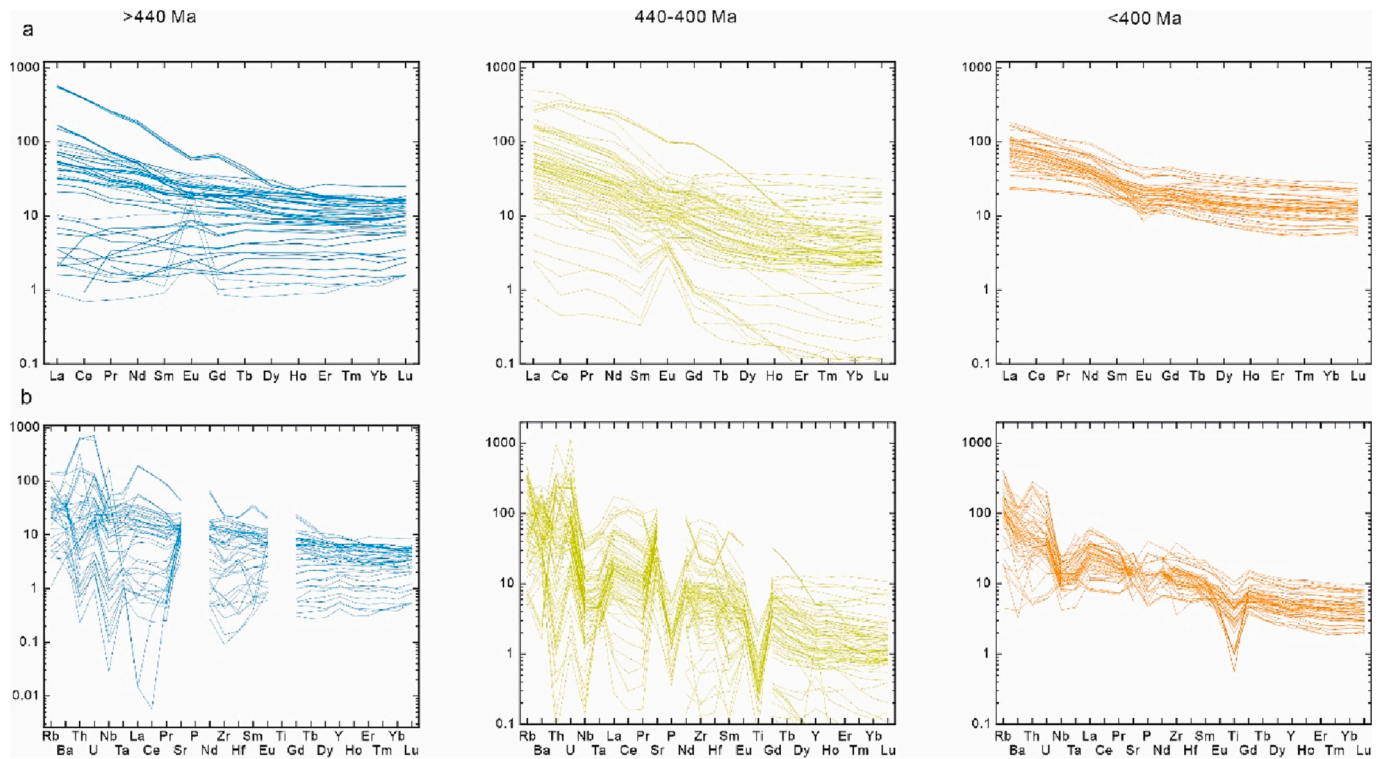


Fig. 9. Rare earth element and primitive mantle-normalised trace element patterns for Palaeozoic magmatic rocks from the NQUB. Data sources as for Fig. 8.

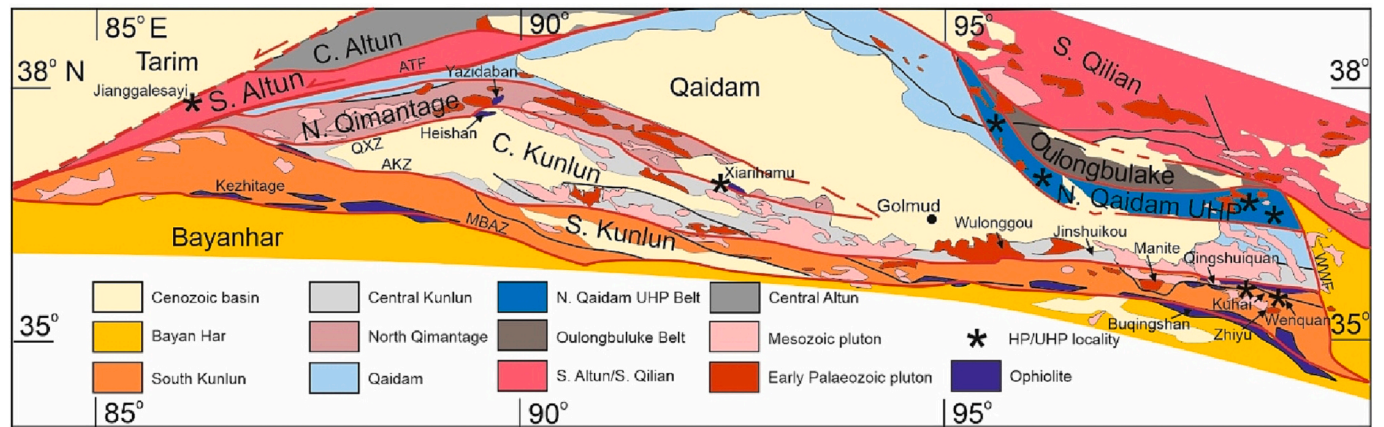


Fig. 10. Tectonic units and major structures of the East Kunlun Orogen. ATF – Altyn Tagh Fault; QXZ – Qimantage-Xiangride Zone (= North Kunlun Fault); AKZ – Aqikekule-Kunzhong Fault (= Central Kunlun Fault); MBAZ – Muztagh-Buqingshan-A'nyemaqen Zone (= South Kunlun Fault); WWF – Wahongshan-Wenquan Fault. From Dong et al. (2018).

#### 2.14. Qaidam Block

Most of the basement of the Qaidam Block is covered by Mesozoic-Cenozoic strata of the Qaidam Basin (Fig. 10), but there are outcrops of Precambrian basement and plutons at the margins, and Cambrian-Ordovician carbonates in the north (Dong et al., 2021) (Fig. 6). The basement has also been penetrated by some of the hydrocarbon wells near the basin margins, where the sedimentary succession is thinner. Cheng et al. (2017) analysed basement samples from such wells, and found a range of zircon U-Pb ages equivalent to the surrounding ranges: early Neoproterozoic (955 and 916 Ma), early Palaeozoic (467–381 Ma), and late Palaeozoic to Mesozoic (291–236 Ma). Palaeozoic magmatism had two main age peaks (Fig. 7i), which are slightly younger than belts to the north and south, and 463 and 403 Ma. Sm-Nd model ages for the early Palaeozoic plutons lie between 2.3 and 1.0 Ga (Cheng et al., 2017),

indicating the involvement of Paleoproterozoic and Mesoproterozoic continental crust in the sources of these rocks. The chemistry of these rocks is broadly I-type granite, with subduction characteristics (Cheng et al., 2017). There are no discernible differences in chemistry or age range between the samples encountered under the north and south parts of the basin. To our knowledge, there are no Palaeozoic igneous rocks with ages >500 Ma reported from the Qaidam Block, but metamorphic zircons in the range 540–520 Ma have been reported from granulites at the western end of the block (Teng et al., 2020). These ages suggest metamorphism and orogeny were underway in the Qaidam region by the earliest Cambrian, similar to or even older than in adjacent areas.

Devonian-Carboniferous plutons exposed in the Dulan region at the eastern side of the present basin are quartz diorite, granodiorite, and granite, with calc-alkali, subduction characteristics (Wu et al., 2014a). Permian-Triassic plutons exposed at the eastern side of the Qaidam

Block are mainly high-K calc-alkaline metaluminous, I-type granitoids, also with subduction zone chemical signatures (Chen et al., 2015). Nd model ages of model ages of 1.28–1.78 Ga indicate derivation from mid Proterozoic basement (Chen et al., 2015), similar to early Palaeozoic plutons in the same region, although derivation from melting of subducted MORB has also been suggested (Shao et al., 2017). The Triassic plutons that intruded the Qaidam Block and its surroundings were part of the Palaeo-Tethyan subduction system under the region (Wu et al., 2009a; Shao et al., 2017).

### 2.15. West Qinling Belt

The West Qinling Belt is a triangular region to the east of the Qaidam Block, that wedges out northwards (Fig. 2). The western boundary to the region is the Wahongshan-Wenquan Fault (Fig. 10); this is the same structure as the active Elashan Fault, but the different names are commonly used in studies of the ancient and modern tectonics respectively (Li et al., 2014a; Yuan et al., 2011). Most of the exposure across the West Qinling Belt consists of Permo-Triassic marine clastic strata (e.g., Li et al., 2014a), making a distinct contrast from the Palaeozoic geology that dominates to the west and north. Relatively deep marine environments are interpreted for these sediment gravity flow deposits, deepening northwards (Li et al., 2014a). Triassic volcanic rocks crop out in the west, adjacent to the Wahongshan-Wenquan Fault. Permo-Triassic granitoids intrude the region (Wu et al., 2019b).

The south boundary of the West Qinling Belt is the Maqin-Lueyang Fault (Fig. 2). This structure is apparently the link between the ophiolite-bearing A'nyemaqen and Mianlue suture zones to the west and east, respectively (Meng and Zhang, 2000), but it lacks ophiolitic lithologies. The Maqin-Lueyang Fault separates the West Qinling Belt from the much larger Songpan-Ganzi Zone to the south. This latter region is a vast area of Triassic flysch deposits, interpreted as having formed during the closure of Palaeo-Tethys and the irregular collision of the Qiangtang and South China blocks with each other and the southern margin of the Proto-Tethys collage to the north (Şengör, 1987).

### 2.16. East Kunlun Orogen: overview

The Kunlun is divided into eastern and western sectors by the Altyn Tagh Fault (Fig. 2), but the relationships between this active structure and the Palaeozoic and early Mesozoic belts in the region are not straightforward. The Altyn Tagh Fault cross-cuts Proto-Tethyan belts in the Altun region, and specifically offsets the North Qilian Orogenic Belt and the NQUB by ~350–475 km in a sinistral sense, displacing these regions from equivalents in the North Altun and South Altun, respectively (Cowgill et al., 2003). Further west, the Altyn Tagh Fault swings in strike to a more east-west orientation, and closer to the trend of the Palaeozoic and Mesozoic structures. The East Kunlun Orogen is divided into four sectors (Fig. 10; Dong et al., 2018). All sectors are intruded by Palaeozoic and/or Triassic plutons.

Three ophiolite belts have been identified in the East Kunlun (Dong et al., 2018) and interpreted as sutures: the Qimantage-Xiangride Zone (= North Kunlun Fault), the Aqikekule-Kunzhong Zone (= Central Kunlun Fault), the Muztagh-Buqingshan-A'nyemaqen Zone (= South Kunlun Fault) (Fig. 10). These ophiolite belts divide the East Kunlun into the North Qimantage (Qimantagh) Belt, the Central Kunlun Belt, the South Kunlun Belt and the Bayanhar Terrane, from north to south (Li et al., 2013a; Dong et al., 2018; Wen et al., 2022b). Other divisions and names vary from this scheme, e.g., Meng et al. (2015) and Yu et al. (2020) grouped the North Qimantage and Central Kunlun belts into a single North Kunlun Terrane. There are also variations in how these terranes are mapped out, e.g., for example, whether the Central and South Kunlun trend parallel to each other for the length of the range, or the Central Kunlun pinches out at ~97° E (Zhou et al., 2016b).

### 2.17. North Qimantage Belt

In the north of the Kunlun, the North Qimantage Belt is a region of mainly early Palaeozoic rocks that are tectonically-interleaved with strips of metamorphic rock of Precambrian age. The Palaeozoic rocks are interpreted as the result of arc and accretionary belt processes, and the latter are interpreted as pre-existing continental basement (Dong et al., 2018). It is not clear what are the North Qimantage Belt's relationships to, and boundary with, the Qaidam Block to its north (Fig. 10). The Precambrian basement is locally overlain by early Palaeozoic volcanic sequences (Dong et al., 2018). The west side of the North Qimantage may wrap around the western side of the Central Kunlun Belt (Fig. 10), thereby separating the latter region from the Altyn Tagh Fault (e.g., He et al., 2018; Dong et al., 2018), but other regional maps show the Central Kunlun Belt continuing as far west as the Altyn Tagh Fault (e.g., Yu et al., 2020). Yu et al. (2017b) referred to North and South Qimantage belts, but what they defined as the South Qimantage is also interpreted as the northern part of the Central Kunlun (e.g., Dong et al., 2018), and that interpretation is followed here. Deformed and fragmented ophiolites have been dated to 537–435 Ma (e.g., Li et al., 2018c; Li et al., 2021a), with both N-MORB and E-MORB chemistry (Yang et al., 1996; Qi et al., 2016).

The oldest volcanic rocks are high Mg-andesites and diorites dated to ca. 520–515 Ma (Wang et al., 2021), with depleted mantle sources (zircon Hf compositions,  $\epsilon\text{Hf}(t)$  of +10 to +15). Early Ordovician basic and intermediate rocks ( $480 \pm 3$  Ma; Cui et al., 2011) have island arc compositions. Younger volcanism is also present, with continental arc signatures (Yu et al., 2017b). Devonian basalts (ca. 395 Ma) have more enriched source compositions, and a mixture of subduction and within plate signatures; these rocks were interpreted as erupted in a post-collisional setting by Zhong et al. (2017). Plutons have a similar age range to the volcanic rocks, from 500 to 390 Ma (Cowgill et al., 2003; Guo et al., 2011; Li et al., 2013b; Wu et al., 2014b; Wang et al., 2014b). Wang et al. (2014b) described a progression in chemical signatures over time, with high-K calc-alkaline granodiorites at ca. 485–445 Ma, A-type granites at 430–420 Ma, and alkali granite with associated minor mafic dykes at 400–380 Ma. Tin-tungsten mineralisation is a feature of this belt, and is associated with both S-type granites (dated at ca. 432 Ma by Zheng et al., 2018) and monzogranite (Gao et al., 2014). Overall, the peak in Palaeozoic magmatism was at ca. 429 Ma (Fig. 6), with a second cluster of ages around 500 Ma (Fig. 7j). Permian-Triassic granitoids are also present (e.g., Li et al., 2013b; Yu et al., 2017b), although less common than in the Kunlun to the south.

### 2.18. Qimantage-Xiangride Zone (North Kunlun Fault)

The Heishan mafic-ultramafic complex in the western part of the Qimantage-Xiangride Zone (Fig. 10) contains gabbro that yielded zircon ages of ca. 486 Ma (Meng et al., 2015). These rocks were interpreted as the products of magmatism in an island arc setting by Meng et al. (2015), but Yu et al. (2017b) considered them to be ophiolitic, albeit with supra-subduction zone characteristics. Dong et al. (2019) dated the Yazidaban ophiolite in the western part of the Qimantage to 421 Ma.

High-pressure and UHP metamorphic rocks have recently been reported from this zone, as eclogite lenses in metasedimentary matrixes from Xiarihamu in the west to Wenquan in the east for ~500 km (Meng et al., 2013; Qi et al., 2014; Song et al., 2018). Coesite inclusions were found in zircons from both eclogites and meta-pelitic gneiss (Bi et al., 2018, 2020). U-Pb zircon ages from this eclogite are in a narrow range of 428–410 Ma, interpreted as the time of peak metamorphism. Zircon cores from the metapelite matrix include similar ages, but also rims of ca. 410 Ma, interpreted as the time of retrograde, amphibolite metamorphism during exhumation (Song et al., 2018).

## 2.19. Central Kunlun Belt

Precambrian basement outcrops in the East Kunlun Orogen are concentrated within the Central Kunlun Belt (Fig. 6). Fault-bound strips and lenses are interspersed with younger rocks, rather than a regional massif. Highest grade rocks are assigned to the Jinshuikou Group, which is dominated by gneiss and includes migmatites. These rocks are assigned to the Palaeoproterozoic, and contain detrital zircons with a spread of Palaeoproterozoic and even Archaean ages (He et al., 2016a), although the depositional age is uncertain. Protoliths are interpreted as continental sedimentary rocks, with peak metamorphism at ca. 1.8 Ga and a Neoproterozoic overprint at ca. 1.0–0.9 Ga (He et al., 2016a). Some ultrahigh-temperature (UHT) granulites were reported in Jinshuikou region, with metamorphic age of  $995 \pm 34$  Ma (He and Song, 2020).

Mafic and pelitic granulite-facies metamorphic rocks in the Qingshuiquan region of the EKO records a clockwise P-T path with high-pressure and ultrahigh-temperature (HP-UHT) conditions, with a long-lived metamorphic age span of 530–465 Ma (Bi et al., 2021). The Jinshuikou Group metamorphic rocks also include early Palaeozoic zircons, indicating that they were involved in metamorphism and deformation of this age (ca. 400 Ma; He et al., 2016a). What is not yet determined is the timing of peak metamorphism of these rocks, and any differences between rocks of similar grade but very different ages and metamorphic histories. Given the existence of high-pressure and UHP metamorphic rocks in the Kunlun of early Palaeozoic age, it is possible that there are rocks now classified in the Jinshuikou Group that have exclusively Palaeozoic origins.

Metasedimentary rocks of the Xiaomiao Group crop out in the east of the Central Kunlun, with detrital zircons that indicate deposition in the Mesoproterozoic. These rocks were also metamorphosed at ca. 400 Ma (He et al., 2016a).

The Central Kunlun contains Neoproterozoic, Cambrian-Devonian and Permian-Early Jurassic granitoids. The Neoproterozoic intrusions are largely S-type granites and granite-gneiss, intruded at ca. 1000–870 Ma (He et al., 2016b). Early Palaeozoic intrusions have a wide age range, mainly between 466–390 Ma (Dong et al., 2018; Wu et al., 2019a; Li et al., 2020a). Detrital zircons from modern rivers that flow across the Central Kunlun have ages back to ca. 550 Ma (Feng et al., 2023), as well as older Precambrian ages. Plutons generally have arc chemical signatures, including I-type granitoids, high-K calc-alkaline tonalites, granodiorites and diorites (Dong et al., 2018). Arc chemistry is also present in gabbros, dated at  $435 \pm 2$  Ma (Zhou et al., 2020). Mafic magmatism was common from Late Silurian to Early Devonian times (Yan et al., 2019c), with subduction-influenced signatures, e.g., Nb-Ta depletion. Silurian to Early Devonian A-type granite plutons were intruded in the Wulonggou region (Xin et al., 2018; Chen et al., 2020c). These granites were sourced from anhydrous, low pressure melting of continental crust with calc-alkaline signatures (Xin et al., 2018), most likely older early Palaeozoic intrusions in the same region (Chen et al., 2020c). Bimodal volcanic rocks dated at 420–409 Ma have mainly asthenospheric sources (Li et al., 2020b). Overall, peak Palaeozoic magmatism was broadly between 420–395 Ma (Fig. 7k). Further information on the Palaeozoic subduction history is provided by the metamorphic record. The P-T-t pathways of HP-UHT metamorphic rocks are interpreted to reveal a complete process from arc compression at the early stage of subduction to extension on the active continental margin related to rollback of the subducted slab in the early Palaeozoic (Bi et al., 2021).

There are also widespread Late Permian-Triassic granitoids (Fig. 7k), mainly in the range 250–200 Ma (He et al., 2016a), but with some examples as young as Early Jurassic (Dai et al., 2013). These plutons have I-type chemistries and high-K calc-alkaline signatures, and include adakites (Xia et al., 2014; Xiong et al., 2014b). A variety of crustal sources with varying mantle inputs have been identified (Xiong et al., 2014b). Magmatism has been previously interpreted as related to subduction of the Palaeo-Tethyan Ocean from the south, based on the arc-

like chemistry of these intrusions (e.g., Xiong et al., 2014b). The number of Permian-Triassic age determinations exceeds the Early Palaeozoic age dataset (Fig. 7k).

## 2.20. Aqikekule-Kunzhong Zone (Central Kunlun Fault)

The Aqikekule-Kunzhong Zone is marked by discontinuous exposures of ophiolitic melanges and volcanic and sedimentary assemblages with subduction zone affinities (Dong et al., 2018). Orthogneiss from Qingshuiquan yielded Proterozoic ages for magmatic zircons at 955 Ma, 895 Ma and 657 Ma, with metamorphic rims at  $559 +12/-17$  Ma and  $516 \pm 13$  Ma (Chen et al., 2008). Amphibolites from the same locality range in age from  $549 \pm 10$  Ma to  $482 \pm 10$  Ma (Chen et al., 2008). Ophiolites reported from the zone have a wide range of ages from latest Proterozoic through Cambrian and Ordovician, summarised in Dong et al. (2018). Silurian and even Devonian ages are also reported, but it is less clear that these ages are from true oceanic crust rather than other igneous rocks interleaved or intruded along the fault zone. The oldest published age is  $555 \pm 9$  Ma (Kuhai gabbro; Li et al., 2007a). Both supra-subduction zone and E-type MORB chemistries are represented, with overlapping age ranges (Du et al., 2017; Dong et al., 2018). The Aqikekule-Kunzhong Zone also contains eclogites. Eclogite outcrops in the east at Wenquan and Kehete have UHP assemblages. Metamorphic zircons in these eclogites have U-Pb ages of 428–425 Ma (Meng et al., 2013; Song et al., 2018), i.e., the same as in the Xiarihamu eclogite along the Qimantage-Xiangride Zone and the NQUB to the north.

## 2.21. South Kunlun Belt

Overall, the South Kunlun Belt contains younger units at lower degrees of burial than the Central Kunlun. Much of the outcrop consists of Permian-Triassic plutons, sedimentary rocks and volcanic rocks, but these are interspersed with several Precambrian units (Dong et al., 2018; Yu et al., 2020).

Mesoproterozoic granitic gneisses are dated to 1200 – 950 Ma (He et al., 2016b). Late Neoproterozoic sedimentary rocks contains detrital zircons as young as 802 Ma (Song et al., 2018). Mesoproterozoic metasedimentary rocks and volcanic rocks are assigned to the Wanbaogou Group, with a smaller area of Palaeoproterozoic metamorphic rocks assigned to the Kuhai Group (He et al., 2016b).

The Ordovician-Silurian Nachitai Group contains volcanic rocks with arc compositions, as well as turbiditic clastic rocks and minor carbonate (Dong et al., 2018) (Fig. 6). Early Palaeozoic plutons are also reported from the South Kunlun Belt, e.g., the Manite granodiorite (487 – 479 Ma according to Li et al. (2017), with an age of  $495.6 \pm 1.1$  Ma recorded by Zhao et al. (2017a)) and the Zhiyu monzogranites and biotite granites, dated as 448 to 408 Ma by Zhou et al. (2016b) (Fig. 10). The oldest magmatism is at least as old as the Late Cambrian, and may be older (Feng et al., 2023). These plutons and volcanic rocks have broadly arc-like, subduction characteristics. Mafic magmatism took place by Early Devonian times (e.g., Dong et al., 2020), with within-plate signatures more prominent than in the Ordovician and Silurian rocks.

There is a smaller area of Permian-Triassic granitoids in the South Kunlun than the Central Kunlun, although they appear similar in age and continental arc chemistry (Roger et al., 2003; Li et al., 2018d). There is a reversal in the proportion of Palaeozoic versus Permian-Triassic ages for magmatism in the South Kunlun compared with the Central Kunlun: relatively more Palaeozoic rocks have been recorded in the South Kunlun (Fig. 7l), with a main peak at 439 Ma and a subsidiary peak at 493 Ma. There is a large area covered by Triassic sedimentary rocks. These include volcanic rocks, but also a mixed clastic-carbonate succession that passes upwards into terrestrial molasse deposits by the Late Triassic.

## 2.22. Muztagh-Buqingshan-A'nyemaqen Zone (South Kunlun Fault)

Fragments of ophiolite in this melange belt are dated at 515–450 Ma (Li et al., 2013a; Li et al., 2021a), which is a similar age range to the Aqikekule-Kunzhong Zone to the north in the Kunlun, as well as other ophiolite belts in the Qilian and Qinling ranges. The ophiolite at Buqingshan (Fig. 10) includes mafic rocks with N-MORB and T-MORB chemistries, indicating the presence of a mature ocean basin in this region (Bian et al., 2004). Fossils in sedimentary rocks in the same part of the mélangé in this region are Early Permian in age (Zhang et al., 2004a). These fossils indicate the existence of deep marine conditions at the south side of the CCOB at this time. The Kezhitaga ophiolite in the western part of the East Kunlun (Fig. 10) has a reported Carboniferous-Permian age (Zhang et al., 2009b), although there are not tight constraints. Combined with the stratigraphic evidence, it appears that the Muztagh-Buqingshan-A'nyemaqen Zone was an active margin at much younger times than the arc and ophiolite belts further north in the CCOB.

The South Kunlun Fault has been reactivated in the Cenozoic to create the active structure known simply as the Kunlun Fault. Some accounts (e.g., Yu et al., 2020) describe a separate Muztagh (or Muz Tagh – A'nyemaqen) Terrane, as a discontinuous belt between the South Kunlun Belt and the Bayanhar Terrane, but here we follow models such as Dong et al. (2021) that do not identify a separate Muztagh Terrane.

## 2.23. Bayanhar Terrane

The Bayanhar Terrane (or Hoh Xil – Bayanhar Terrane) is the western part of the Songpan-Ganzi Zone, which is a triangular-shaped region exposing Middle Permian to Triassic flysch (Figs. 2 and 9). Deposits in the west are named the Bayanhar Group (e.g., Feng et al., 2009). The region represents the irregular zone of accretion between the south side of the Kunlun, the Qiangtang Block and the South China Block (Şengör, 1987; Roger et al., 2008; Metcalfe, 2013). The region contains some Triassic quartz-diorite and granodiorite intrusions (e.g., Lü et al., 2006;

Liu et al., 2006b; Cai et al., 2009; Zhang et al., 2014), but fewer than in the main Palaeo-Tethyan arc system exposed within the Kunlun to the north. There are rare Palaeozoic intrusions (Fig. 7m).

## 2.24. West Kunlun Orogen: overview

The West Kunlun Orogen (Fig. 11) preserves a record of Palaeozoic subduction and accretion at the southwestern margin of the Tarim Block. Unlike the East Kunlun Orogen and the Qilian Shan/Qaidam regions, the West Kunlun Orogen has no recorded high-pressure or UHP rocks. Although Precambrian basement has been reported (e.g., Zhang et al., 2018a), there are not the continuous basement terranes present within regions to the east, at least south of the North Kunlun Terrane (Tarim Block). Outcrops of Precambrian rocks are a relatively minor component of the region (Liu et al., 2019). Instead of a pattern of adjacent Precambrian basement strips and accretionary Palaeozoic rocks, there is a more continuous exposure of arc-related metasedimentary rocks and volcanic rocks at the south side of the Tarim Block, intruded by granitoids (Şengör and Okurogullari, 1991; Mattern and Schneider, 2000; Xiao et al., 2002a, 2002b; Yuan et al., 2002; Xiao et al., 2005; Zhang et al., 2019b). Ophiolite belts and major shear zones have been used to divide the range into three units, the North Kunlun, South Kunlun and Tianshuihai terranes (e.g., Xiao et al., 2005; Zhang et al., 2019b), but the southern two terranes are not highly distinct from each other in terms of their lithologies, age ranges or structure. This is especially true in the west of the West Kunlun Orogen, where the local terminology refers to a Tashikorgan Terrane (Zhang et al., 2018b), covering the whole region in between the North Kunlun and South Pamir terranes – the latter being a lateral equivalent of the Gondwana-derived Qiangtang Block (Robinson et al., 2012). The westward continuation of tectonic units beyond the West Kunlun Orogen is debated, with the lateral correlations disrupted by Mesozoic-Cenozoic collision tectonics and major strike-slip faulting. Structural vergence is commonly to the south (Şengör and Okurogullari, 1991; Mattern and

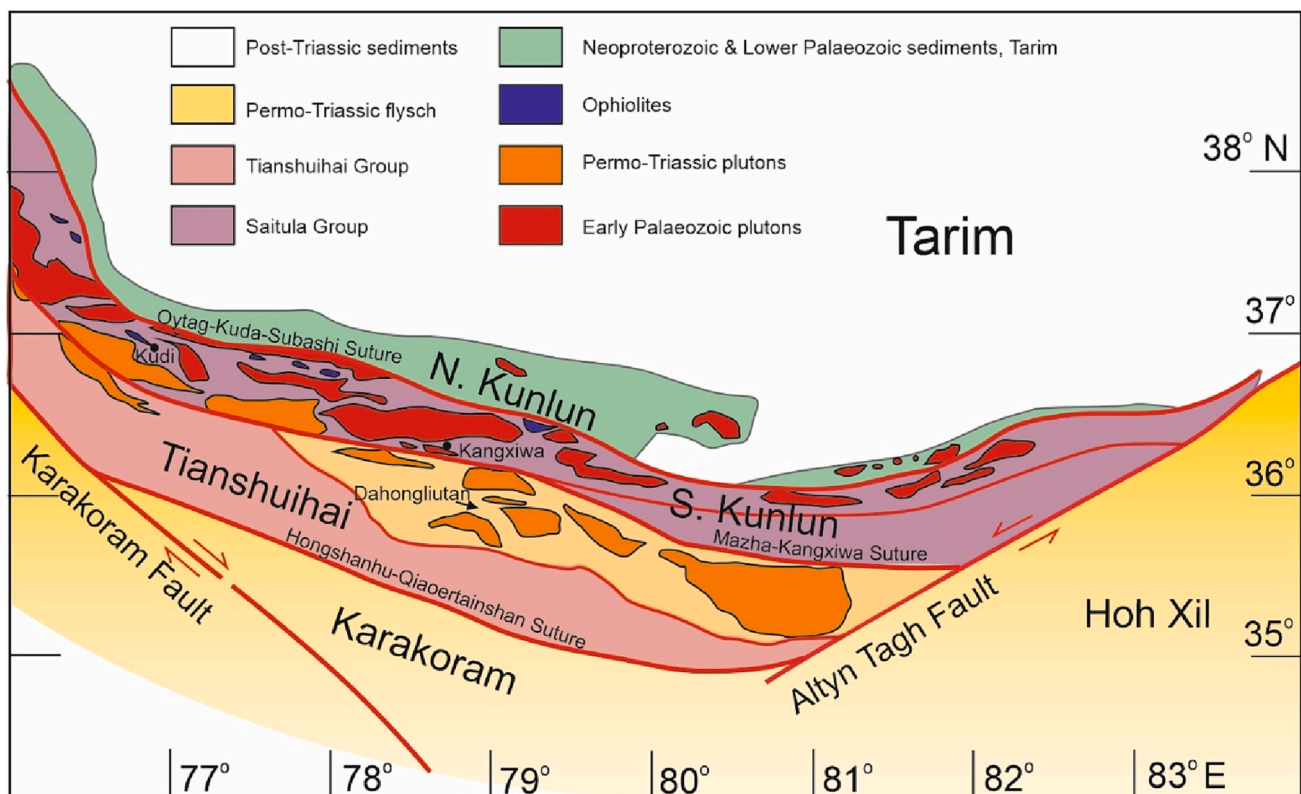


Fig. 11. Tectonic units of the West Kunlun Orogen. From Zhang et al. (2019d).

Schneider, 2000).

## 2.25. North Kunlun Terrane (southwest Tarim Block)

The North Kunlun Terrane (Fig. 11) is equivalent to the southwestern margin of the Tarim Block, and is well-established to have Precambrian basement (e.g., Yuan et al., 2003; Wang, 2004): gneiss, schist and migmatites are intruded by Palaeoproterozoic granitoids, and these rocks are unconformably overlain by Sinian metasedimentary rocks (Fig. 6). This succession continues into the Cambrian (Zhang et al., 2019b). There is an unconformity beneath Devonian red bed clastics (molasse) (Zhang et al., 2019b).

There is rarer early Palaeozoic magmatism in the North Kunlun Terrane compared with some of the other tectonic units of the CCOB, but granitoids dating from 466–428 Ma have been identified (Zhang et al., 2019c, 2019d). These rocks have a variety of chemistries, with I-, S- and A-type granites all present (Zhang et al., 2019c). The oldest of these rocks are notably younger than magmatism in the South Kunlun and Tianshuihai terranes to the south, consistent with interpretations that have the North Kunlun Terrane as a south-facing passive margin for at least the early stages of Proto-Tethyan subduction (Zhang et al., 2019c). This is one of the few regions in the CCOB where there are not common, alternative interpretations of subduction polarity through the early part of the early Palaeozoic.

The south margin of the North Kunlun Terrane is marked by scattered ophiolites of the Oyttag-Kuda-Subashi suture zone (Yang et al., 1996; Mattern and Schneider, 2000), also known as the Akaz suture zone (Xiao et al., 2005) or the Oyttag-Kudi-Qimanyute suture (Zhang et al., 2019b). These ophiolitic rocks are predominantly Cambrian in age, from 525 to 484 Ma (Xiao et al., 2003; Zhang et al., 2004b). One much younger, Silurian (428 Ma) age for basalt in the Kudi ophiolite (Zhang et al., 2004a) may represent separate magmatism, related to the plutonism of similar age in the region. Both mid ocean ridge and subduction-related signatures have been reported from the ultramafic and mafic rocks (e.g., Yang et al., 1996).

## 2.26. South Kunlun Terrane

A widely-distributed volcanosedimentary sequence within the South Kunlun Terrane has been metamorphosed to amphibolite facies (Zhang et al., 2019b), and is known as the Saitula Group (Zhang et al., 2018c). Its zircon age distributions indicate that it was originally deposited during the late Neoproterozoic to Cambrian (ca. 600–500 Ma); the metamorphism was an early Palaeozoic process over ca. 100 Myr from 500 to 400 Ma (Ye et al., 2008), with a possible peak at ca. 440 Ma (Zhang et al., 2019c).

Early Palaeozoic magmatism in the West Kunlun is concentrated in the South Kunlun Terrane (Fig. 6). Yin et al. (2020) deciphered a northern progression of magmatism from the Tianshuihai Terrane into the South Kunlun Terrane from 533 Ma until ca. 513 Ma, with I-type granite magmatism until ca. 450 Ma (Liu et al., 2019). There is a long record of magmatism from this time onwards into the Silurian and Devonian (Fig. 7n); subduction-related plutons are widely-distributed across the South Kunlun Terrane (Yuan et al., 2002; Ye et al., 2008; Jia et al., 2013; Liu et al., 2014; Li et al., 2019b; Zhang et al., 2019b; Yin et al., 2020). Melt was contributed from metasedimentary and metaigneous sources (Yin et al., 2020). High Ba-Sr and A-type granites were intruded between 430 and 400 Ma. The region was also intruded by granitic plutons in the Triassic, as the result of melting of thickened Precambrian crust that interacted with mantle melts (e.g., Jiang et al., 2013).

Structural vergence is predominantly to the south, with dips of strata and metamorphic foliation to the north or northeast (e.g., Şengör and Okurogullari, 1991; Zhang et al., 2018c), but the orientation is variable. The Mazar-Kangxiwa suture (Bian et al., 2001) separates the South Kunlun and Tianshuihai terranes. Metasedimentary rocks along the

Mazar-Kangxiwa suture were originally deposited in the Ordovician and Silurian periods. Similar rocks are not found north of the early Palaeozoic plutonic belt, interpreted by Wang et al. (2017b) as evidence for a paired arc-accretionary complex developed above a north-dipping subduction zone (Yang et al., 2010; Zhang et al., 2007c).

## 2.27. Tianshuihai Terrane

Precambrian basement crops out in the far west of the Tianshuihai Terrane. Latest Archaean protoliths were metamorphosed at ca. 2 Ga and intruded by plutons at 840–835 Ma (Zhang et al., 2018a). The Tianshuihai Group consists of a thick, partly metamorphosed succession of marine clastic sedimentary rocks, including turbidites and tuffites (Mattern and Schneider, 2000). Bedding and cleavage of these rocks generally dips north, or NNE. The Tianshuihai Group is regarded as the oldest unit of the greater part of the Tianshuihai Terrane, with late Neoproterozoic depositional ages (Zhang et al., 2019b), although firm age constraints are rare. Sedimentary banded iron formation (BIF)-type Fe deposits occur within the Tianshuihai Group. Combined zircon U-Pb ages from cross-cutting intrusions and detrital grains led Hu et al. (2016a) to interpret a depositional age for sedimentary rocks at the Dahongliutan Fe-ore deposit of 593–532 Ma, i.e., Neoproterozoic to Early Cambrian.

In the western part of the Tianshuihai Terrane, metasedimentary rocks are grouped as the Bulunkuole Group (Ji et al., 2011; Zhang et al., 2018c). Conditions reached amphibolite or even granulite facies, although the timing of this metamorphism is unclear. Zircon U-Pb ages from meta-volcanic rocks intercalated with the sedimentary rocks yield Cambrian ages (Zhang et al., 2018c), younging northwards from 530–520 Ma in the south to 508 Ma in the north. Devonian red bed molasse sedimentary rocks of the Tisnab Group lie unconformably over older sequences in the region (Şengör and Okurogullari, 1991).

The oldest plutonism in the Tianshuihai Terrane related to Proto-Tethys is dated at 550 Ma (Sui et al., 2021), with other plutons at ca. 530 Ma (Yin et al., 2020), indicating magmatism had begun by the Early Cambrian in this region, if not earlier (Fig. 7o). Published magmatic ages are predominantly Cambrian (e.g., Zhu et al., 2016; Liu et al., 2019), but it is not clear if this is because of incomplete sampling, or a real switch-off of magmatism by the Early Ordovician. If real, it is a different and older age distribution to other units of the CCOB (Fig. 6). There are also rare Triassic plutons (Liu et al., 2015). Both gabbro and granodiorite intrusions are present among the early Palaeozoic rocks. There are enclaves in the evolved plutons with intermediate compositions (Sui et al., 2021). Chemical signatures indicate a subduction setting (Sui et al., 2021), including I-type granitoid chemistry and sample distributions in tectonic discrimination diagrams such as the Th/Ta–Yb plot.

The south side of the Tianshuihai Terrane is marked by the Hongshanhu-Qiaortianshan (Banggong-Nujiang Suture), representing the Palaeo-Tethyan collision with the north side of the Karakorum (Qiangtang) Block.

## 2.28. Qinling: overview

The Qinling range (Fig. 12) contains several tectonic units whose significance and extent is still being unravelled (Bader et al., 2013; Liu et al., 2016; Dong and Santosh, 2016). A major step forwards was the recognition that both Palaeozoic and Triassic orogenies are involved in the Qinling (Mattauer et al., 1985), and that these events acted on tectonic units with Proterozoic histories of deformation and magmatism (Ratschbacher et al., 2003; Dong and Santosh, 2016). The Palaeozoic events accreted elongate continental units to each other and to the southern margin of the North China Block; the Triassic suturing marked the addition of the South China block to the south side of this collage (Meng and Zhang, 2000). It is noteworthy that the Qinling is a narrow range; there is only ~100 km between the margins of the North and South China blocks where they approach each other at the nearest point.

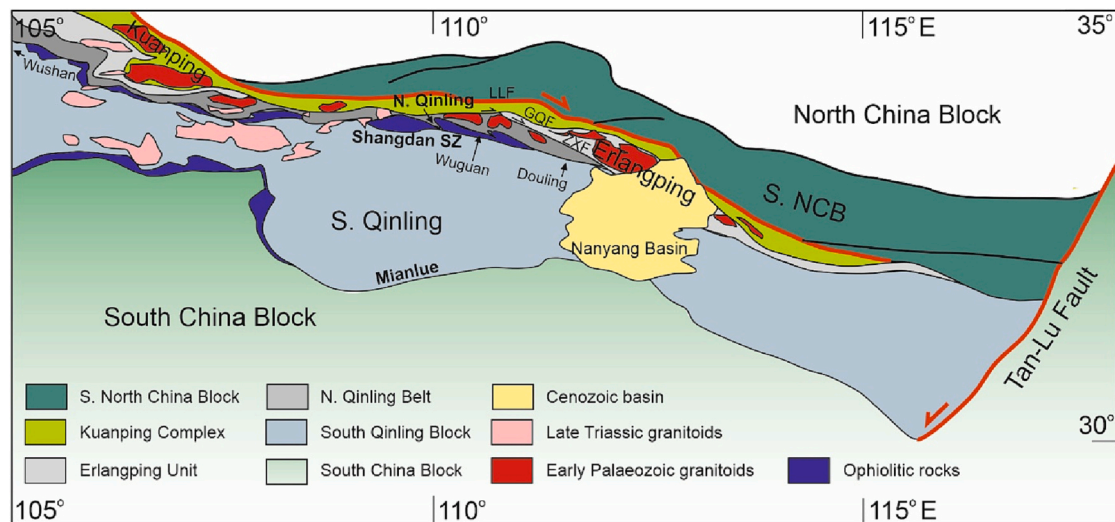


Fig. 12. Tectonic units of the Qinling Orogen. LLF – Luonan-Luanchuan Fault; GQF – Guanpo-Qiaoduan Fault; ZXF – Zhuyangguan-Xiaguan Fault. From Dong and Santosh (2016).

This is in contrast to the CCOB further west, where there are more tectonic units across the entire belt, and the width of individual units increases westwards. The individual tectonic units across the Qinling are described below from north to south.

### 2.29. North China Block

Most of the North China Block consists of Archaean crust, commonly reworked during the Palaeoproterozoic, and hence the term North China Craton is commonly used for the same region, especially for times of stability through much of the Precambrian (Zhao and Cawood, 2012). Magmatic and metamorphic ages of 2.5 Ga and 1.9 Ga are typical, with relative quiescence and mixed carbonate-clastic sedimentation through much of the Proterozoic. The Archaean and Palaeoproterozoic tectonics of the North China Block are the subject of intense debate. One school of thought proposes that eastern and western Archaean blocks were brought together along the Trans North China Orogen in the Palaeoproterozoic (Zhao et al., 2005). An alternative view is that Palaeoproterozoic reworking of Archaean crust is much more widespread across the block, and that the NNE-SSW trend of the Trans North China Orogen reflects later reactivation (Kusky et al., 2016).

There is a Mesoproterozoic ophiolite belt along the south side of the North China Block: the Kuanping Complex (Fig. 12) (also called the Kuanping Mélange, although it does not appear to be a sedimentary mélangé; Dong et al., 2014). Although this unit is commonly included in accounts of the tectonic units of the Qinling, its Precambrian evolution seems unrelated to the opening or closure of Proto-Tethys to the south. The other unit involved in the closure of the ocean that led to the formation of the Kuanping Complex was the North Qinling Belt (see below).

The eastern side of the North China Block is terminated by the strike-slip Tan-Lu Fault (Fig. 12), which was generated by the Triassic collision of the South China Block with the southern side of the North China Block and the amalgamated belts along the Qinling (e.g., Dong and Santosh, 2016). Therefore, the original eastern extent of the North China Block, and all the units within the Qinling to the south, is hypothetical.

### 2.30. Erlangping unit

The northernmost Palaeozoic tectonic division in the Qinling is the Erlangping Unit (Fig. 12), which is located between the Kuanping Complex to the north and the North Qinling Belt to the south. It has previously been interpreted as the relicts of an early Palaeozoic back-arc basin, that opened during northwards subduction of the Shangdan

Ocean beneath the North Qinling Belt (Dong and Santosh, 2016). Closure of this back-arc basin is suggested to have taken place at or shortly before the closure of the Shangdan Ocean (Dong and Santosh, 2016). Metamorphic age ranges reported from the Erlangping Unit cover a wide time span. Zhao et al. (2017b) reported age ranges of 440 – 360 Ma.

Ophiolitic rocks within the Erlangping Unit are termed the Erlangping Group. Interpretation of origins in a back-arc environment comes partly from the presence of rhyolitic rocks within the zone (Dong et al., 2011a). Ages of volcanic rocks vary widely, from ca. 475 Ma to 440 Ma (Dong et al., 2011a); this range is similar to the recorded ages of plutons within the same unit. Early Cambrian microfossils from ophiolitic cherts record earlier crust (Wang et al., 1995).

Early Palaeozoic granitoids are common within the Erlangping Unit (Fig. 6), with ages commonly between 490 and 440 Ma, and a peak at ca. 461 Ma (Fig. 7p; Bader et al., 2013; Wang et al., 2016; Abdallsamed et al., 2017). These rocks indicate that the belt is not simply a zone of oceanic rocks but contains a record of a variety of subduction-related magmatism. Crustal melt granite was produced and intruded at ca. 460 Ma (Guo et al., 2010). High-Mg granodiorite was intruded at ca. 440 Ma, with an interpreted source in the supra-subduction zone mantle wedge (Abdallsamed et al., 2017). Dacitic and rhyolitic extrusive rocks are recorded at ca. 435 Ma (Hu et al., 2019), erupted among basaltic lavas.

### 2.31. North Qinling Belt

Most of the area of the North Qinling Belt (Fig. 12) consists of metamorphic basement termed the Qinling Group. The Qinling Group consists of granite-gneiss, eclogite, granulite, amphibolite, and meta-sedimentary lithologies such as marble. Protoliths are late Mesoproterozoic and Neoproterozoic in age (Shi et al., 2013; Diwu et al., 2014), but underwent regional peak metamorphism in the early Palaeozoic at ca. 490 Ma (Su et al., 2004), or slightly earlier at 516–509 Ma, according to Shi et al. (2018). Retrograde metamorphism took place at ca. 465 Ma (Yu et al., 2016) and at 420–400 Ma (Diwu et al., 2014). Detrital zircons from metasedimentary units cover a wide spectrum of Precambrian ages, with peaks in the ranges of 660–1000 Ma, 1500–1900 Ma, 2226–2172 Ma, and >2400 Ma (summarised in Yan et al., 2016). This spread is claimed to distinguish the North Qinling Belt from either the North China Block or the South China Block (Diwu et al., 2012). This Neoproterozoic clustering is different from the Archaean signatures of the North China Block, but a separate identity from the South China

Block is more speculative, given the range of basement ages across that continent (see below).

Lenses of eclogite within gneiss record peak UHP conditions at ca. 500–490 Ma (e.g., Wang et al., 2011; Bader et al., 2013; Liu et al., 2016). Exhumation ages based on Ar-Ar dating have a wide range (Hu et al., 2020), from at least 484 Ma to 396 Ma. Eclogites have continental protoliths, with zircon cores yielding Neoproterozoic ages of ca. 800 Ma (Wang et al., 2013). UHP metamorphism is interpreted as the result of subduction of the basement of the North Qinling Belt under an arc located to its north, in the Erlangping region (Wang et al., 2013).

Granitoid plutons were emplaced in the North Qinling Belt between 510–400 Ma (e.g., Wang et al., 2009; Zhang et al., 2013b; Li et al., 2018e). Zhang et al. (2013b) identified three peaks for pluton generation, at ca. 500 Ma, ca. 452 Ma and ca. 420 Ma. These authors related the earlier phase of magmatism to the melting of metasedimentary rocks during continental collision, with the successive phases caused by slab break-off and the onset of extension, respectively. As more dates and geochemical analyses are published (e.g., Qin et al., 2014b; Qin et al., 2015; Li et al., 2018e; Ren et al., 2018), it is not clear that this tripartite division is tenable. In Fig. 7q, the main peak shows at 440 Ma, with a subsidiary at 489 Ma.

### 2.32. Shangdan Suture Zone

The Shangdan Suture Zone is an east-west trending strip of ophiolitic rocks within the interior of the Qinling, that represents the early Palaeozoic collision of the North and South Qinling blocks (Dong et al., 2011b; Li et al., 2015b), via closure of the intervening Shangdan Ocean. Mafic rocks include MORB lavas, boninites and lavas with island arc affinities (Li et al., 2015b). Ophiolites have a wide range of ages from ca. 518–457 Ma (summarised in Dong et al., 2007). The Danfeng Group consists of ophiolitic melange (Dong et al., 2015) and island arc volcanic rocks (Zhang et al., 2015b) in the north, and metasedimentary rocks in the south that are collectively known as the Wuguan Complex, and interpreted as the metamorphosed product of an accretionary prism (Yan et al., 2016). A mafic intrusion dated at 485 Ma was interpreted by Wu et al. (2020) as the product of back-arc extension. Younger intrusions have been dated at 437 to 403 Ma by Qin et al. (2021), and interpreted to reflect melting at decreasing pressures through this time, from >1.5 GPa to <1.0 GPa. The KDE plot (Fig. 7r) shows a notably bimodal age distribution, with peaks at 430 and 488 Ma.

A distinctive feature of the Shangdan Suture zone is the elongate shape of many of the plutons and other rock units distributed along it (see maps in Wu et al., 2020 and Qin et al., 2021, for example). The Diaozhuang pluton in the Wuguan region has an aspect ratio of >50:1. More structural studies are needed to determine the kinematics and timing of this deformation, to build on the few reports already published (Liang et al., 2017; Zhao et al., 2017b).

### 2.33. South Qinling Block

The South Qinling Block (Fig. 12) has a similar latest Neoproterozoic and Lower Palaeozoic succession to the South China Block, and is interpreted as having derived from this larger continental parent (Zhang et al., 2001). Much of the basement of the South Qinling Block formed in the Late Neoproterozoic in accretionary orogenic events (Hu et al., 2016b), as represented in the Xiaomoling ophiolitic mélangé (Dong et al., 2017). There is also evidence for older crust: Nie et al. (2016) recorded detrital zircon grains of ca. 2.5 Ga in paragneiss of the Douling complex.

The South Qinling Block is distinctive from the tectonic zones to its north (Fig. 6): it is much wider (up to 200 km across), lacks equivalent evidence for intense regional shearing, and does not carry a record of early Palaeozoic magmatism, but has Triassic magmatic centres (Fig. 7s).

### 2.34. Mianlue Suture

The Mianlue Suture (Fig. 12) was correlated with the South Kunlun Suture (A'nyemaqen Suture) by Meng and Zhang (2000); there is a section along the West Qinling Belt that lacks the ophiolitic slivers found to the east and west. Discontinuous ophiolites within the suture zone are Devonian to Triassic in age (Lai et al., 2004), i.e., distinctly younger than the Proto-Tethyan ophiolites to the north and west through the rest of the Qinling and in the Qilian Shan and Kunlun ranges. Fragmentary slivers of the ophiolite stratigraphy are represented, from ultramafic complexes through to sheeted dyke units and lavas. Parts of the ophiolites have MORB characteristics, but some units show ocean island basalt or supra-subduction zone signatures (Zhang et al., 2004c). The Mianlue Suture records the Triassic collision between the South China Block and the south side of the South Qinling Block, and is regarded as the main suture zone of the closure of Palaeo-Tethys. Triassic granitoid plutons and dykes are recorded as intruding the suture zone (e.g., Yang et al., 2015; Fig. 7t). Dextral shear has been recorded along the Mianlue Suture, dated to the Middle to Late Triassic, and interpreted as the result of oblique closure of this part of Palaeo-Tethys (Liu et al., 2015).

### 2.35. South China Block

The main part of the South China Block was assembled in the Neoproterozoic through collision of the Yangtze and Cathaysia cratons (Cawood et al., 2020). Zircon U-Pb age studies of basement rocks and sedimentary cover have revealed a long and complex history of Precambrian magmatism and crustal growth (e.g., Wang et al., 2012; Cawood et al., 2020). The South China Block has distinctly different age signatures from the North China Block, but more in common with the basement units distributed across the CCOB (e.g., Yao et al., 2014; Jian et al., 2020), with zircon age dates clustering at 1100 – 950 Ma (Cathaysia) and 1000 – 750 Ma (Yangtze).

## 3. Correlation between tectonic units

Previous studies have compared and correlated tectonic and magmatic units between the western and eastern halves of the CCOB (e.g., Meng and Zhang, 2000; Tseng et al., 2009; Yang et al., 2018; Fig. 2). This study is partly a summary and refinement of these correlations, but also makes some new proposals to increase the number of correlated units along the entire orogen.

The origin and evolution of the Alashan Block remain controversial. It may have connections to the South China Block in the Precambrian (Song et al., 2012; Song et al., 2017a). Alternatively, it was a part of the Tarim Block, cut by the Altyn-Tagh Fault (Song and Li, 2019). A third option is that it has affinities with the North China Craton (Gong et al., 2016).

The North Qilian Orogenic Belt is potentially equivalent to the Erlangping Unit in the Qinling (Fig. 2): both units contain early Palaeozoic arc and ophiolitic fragments, accreted to the adjacent southern margins of the Alashan and North China Block respectively. This correlation assumes that if the Alashan and the North China Block were not fully amalgamated by the Ordovician, they were in close proximity.

Exposure of the North Qilian Orogenic Belt disappears at around 105° E, where it is covered by younger strata. Similar Ordovician volcanic rocks and plutons with ages of 450–440 Ma crop out ~200 km to the southeast, east of Tianshui (Yang et al., 2018). This area is contiguous with the rest of the northern Qinling to the east (Liu et al., 2016), such that the continuity of the North Qilian Orogenic Belt and the Erlangping Unit can be suggested by ca. 440 Ma. The four-fold tectonic sub-division of the North Qilian Orogenic Belt is not recorded in the much narrower Erlangping Unit, meaning that the correlation is a simplification (Fig. 2). Tseng et al. (2009) used the presence of intrusive adakites of ca. 450–430 Ma in the North Qilian and similar rocks of ca. 430 Ma in the North Qinling to draw a broad correlation between the

two regions. However, their correlation matches the south side of the North Qilian Orogenic Belt to the south side of the Shangdan Suture Zone, which we consider less likely than the options considered below.

The Central Qilian Block can be correlated along strike with the North Qinling Belt (Dong and Santosh, 2016); the two units are aligned with one another, and form a continuous band with Proterozoic basement linking the Qilian and Qinling ranges (Fig. 2). Likewise, there is continuity between the South Qilian Accretionary Belt and the Shangdan Suture Zone in the Qinling (Song et al., 2017b; Yang et al., 2018).

There is a more tentative correlation between the Oulongbuluke Block and the South Qinling Block, which are the next two belts moving southwards in the Qilian and Qinling ranges respectively (Fig. 2). Not only is there a lack of structural continuity between exposures of the two belts, but the basement characteristics have differences as well as similarities. The broad similarity is that both regions contain Precambrian basement, and are not the largely accretionary crust of adjacent regions to the north in each area. The difference is that the Oulongbuluke Block contains late Palaeoproterozoic basement (ca. 2.47–1.85 Ga) whereas the South Qinling Block seems to have largely formed in the late Neoproterozoic, notwithstanding the 2.5 Ga detrital zircons recorded by Nie et al. (2016).

Along-strike continuity along the Qilian and Qinling belts breaks down east of the Qaidam Block (Fig. 2), where the Triassic sedimentary rocks of the West Qinling Belt are juxtaposed along the Wahongshan-Wenquan Fault with the Precambrian and Palaeozoic rocks to the west. We do not correlate the Qaidam Block, North Qimantage, Central Kunlun or South Kunlun with any units within the Qinling, on structural grounds. These units to the west of the West Qinling Belt terminate at the Wahongshan-Wenquan Fault, to the east of which there are Triassic marine clastic strata; these Triassic rocks are similar to sequences in the much larger Songpan Ganzi Zone to the south.

The great majority of studies on the Kunlun focus on local areas within either the East or West Kunlun, so that there are relatively few papers that cover the correlation between the regions. According to Cowgill et al. (2003), the North Kunlun Terrane (West Kunlun Orogen) is the lateral equivalent of the North Qimantage and North Kunlun Belt of the East Kunlun Orogen. But, the former region is also the southwestern margin of the Tarim Block (Fig. 11), so it cannot be a simple lateral equivalent of any region exposed within the East Kunlun. The Oyttag-Kuda-Subashi or Akaz suture zone (Xiao et al., 2005) is a narrow but distinct ophiolite belt that separates the North Kunlun Terrane and the South Kunlun Terrane (Fig. 11). Precambrian basement in the west of the South Kunlun Terrane may preclude it from being a lateral continuation of the Triassic accretionary Bayanhar Terrane (Songpan-Ganzi Terrane), despite the apparent lateral continuity between these two zones in the region of 81°. The Tianshuihai Terrane appears to continue eastwards into the remainder of the Qiangtang Block, to the south of the East Kunlun (Cowgill et al., 2003), but it appears to be an early Palaeozoic accretionary complex, rather than having the continental affinities of much of the Qiangtang Block. We group the South Kunlun Terrane and Akaz suture zone of the West Kunlun as a pair of basement/accretionary complex slivers, with the Tianshuihai Terrane representing a south-facing accretionary complex that grew above a separate subduction zone (Xiao et al., 2005).

There have been many recent attempts to reconstruct the affinities of Precambrian basement exposed with the CCOB, commonly based on age spectra of detrital zircons. The consensus is that the closest match is with the South China Block (e.g., Jian et al., 2020; Li et al., 2022a). Detrital zircons from Neoproterozoic and early Palaeozoic strata within the South China Block show a dominance of Neoproterozoic ages (ca. 950–800 Ma), with slightly younger ages in the component Yangtze Block than the Cathaysia Block. A similar age distribution occurs within the basement of the Kunlun and Qaidam regions, but the Tarim Block contains dominantly Palaeoproterozoic ages, while the north China Block has a combination of Palaeoproterozoic and Archaean ages (Jian et al., 2020 and references therein).

Isotopic signatures of plutonic rocks also fingerprint tectonic units. Chen et al. (2015) used Pb isotope compositions of Permian-Triassic granitoids in eastern Qaidam to suggest an affinity between the basement of this region and the South China (Yangtze) Block.

#### 4. Evidence for dextral shear

There are references to range-parallel, dextral shear scattered through the literature for the Proto-Tethyan belts, using the term shear to cover both brittle and ductile deformation and the strike-slip offsets generated. Whereas previously these observations have been regarded as incidental, or not included in many models for the evolution of Proto-Tethys, we regard them as highly important evidence for the tectonic history of the CCOB, and evidence that the orogen has a three-dimensional aspect not captured by two dimensional reconstructions. This section summarises these data, taking the belts in the same order as in the previous sections.

Ductile dextral shear was noted along the boundary between the Central Qilian and the North Qilian Orogenic Belt, dated loosely to between 440 and 380 Ma by Qi et al. (2004). The same zone contains the dextrally-sheared Xiaodongcao pluton (Fig. 5); intrusion is dated at  $517 \pm 3$  Ma by Fu et al. (2020a), although the timing of deformation is not constrained. Pre-Devonian dextral shear occurred within the Central Qilian Block, parallel to the margins of this unit. It has been identified in a mylonitic gneiss with an Ordovician granitoid protolith (Wu et al., 2017), and within felsic mylonite ~300 km along strike to the southeast (Xiao et al., 2009a). Sun et al. (2022) recorded U-Pb ages of 452–449 Ma for zircon rims, interpreted as formed during metamorphism of the Central Qilian Block, but before ductile dextral shear of the same rocks.

Zhang et al. (2009c) reported dextral shear along NW-SE trending shear zones in the Tanjiashan gold deposit, in the northwestern part of the Oulongbuluke Block. An Ar-Ar age of 409 Ma from sericite along a shear zone is regarded as the age of this deformation. Later, sinistral, shear took place along these shear zones in the Late Palaeozoic–Early Mesozoic.

The Dulan zone is the eastern part of the NQUB (Fig. 5), and underwent dextral shear during exhumation of the metamorphic rocks, with an Ar-Ar age of syn-kinematic muscovite of 406 Ma (Xu et al., 2006). Early Palaeozoic dextral shear has also been reported along strike, in the Xitieshan region (Fu et al., 2015).

Dextral shear within the western Qimantage is recognised, and constrained as pre-dating the tungsten-tin mineralisation that took place at ca. 415 Ma (Feng et al., 2013). The Central Kunlun Fault in the East Kunlun experienced dextral slip after sinistral oblique thrusting dated at 427–408 Ma (Chen et al., 2002; Li et al., 2014b). Dextral shear is reported along range-parallel, Palaeozoic fault zones in the West Kunlun Orogen (Mattern and Schneider, 2000; Xiao et al., 2005), although there are few absolute constraints on the timing of the offset.

Dextral shear is widespread in the different units of the Qinling Belt, across strike. There is also evidence for sinistral shear at different times (e.g., Zhao et al., 2017b) although this appears to be subordinate to the dextral shear, and reported in fewer localities. Early Palaeozoic dextral shear was noted in the Qinling along the Kuanping Complex at the northern side of the Qinling by Li et al. (2018a). Zhao et al. (2015) and Zhao et al. (2017b) recognised dextral shear along three of the main fault zones along the northern side of and within the North Qinling Belt (Fig. 12; Luonan-Luanchuan, Guanpo-Qiaoduan and Zhuyangguan-Xiaguan faults). The Huamenlou pluton was intruded at ca. 462 Ma into Precambrian basement of the Qinling Group, within the North Qinling Belt, during dextral shear (Li et al., 2018e). Other elongate plutons of this age are widespread in the North Qinling (Zhang et al., 2013b), may also have been emplaced during regional shear. Synchronous dextral and sinistral shear is reported from the Qinling Group on the north side of the Shangdan Suture Zone, in the mid Palaeozoic (400–350 Ma) (Wang et al., 2005b; Mao et al., 2020). The Shangdan Suture Zone underwent dextral shear in the Wushan region (Liang et al., 2017),

no later than 403 Ma (constrained by the zircon U-Pb age of a cross-cutting dyke). Zhao et al. (2017b) also reported dextral shear along the Shangdan Suture, but overprinted by later sinistral motion at lower temperatures. The Mianlue Suture includes relatively late dextral strike-slip, superimposed on earlier sinistral motion (Li et al., 2007b).

In summary, there is evidence for early Palaeozoic ductile dextral shear along the strike of the different tectonic units within the CCOB, both in eastern and western sectors along strike, and from north to south across the regional strike. Although sinistral shear is also reported (e.g., Zhang et al., 2009c; Mao et al., 2020), it typically seems subordinate to the dextral deformation, and/or more important further south, in late Palaeozoic or Mesozoic shear zones. Shear occurred both at the boundaries between major units, and within them. It was contemporary with arc magmatism within these units (Li et al., 2018e). There are more instances reported from the Qinling than regions to the west; this difference may simply reflect a greater number of studies in the Qinling, but it may be an indication of greater shear, especially in the North Qinling Belt.

## 5. Discussion: sequence of tectonic events

### 5.1. Previous models: multiple subduction zones

There is broad agreement that the crust within and at the margins of the CCOB originated on the northern margin of Gondwana, in the late Precambrian and early Palaeozoic (Fig. 4) (Han et al., 2016; Li et al., 2018a; Cawood et al., 2021). Numerous studies on the Qilian Shan, Kunlun and Qinling focus on one or other suture zone identified as a site for the closure of at least a branch of Proto-Tethys, if not the main ocean. Younger ophiolite belts and magmatic arcs are identified with the evolution and eventual closure of Palaeo-Tethys. Most models treat each ophiolitic belt as a unique suture between arcs and/or continental blocks, representing closure of a distinct ocean basin (e.g., Yu et al., 2020). Therefore, many individual papers propose configurations represented by Fig. 13, where more juvenile tectonic units are juxtaposed with Precambrian terranes across a suture zone, which represents closure of an intervening ocean basin.

It is clear that there is no single, unique, suture within the CCOB, based on the number of reported ophiolite belts across the whole orogen, especially in the East Kunlun to Qilian Shan section where the CCOB is widest. The schematic cross-section of Fig. 13 applies multiple times

across the whole belt. For example, Xiao et al. (2009a) depicted four long-lived subduction zones operating through the Late Cambrian to Early Silurian interval within the Qilian Shan, i.e., not including the Kunlun, where further subduction zones are identified in the same time interval (e.g., Meng et al., 2015). The implications of such models become obvious when palaeogeographic reconstructions are attempted: models with multiple synchronous subduction zones require small and isolated blocks to “float” within minor ocean basins for roughly one hundred million years before colliding with each other, nearly simultaneously (e.g., Bian et al., 2001; Zhao et al., 2018a; Yu et al., 2020; Liu et al., 2021; Metcalfe, 2021; Dong et al., 2021; Yu et al., 2021). Although the modern example of the southwest Pacific shows that more than one subduction zone can operate in a region simultaneously, the caveat is that such zones tend to be small, highly arcuate and unstable, disappearing after a few million years (e.g., Hall, 2017), and may relate to short-lived oceans formed after initial collision elsewhere (Schliffke et al., 2021). Stable, major, subduction zones do not group in bundles (Şengör et al., 2018). Long-lived subduction zones around the Pacific are linear features, e.g., the Andean margin of South America.

All the major tectonic boundaries within the Qilian Shan have previously been interpreted as representing opposing senses of subduction, by different authors. The list that follows is not exhaustive, and it should be read as an illustration of the amount of variation between different interpretations of the same areas. The North Qilian Orogenic Belt is interpreted as formed exclusively above north-dipping subduction zone by Wang et al. (2005a) and Pan et al. (2020), and above a south-dipping zone by Xiao et al. (2009a), Yan et al. (2010) and Zhang et al. (2019a). A common scenario is of north-dipping subduction under the south side of the region coupled with synchronous south-dipping subduction zone along the northern side (e.g., Xu et al., 2010b), with the latter process closing a back-arc basin. Fu et al. (2019) suggested that the North Qilian Orogenic Belt includes two north-dipping subduction zones, based on the identification of paired arc and accretionary complexes. The South Qilian Accretionary Belt has been described as developing above a north-dipping subduction zone by Yang et al. (2018) and above a south-dipping subduction zone by Fu et al. (2018), based largely on the sense of thrust motion of arc and ophiolite rocks within this belt over adjacent units. Zhao et al. (2020) showed the Central Qilian block as lying over a south-dipping subduction zone, with a back-arc basin forming to its south. Yan et al. (2022) interpreted three separate subduction zones in the accretion of the SQAB, with initial south-dipping subduction from

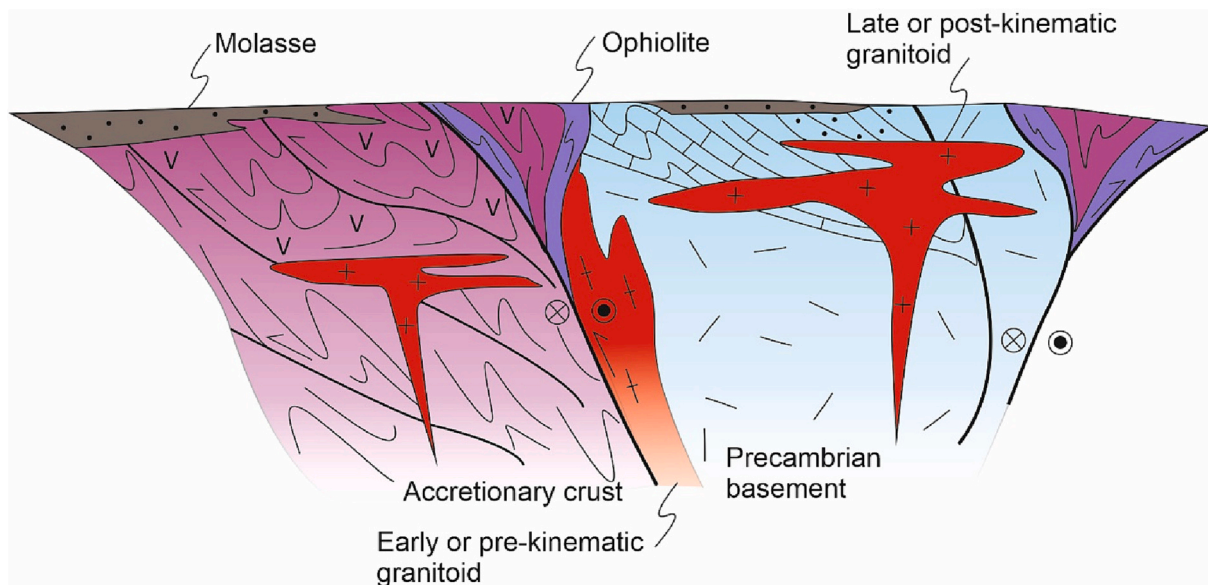


**Fig. 13.** Schematic illustration of typical tectonic units within the CCOB, their components and their relationships to each other: Precambrian basement-cored terrane (light blue); accretionary arc/prism (purple); ophiolitic suture zone (deep blue).

530–480 Ma, followed by arc collision with the Central Qilian and two later north-dipping zones, punctuated by docking of a Hualong microcontinent.

Most accounts of the NQUB propose north-dipping subduction prior to exhumation of the metamorphic rocks (although see Li et al. (2021b) for a contrary view), but there is disagreement as to whether the continental subduction took place entirely within crust of the Qaidam Block, or whether there was an oceanic tract between the UHP belt and the Oulongbuluke Block to the north (Zhang et al., 2009a). Similar debate occurs for the belts within the East Kunlun, and the relationships between the ophiolites and high-pressure and UHP rocks and former subduction zones in this region.

Some interpretations of the West Kunlun favour northward-dipping subduction through the greater part of the evolution of the West Kunlun Orogen (Şengör and Okurogullari, 1991; Wang, 2004; Wang et al., 2017b), but at least initially subduction may have been to the south (Mattern and Schneider, 2000; Xiao et al., 2005; Zhang et al., 2018a; Liu et al., 2019), and underneath the South Kunlun Terrane. Initial south-dipping polarity is interpreted from the northwards-younging of both Cambrian plutonism by Yin et al. (2020) and sedimentation (Zhang et al., 2018b). However, the eastwards trend of Mesozoic-Cenozoic magmatism in the Central Andes shows the potential flaw in this reasoning. The reversal in subduction polarity took place at ca. 513 Ma according to Wang et al. (2017b), at ca. 470 Ma according to Xiao et al. (2005), in the Late Silurian (Li et al., 2019b) or the Late Palaeozoic (Zhang et al., 2019b).

Here, we follow the studies that argue for early southwards subduction in the West Kunlun, not least because there is no apparent record of early Palaeozoic arc magmatism in the southwestern part of the Tarim Block (North Kunlun Terrane), as would be expected if there was a northwards-dipping subduction zone under this continental margin in the Cambrian. Later arc-signature magmatism in the early Palaeozoic is widespread across the South Kunlun Terrane up to ca. 400 Ma, i.e., the same time interval as other sectors of the CCOB. We suggest that there was a Late Cambrian (ca. 500 Ma) reversal in subduction polarity, following collision of a passive margin at the south side of Tarim with a north-facing arc in the Central Kunlun Terrane. North-dipping subduction continued through the remainder of the early Palaeozoic. This is essentially the model of Wang et al. (2017b).

Most recent models for the Qinling are variations on the scheme of Dong and Santosh (2016), with early southwards subduction under the

North Qinling Belt followed by northwards subduction of the Shangdan Ocean under the south margin of this unit, possibly accompanied by opening and then (southwards?) subduction of an Erlangping back-arc basin. Closure of the Shangdan Ocean docked the South Qinling Belt to the North Qinling Belt, and was followed by northwards subduction of the Mianlue Ocean (i.e., main branch of Palaeo-Tethys), with eventual collision of the South China Block in the Triassic.

The plethora of different models for subduction polarity within the CCOB is understandable: the tectonic units of the Qilian Shan, Qaidam and Kunlun are arranged as alternating belts of Precambrian basement and early Palaeozoic orogenic rocks (Fig. 6), so that there is no unique solution as to which arc sat outboard of which continental unit. Structural transport direction may vary along individual boundaries, and in any case is strongly modified by Mesozoic-Cenozoic deformation (Allen et al., 2017; Zuza et al., 2018).

If all the individual subduction zones that have been interpreted for different parts of the CCOB are shown on the same cross-section, the implication is that as many as nine separate subduction zones were active at roughly the same time in the early Palaeozoic (at ca. 480–450 Ma) in the region of the CCOB that is currently widest (seven are shown in Fig. 14). The full sub-division is: two subduction zones represented in the North Qilian Orogenic Belt (Fu et al., 2019), two under the Central Qilian Block (e.g., Yang et al., 2018; Fu et al., 2018), another one under the SQAB (Yan et al., 2022), one between the Qaidam Block and the Oulongbuluke Block (e.g., Zhang et al., 2009a; Xiong et al., 2014a) and up to three across the Kunlun (Dong et al., 2018; Yu et al., 2020). This scenario, of multiple independent subduction zones operating at the same time (Fig. 14), does not seem likely. More recent reconstructions of the Gondwana margin include “archipelago” configurations of narrow arcs and continental slivers (Fig. 15a,b; Zhao et al., 2018a; Dong et al., 2021; Yan et al., 2022).

## 5.2. Oroclinal bending model

In contrast, Li et al. (2018a) described a single subduction zone on the northwest margin of Gondwana (Fig. 15c). This subduction zone opened a back-arc basin to its east, and rifted a linear continent away from Gondwana, consisting of crust now preserved from the Kunlun to the Qinling. A key feature of the model is the tight, oroclinal, bending of this subduction zone through the early Palaeozoic, such that the original subduction front developed two hairpin loops (Fig. 15c). These loops are

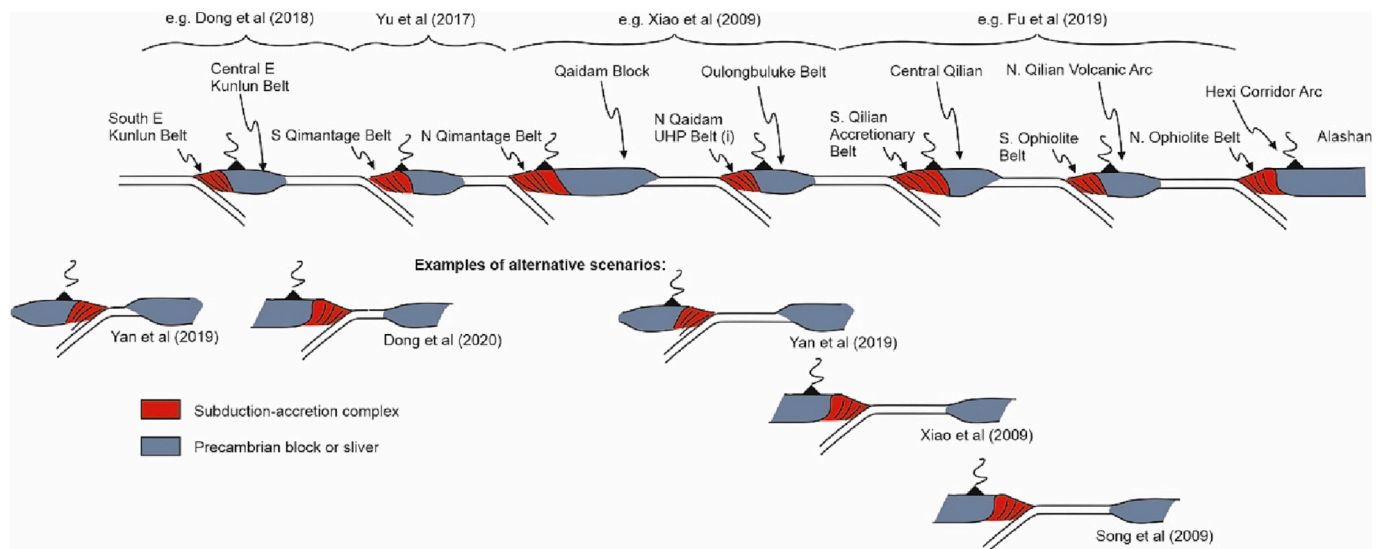
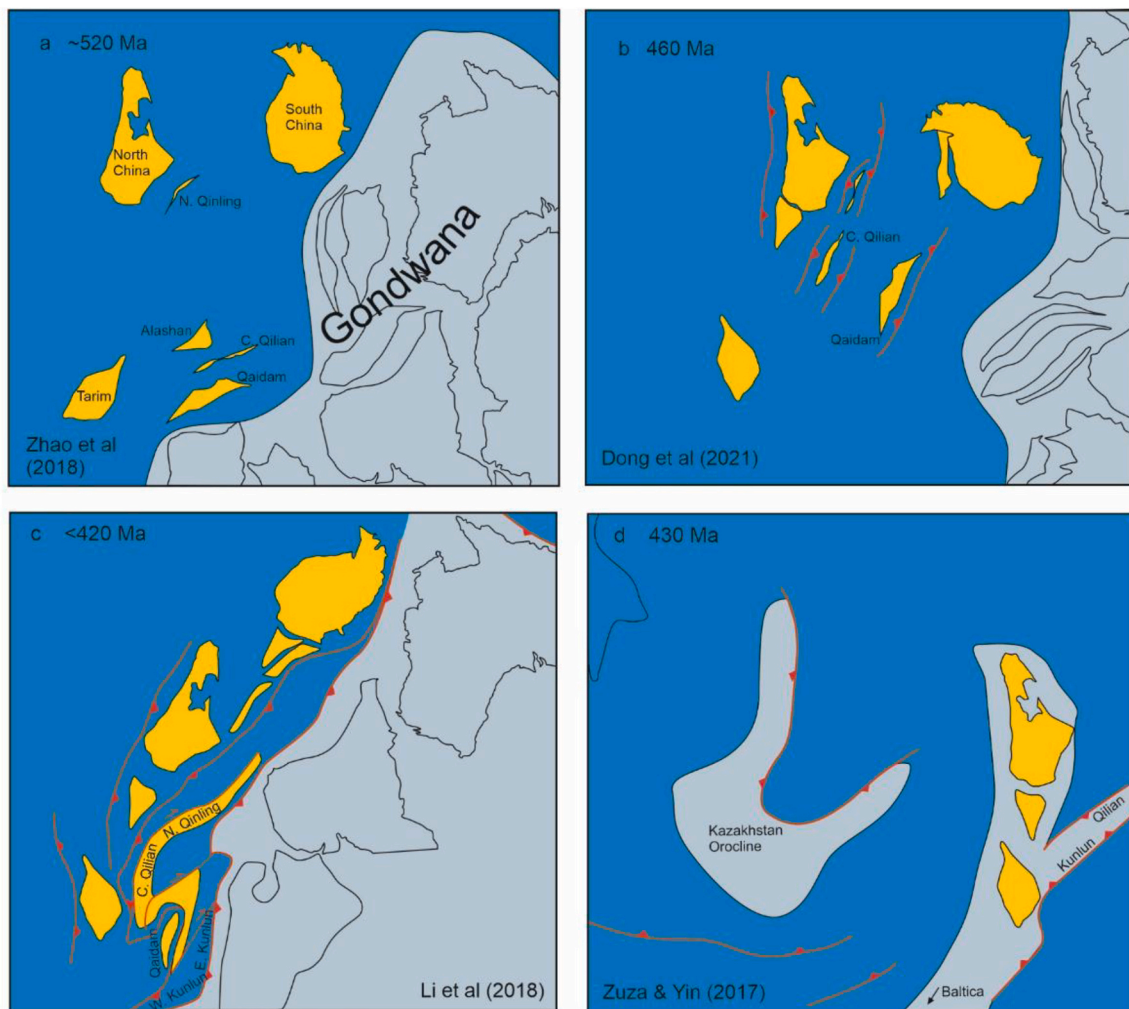


Fig. 14. Summary of separate subduction zones previously suggested for the CCOB, across a transect from the Alashan to the Eastern Kunlun. This compilation is intended to show the implausible configuration of all arcs, microcontinents and palaeo-oceans (represented by ophiolites) reported for the CCOB at roughly Late Ordovician times (ca. 450 Ma).



**Fig. 15.** Previous palaeogeographic reconstructions for the CCOB at different time intervals in the Palaeozoic. The sequence of figures is not a progression in time. (a) Mid Cambrian archipelago reconstruction, [Zhao et al. \(2018a\)](#). (b) Mid Ordovician archipelago reconstruction, [Dong et al. \(2021\)](#). (c) Double orocline model of [Li et al. \(2018a\)](#). (d) Balkatach model of [Zuza and Yin \(2017\)](#), with continental basement of the Kunlun and Qilian regions attached to the Tarim Block.

identified as occurring i) west of the Altun region, on the northwest side of the Altyn Tagh Fault, and ii) east of the eastern end of the Qaidam Basin. The issue with both loops is that they are speculative, rather than firmly established.

The proposed loop west of the Altun is in an unexposed area, covered by sediments of the Tarim Basin. The South Altun UHP belt has continental protoliths for its eclogites; the North Altun high-pressure belt has oceanic protoliths. These metamorphic grades and protoliths correlate with the NQUB and North Qilian Orogenic Belts offset to the east by the Altyn Tagh Fault ([Yang et al., 2001](#)). The loop proposed at the eastern end of the Qaidam Basin is also equivocal. It would link UHP belts at the north side of Qaidam and the eastern Kunlun, but whereas the former is a large terrane of Neoproterozoic continental protoliths (e.g., [Song et al., 2010, 2012; Zhang et al., 2010](#)), the latter region contains eclogites derived from oceanic crust ([Song et al., 2018](#)) associated with mica-schists that also contain UHP minerals ([Bi et al., 2018, 2020](#)). The East Kunlun eclogites are associated with numerous scattered Cambrian ophiolites ([Li et al., 2018c; Jia et al., 2018](#)). In summary, the ages of metamorphism are similar between the NQUB and the East Kunlun, but the host lithologies and degrees of metamorphism are not. Additionally, the Kunlun UHP rocks are found along at least two separate ophiolite belts within the Kunlun, the Qimantage-Xiangride Zone and the Aqikekule-Kunzhong Zone. Thirdly, structural vergence across easternmost Qaidam is predominantly to the south ([Chen et al., 2012b](#)),

consistent with regions further west along the north side of the Qaidam Basin, but also consistent with the north side of the eastern Kunlun ([Yin et al., 2008; Meng et al., 2015; Li et al., 2018c](#)). There is no reversal in structural vergence, as would be expected if a single subduction front had been folded round to face itself.

The final issue with this model with the model of [Li et al. \(2018a\)](#) is that the Shangdan Ocean (i.e., a branch of Palaeo-Tethys) is shown as opening roughly in Devonian times, and being in existence by < 380 Ma, but the Shangdan Suture Zone records the collision of the North Qilian and South Qilian Blocks and took place before 400 Ma ([Dong and Santosh, 2016](#)). A key question in understanding the evolution of Proto-Tethys is the implication for when, where and how did the Palaeo-Tethys Ocean open.

[Zuza and Yin \(2017\)](#) correlated cratonic blocks from Baltica to North China as a single continental strip in the Neoproterozoic ("Balkatach"). Proto-Tethys closure in this model is summarised as a single collision between a unified Qaidam-Kunlun continent (possibly linked laterally to south Tarim), and the south side of the North China Block ([Fig. 15d](#)). This collision closed a single Qilian Ocean, which pinched out to the west, within the interior of the region covered by deposits of the Tarim Basin (see also [Wu et al., 2017](#)). Given the evidence for multiple remnant oceanic tracts preserved within the Qilian Shan and Kunlun, this scenario must be at least a simplification. Nor does it explain the correlations between tectonic units in the Qilian Shan and counterparts in the

Qinling.

In summary, none of the existing tectonic models fully accounts for the evolution and destruction of the Proto-Tethys Ocean, because all have problems in explaining the distribution of Precambrian basement blocks and early Palaeozoic accretionary crust across the CCOB.

### 5.3. Proto-Tethys evolution

In this section we propose a new model to explain the evolution of Proto-Tethys Ocean and the creation of the CCOB. Any such model has to cover the following key points: the juxtaposition of multiple slivers of basement and accretionary crust; the timing of the oceanic lithosphere (ophiolites) and subduction-related magmatism within these belts; possible correlations along and across the strike of different regions; implications for the evolution of the Palaeo-Tethys Ocean.

We suggest that the segments of Precambrian basement now juxtaposed with each other along the south sides of the Tarim and North China blocks were originally part of a single continent, herein named KQQQ, or K-Qubed. This concept is an extension of the idea of a “KQQ” continent already in use (e.g., Jian et al., 2020), that links the western crustal units exposed in the Kunlun, Qaidam and Qilian regions. The

origin of K-Qubed is not completely clear, but the South China Block is the most likely candidate (Wan et al., 2001; Jian et al., 2020). This match is based partly on the correlation of basement ages between the Proto-Tethyan blocks and the South China Block. Nd model ages of Precambrian basement show similar ranges: e.g., ca. 2.3–1.9 Ga in the Central Qilian Block; 2.2–1.5 Ga in the South China Block (Tung et al., 2007). U-Pb age ranges for Precambrian basement in both the Qilian basement and South China Block are similarly broad through the Proterozoic, including intensive magmatism at  $\geq 900$  Ma, related to the assembly of the Rodinia supercontinent (e.g., Y. Li et al., 2018a; Jian et al., 2020). The Alashan may also have originated as part of the South China Block (Song et al., 2017a), in which case it could be added to the ribbon continent depicted in Fig. 16a.

K-Qubed appears to have developed as a distinct entity following a phase of Neoproterozoic rifting and Cambrian oceanic spreading, which separated it from the South China Block (Fig. 16a). Neoproterozoic–Cambrian rifting of the Precambrian basement preserved within the CCOB is indicated by: i) Late Neoproterozoic (800–700 Ma) bimodal magmatism and rift-related sedimentation in the Qinling (Meng and Zhang, 2000); ii) 600–580 Ma within-plate basic igneous rocks in the North Qilian Orogenic Belt (Xu et al., 2015); iii) Cambrian bimodal

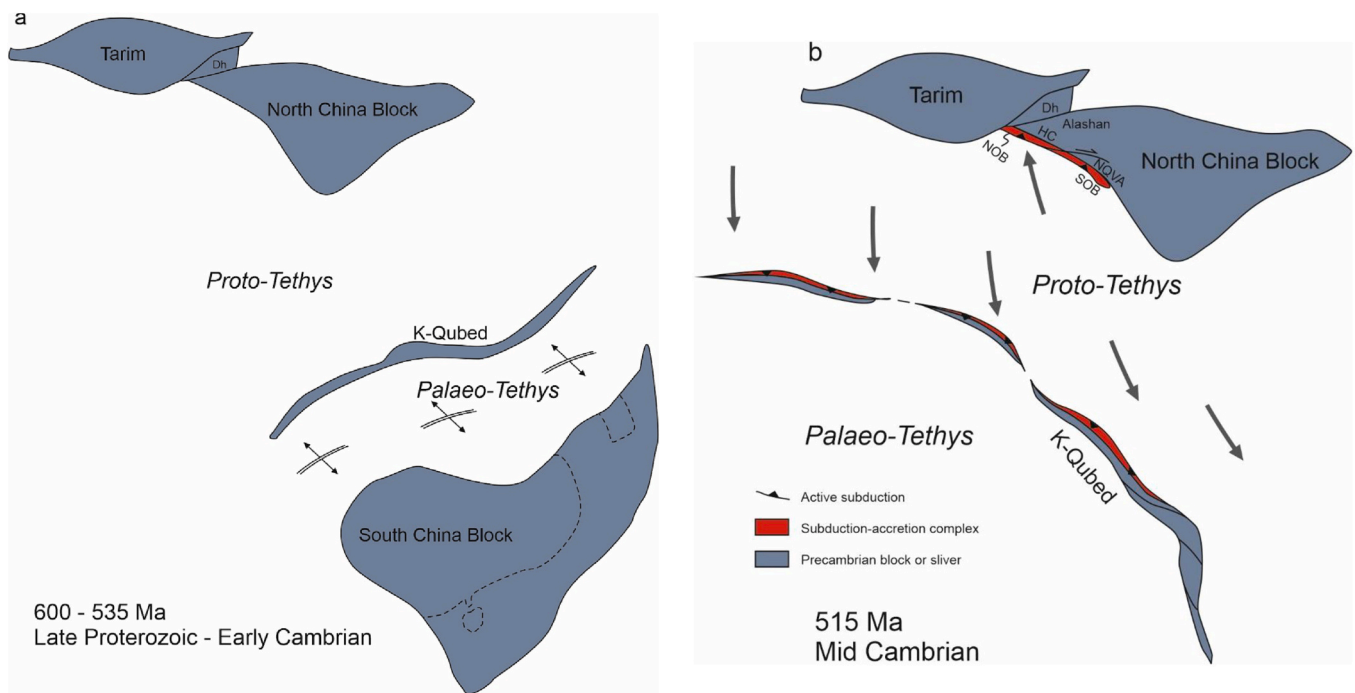


**Fig. 16.** Tectonic evolution of the CCOB as a series of plate scale reconstructions. (a) 600–530 Ma. Rifting and separation of a ribbon continent, K-Qubed, from the South China Block. Abbreviations are as follows. CEKT: Central East Kunlun Terrane. CQB: Central Qilian Block. Dh: Dunhuang. EU: Erlangping Unit. HC: Hexi Corridor. KC: Kuangping Complex. NKT: Northern Kunlun Terrane. NOB: Northern Ophiolite Belt. NQGB: North Qinling Belt. NQim: North Qimantage. NQUB-i: ca. 490 Ma UHP metamorphic rocks in the North Qaidam Ultra High-pressure Belt. NQUB-ii: ca. 440–420 Ma UHP metamorphic rocks in the North Qaidam Ultra High-pressure Belt. NQVA: North Qilian Volcanic Arc. OB: Oulongbuluke Block. SEKT: South East Kunlun Terrane. SKT: South Kunlun Terrane. SOB: Southern Ophiolite Belt. SQAB: South Qilian Accretionary Belt. SQGB: South Qinling Block. QB: Qaidam Block.

(b) 515 Ma. Southwards subduction of Proto-Tethys under the northern side of K-Qubed, and localised subduction northwards under the Hexi Corridor and the Alashan.

(c) 500–490 Ma. Initial collision of continental crust of K-Qubed with the south side of the North China Block, synchronous with strike-slip repetition of slivers of K-Qubed and adjacent subduction-accretion complexes, and a subduction flip to consume Palaeo-Tethys. Ophiolites younger than this age attest to continued oceanic crust (back-arc basins, bab) inboard of the outermost arc.

(d) 460 Ma. Oblique northwards subduction of Palaeo-Tethys under the accreted slivers of K-Qubed, with dextral shear.

(e) 440 Ma. Continued northwards subduction of Palaeo-Tethys and extensive development of arc magmatism over both Precambrian basement of K-Qubed and younger accretionary crust. Peak UHP metamorphism during docking of crust now exposed on either side of the Qaidam Block. Dextral shear continues along the CCOB. Change in geochemical signature of magmatism to “syn-collision” type, at least in the NQUB (Figs. 8 and 9). Peak CCOB magmatism occurs at approximately this time (Fig. 7).

(f) 400 Ma. Assembly of CCOB, with extensive surface uplift and molasse deposition. Magmatism in NQUB has similarities with >440 Ma “pre-collisional” examples.

(g) 300 Ma. Quietness: cessation of subduction or highly oblique subduction, and no arc magmatism.

(h) 250 Ma. Resumption of Palaeo-Tethys subduction leads to renewal of arc magmatism across southern CCOB, before eventual collision with Qiangtang and the South China Block in the Triassic.

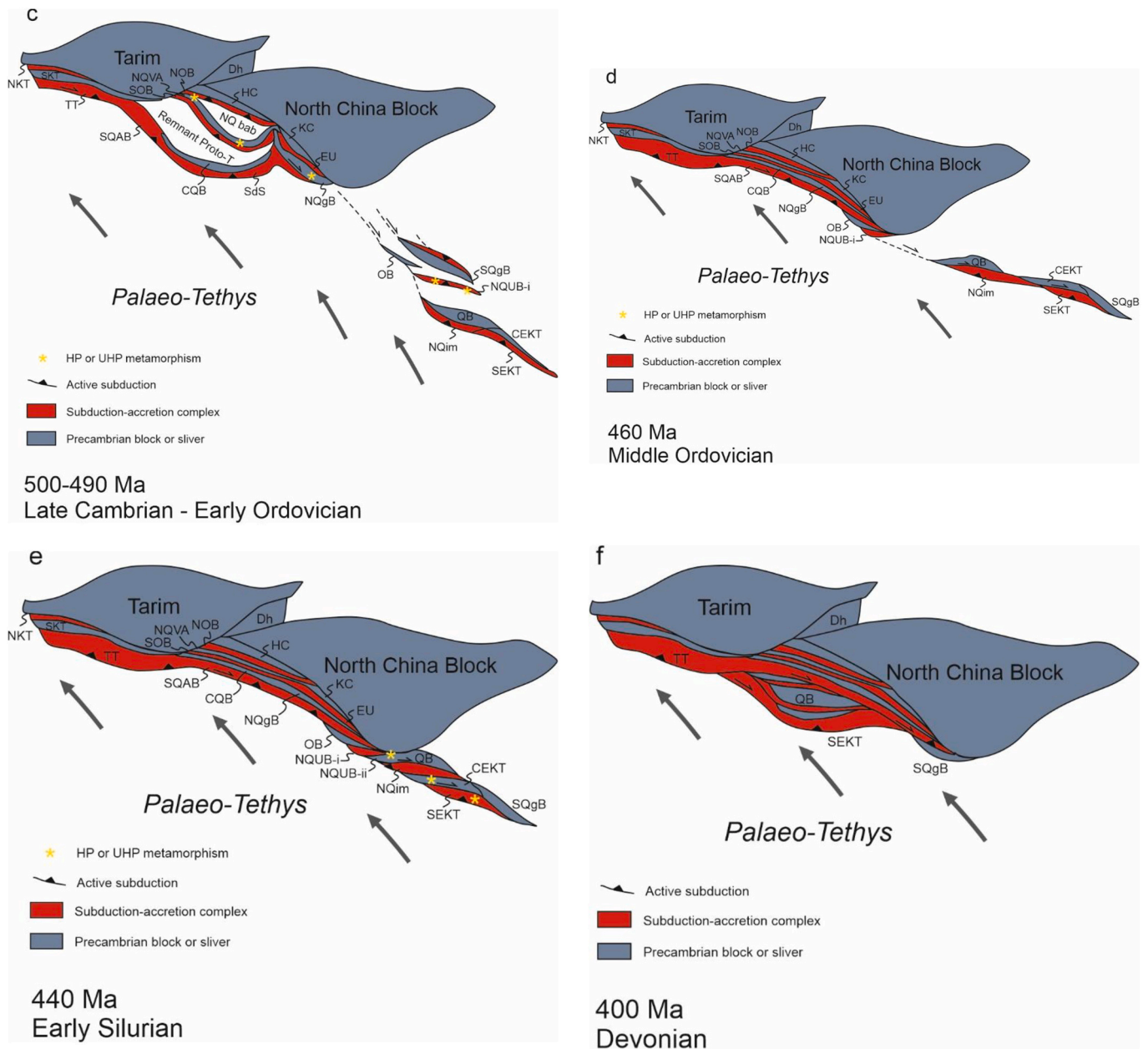


Fig. 16. (continued).

magmatism within the North Qilian Orogenic Belt (Du et al., 2007); iv) Middle Cambrian rift-related volcanic rocks in the Central Qilian (Li et al., 2018b); v) Neoproterozoic rift volcanic rocks and stratigraphy within the West and East Kunlun (Bian et al., 2001 and references therein); vi) Sinian to Cambrian syn-rift stratigraphy and generation of the rift-related Akaz volcanic rocks at the southwest of the Tarim Block (Mattern et al., 1996; Yuan et al., 2004), possibly related to wider rifting across Tarim in the Neoproterozoic (He et al., 2020).

The reconstructed position of the South China Block was in the vicinity of the North China Block in the latest Precambrian and early Palaeozoic, on the northern side of Gondwana. The exact positions of the two blocks are not clear, and Li et al. (2018a) summarised the numerous different scenarios that have been reconstructed. It is plausible that the North China Block was outboard of the main Gondwana continent by earliest Cambrian times (e.g., Zhao et al., 2018a; Fig. 15a), and aligned north-south with the adjacent Alashan and Tarim microcontinents (Fig. 16a) (Dong et al., 2021). The connection between the Tarim and North China blocks is also debated; it is not clear how close the two

continents were to each other through the Palaeozoic. Some reconstructions place them in contact by the Cambrian (e.g., Han et al., 2016), but others imply separation through most or all of the Palaeozoic (e.g., Xiao et al., 2018). The timing of the connection does not matter for first order reconstructions of the CCOB, as long as no additional intervening oceans are involved.

Oceanic spreading was underway by the latest Proterozoic and certainly by the Cambrian (Fig. 16a), given the numerous ophiolitic rocks of these ages distributed within the CCOB (e.g., Bian et al., 2001; Shi et al., 2004; Dong et al., 2007; Song et al., 2013; Song et al., 2019a, 2019b; Yang et al., 2018; Li et al., 2018c). The Middle Cambrian, rift-related volcanic rocks in the Central Qilian (Li et al., 2018b) may indicate either diachronous rifting and break-up, or a second and separate extension event. Oceanic subduction under K-Qubed had started by the Early Cambrian (535 Ma), given the rare examples of subduction-related plutons of this age: high-Mg diorites from the North Altun Belt (Ye et al., 2020) and ca. 530 Ma plutons from the West Kunlun Orogen (Yin et al., 2020). Identification of arc-like plutons as old as 550 Ma in the western

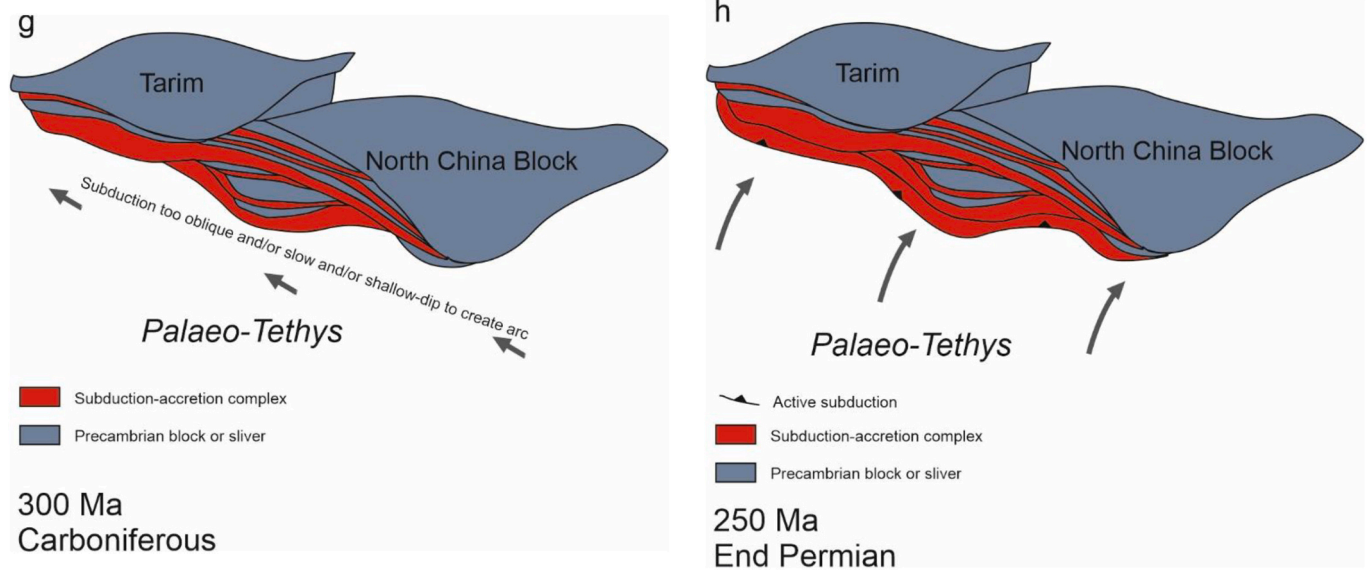


Fig. 16. (continued).

Kunlun (Tianshuihai Terrane) takes the record of subduction back into the Proterozoic (Sui et al., 2021). These early occurrences are in the west of the entire system, giving a hint that subduction began diachronously from west to east. Subduction was regionally underway by the Late Cambrian (ca. 490 Ma), and in full operation by the Early Ordovician (ca. 475 Ma), based on multiple occurrences of arc volcanic rocks and plutons of these ages distributed through the Kunlun, Qilian and Qilian (e.g., Xia et al., 2003; Gehrels et al., 2003a; Zhang et al., 2013b; Wu et al., 2016).

The broad overlaps and similarities in the timing of magmatism across the different belts indicate that one original continental terrane was originally rifted, and then the outboard margin of the continental strip was transformed into a subduction margin. This magmatism (Fig. 6) took place within both accretionary crust and adjacent Precambrian basement slices (Fig. 16b), which is consistent with the narrow width of the rifted K-Qubed continent.

In palaeogeographic terms, the ocean that lay between K-Qubed and the North China Block was Proto-Tethys; this ocean narrowed as K-Qubed approached the North China Block and was ultimately destroyed when K-Qubed collided with it in the Late Cambrian. In this part of the reconstruction, we follow several other models that deal with the creation of the CCOB (e.g., Li et al., 2018a). The ocean that opened behind K-Qubed and separated it from the South China Block was effectively part of Palaeo-Tethys, with the implication that this part of Palaeo-Tethys was older than most models allow for. It is hard to develop an alternative scheme: if the existence of two main oceanic plates on either side of the Precambrian continental crust in the CCOB is recognised, logically only one of these oceans can be termed Proto-Tethys. It follows that this was the ocean that disappeared first, between the North China Block and the K-Qubed continent.

#### 5.4. Palaeo-Tethys evolution

The other main oceanic plate involved in the CCOB, Palaeo-Tethys (e.g., Li et al., 2018a), lay between the K-Qubed continent and the Qiangtang and South China blocks. These continents collided with the south side of the CCOB in the Triassic, which is the age of southernmost sutures in the CCOB (A'nyemaqen and Mianlue). These collisions sealed the CCOB off from the effects of subduction: younger Tethyan continental margins developed further to the south. There is an issue that Palaeo-Tethys is typically understood to be younger: the oldest common ophiolites are Carboniferous in age. There are examples of Palaeo-

Tethyan crust with ages as old as the Cambrian (Zhai et al., 2016), but they are rare. This is an issue because much of the growth of the CCOB is understood to take place by subduction under individual components of K-Qubed (e.g., Xiao et al., 2005; Dong and Santosh, 2016; Yu et al., 2020). This configuration means early Palaeozoic consumption of Palaeo-Tethys northwards under the K-Qubed continent, distinct from the oceanic tract that originated on the other side of K-Qubed (Proto-Tethys).

As noted above, it is highly debated what was the subduction polarity under each arc segment, because of the juxtaposition of multiple strips of Precambrian basement and accretionary crust against each other (Fig. 6), and the degree of shortening and tectonic reactivation – including post-Palaeozoic events such as the India-Eurasia collision. The juxtaposition means that it is not generally possible to be certain which accretionary belt relates to which basement block (Fig. 3). The degree of shortening and reactivation means that many structural fabrics and fault zones dip steeply or sub-vertically, and dips fan across single deformation zones. Our model in Fig. 16 attempts to resolve the polarity issue in the following way. First, south-directed Cambrian subduction of Proto-Tethys under the northern side of K-Qubed produced the earliest arc magmatism recorded, at around 535–530 Ma (Yin et al., 2020). Initial southwards subduction is consistent with the lack of Cambrian magmatism along the margins of Tarim and the North China Block (Fig. 16b). Such southwards subduction would have enhanced the separation of the K-Qubed continent away from the greater South China Block by earliest Cambrian times, if not earlier (Fig. 16b). Subduction generated arc-related magmatism within both the pre-existing basement of K-Qubed and new, accretionary crust at its margins. Some crust does not carry a record of Cambrian and Early Ordovician arc magmatism, including the South Qinling Block and the Central Kunlun Terrane; these blocks are located at the eastern end of the ribbon continent, protected from the effects of the subduction (Fig. 16b).

As Proto-Tethys shrank, there was initial collision of K-Qubed and Tarim in the West Kunlun Orogen, by ca. 500 Ma, evidenced by the end of the northwards migration of magmatism at this time (Yin et al., 2020). Simultaneously, there was UHP metamorphism in the North Qinling Belt and high-pressure metamorphism in the North Qilian Orogenic Belt. The Qinling UHP metamorphism involved continental protoliths, and so indicates continental crust had entered a subduction zone before peak metamorphic conditions were reached, by ca. 495 Ma. This indicates collision of the North Qinling Belt with the North China Block, also by ca. 500 Ma. The high-pressure metamorphism in the North Qilian

Orogenic Belt and early phase of UHP metamorphism in the NQUB are very similar in age, at 495–490 Ma. Although these events in North Qilian and the NQUB involved oceanic rather than continental lithosphere, they also indicate a significant tectonic event at this time, and a reversal in the transport direction of oceanic lithosphere within the subduction zone(s), from normal subduction to extension and eventual exhumation. Many parts of the CCOB record a secondary peak in magmatism at ca. 500–490 Ma, followed by a relative lull (Fig. 7). Examples include the Shangdan Suture Zone, the North Qilian Volcanic Arc and the North Altyn (Fig. 7). This ca. 500 Ma magmatism is similar in age to more distant parts of Gondwana such as Nepal (Cawood et al., 2007).

We suggest that these collisions along the northern side of K-Qubed at ca. 500 Ma caused a flip in subduction polarity, and the development of northwards subduction under the outboard, southern, margin of K-Qubed (Fig. 16c). Subduction generated arc magmatism in both the Precambrian basement blocks (e.g., Central Qilian Block) and accretionary terranes (e.g., the SQAB). Peak magmatism in many of the CCOB regions occurred at ca. 450–430 Ma (Fig. 7). As oceanic lithosphere continued to be consumed under the K-Qubed continent there was simultaneous dextral shear along the ribbon continent, evidenced by syn-tectonic plutons at least as old as 460 Ma (e.g., Li et al., 2018e), and potentially as far back as 500 Ma (Zhang et al., 2013b). This dextral shear was driven by oblique subduction, using many modern arc systems such as Indonesia as analogues. The key feature of this model is that the slicing of arc segments along the Proto-Tethyan subduction zone docked strips of Precambrian basement and adjacent subduction-accretion complexes next to each other and ultimately against the backstop of the North China Block (Fig. 16c). It is plausible that small, short-lived oceanic basins were generated and quickly destroyed during the reshuffling of the ribbon continent. Fragments of these basins are preserved among the ophiolites of the CCOB, commonly with supra-subduction signatures that indicate their origin distinct from conventional ocean basins with MORB-type chemistry (e.g., Li et al., 2015b).

The continental slivers and their adjacent accretionary complexes terminated against the southern side of the North China Block and the southeast side of the Tarim Block (Fig. 16e), and did not reach further west. The West Kunlun Orogen contains fewer and less well-defined regions of Precambrian basement than the regions to the east of the Altyn Tagh Fault, and a more continuous development of accretionary crust across the strike of this region (Şengör and Okurogullari, 1991; Xiao et al., 2005). Oblique motion continued during collision of the continental slivers with each other and with the south side of the North China Block (Fig. 16e), such that exhumation of UHP rocks at ca. 430 Ma was also accompanied by dextral shear (Xu et al., 2006; Fu et al., 2015).

A distinctive feature of the East Kunlun region is how UHP eclogites with identical 440–420 Ma ages for peak metamorphism lie across the strike of the range (Song et al., 2018): Xiaruhamu lies along the Qimantage-Xiangride Zone (= North Kunlun Fault); Wenquan and Kehete are on the Aqikekule-Kunzhong Zone (= Central Kunlun Fault). These ages are identical to the second phase of UHP metamorphism in the NQUB (Song et al., 2019a, 2019b). It is highly unlikely that there were three separate events associated with three different subduction zones, at the same time. Such metamorphism happens continuously during subduction, both oceanic and continental, but if the metamorphosed rocks continue to enter the mantle they are destroyed and not returned to the surface (Agard et al., 2009). Continuous return flow of eclogites along a subduction channel would be expected to produce a range of ages. The narrow age ranges in the Qaidam and Kunlun examples suggest one event caused rocks that had experienced UHP metamorphism at ca. 440–420 Ma to be preserved, and exhumed by 410 Ma (Song et al., 2018). The most likely explanation for exhumation of continental crust is break-off of an attached oceanic slab (Magni et al., 2017), at which point the overall buoyancy of the continental crust causes exhumation, even allowing for the high density of deeper regions converted to eclogite. This is plausible for the NQUB, where the UHP rocks are largely continental in origin, but is an imperfect explanation

for the UHP rocks within the East Kunlun, which have more common oceanic protoliths (Song et al., 2018). However, if all UHP localities were part of a single convergent system at ca. 440 Ma, slab break-off of oceanic lithosphere down-dip of the continental crust of the NQUB would have caused exhumation of adjacent UHP oceanic crust in the same system, brought to the surface by the buoyancy of the adjacent continental crust.

Collision and UHP metamorphism during the Silurian were accompanied by the widespread development of deep-marine clastic (flysch) deposition in basins over and adjacent to the arc centres (e.g., over the northern part of the North Qilian Orogenic Belt and at the southern side of the South Qilian Accretionary Belt). Much of the strike-slip duplication of the continental and arc segments took place after ca. 425 Ma, to replicate the UHP rocks into the four units exposed north and south of the Qaidam Basin (Fig. 16f).

A feature of the K-Qubed model is that Silurian and Early Devonian magmatism in the southern parts of K-Qubed is partly attributable to subduction (i.e., arc magmatism) but also includes components related to the stacking and thickening of crust during accretion (Figs. 8 and 9), leading to higher Sr/Y ratios between 440 and 400 Ma, for example, compared with older and younger periods. Middle Devonian and younger magmatism is post-collisional in the sense that it post-dates these events and associated HP/UHP metamorphism from ca. 440–420 Ma, but also involves arc signatures, which we relate to oceanic subduction under the south side of K-Qubed in the Devonian (<400 Ma; Fig. 16f).

By Devonian times the Proto-Tethyan belts were sub-aerial, and we infer that the individual tectonic units had achieved a configuration close to their present pattern, allowing for >300 km of sinistral slip along the Cenozoic Altyn Tagh Fault. The overall structure of the CCOB resembles a dextral strike-slip duplex (Fig. 16f), which is consistent with kinematic interpretation of fault-bounded units becoming bundled against the southern side of the Tarim Block. There was deposition of terrestrial clastics (molasse) in numerous basins (Fig. 6): these sedimentary rocks lie unconformably over foliated and metamorphosed older rocks. Scattered mafic volcanic rocks, dykes and A-type granites may represent extension of the orogenic (commonly termed collapse) (Zhong et al., 2017; Dong et al., 2020; Xu et al., 2020; Li et al., 2020a, 2020b), but the basic melts could have originated through small-scale convection at the base of the lithosphere without regional extension (Kaislaniemi et al., 2014). Structural evidence, rather than inference, for Devonian extension has yet to be found (e.g., rift basins or metamorphic core complexes), but there are numerous metamorphic ages interpreted as evidence for retrogression and major exhumation at this time (e.g., Xia et al., 2012; Song et al., 2018). Similarities between Cambrian-Ordovician magmatism and Devonian magmatism in the NQUB (Figs. 8 and 9) are consistent with subduction under the region before and after the Silurian UHP metamorphism and collision at ca. 440–420 Ma (Fig. 16d–f), but there is the alternative that the <400 Ma magmatism was unrelated to active subduction, and entirely represents post-collisional melting of sources influenced by the earlier subduction (e.g., Wang et al., 2022a; Wang et al., 2022b).

There was a widespread hiatus in magmatism through the Carboniferous and part of the Permian, indicating a halt in subduction of through this time (e.g., Yuan et al., 2002; Zhang et al., 2009a, 2009b, 2009c). A resumption of northwards subduction of Palaeo-Tethys in the Permian, under the CCOB collage, created new magmatic belts in the Kunlun and Qinling (Fig. 7), which overprinted the early Palaeozoic deformation and magmatism. This was the arc related to the final closure of Palaeo-Tethys (Fig. 16g). Magmatism did not affect the Qilian Shan, north of the northern side of the Qaidam Block, because this region was too far from the active subduction zone. Subduction continued into the Triassic, and the increasing proximity of the North Qiangtang and South China blocks to the south side of the Kunlun and Qinling generated vast quantities of clastic sediment that accumulated in the Songpan-Ganzi accretionary prism. These sedimentary rocks filled

embayments between the colliding plates (e.g., in the West Qinling Belt), and so created the highly irregular margins to the Songpan-Ganzi Zone (Şengör, 1987). Sediment generation and accumulation was presumably helped by low global sea levels in the Triassic period. Collision with the Qiangtang and South China blocks completed the subduction and closure of Palaeo-Tethys, along the A'nyemaqen and Mianlue sutures.

The K-Qubed model satisfies the fundamental features of the Proto-Tethyan terranes (Fig. 13), namely: i) parallel belts of Precambrian basement with the same broad age ranges; ii) intervening early Palaeozoic subduction-accretion complexes with essentially the same magmatic and metamorphic age ranges (Fig. 6), distributed between the North Qilian Orogenic Belt and the East Kunlun; iii) widespread dextral shear within the various units and at their margins; iv) widespread similarity between belts of Silurian flysch sedimentary rocks (composed of turbidites in forearcs and underfilled foreland basins); v) Devonian molasse deposits (i.e. terrestrial clastics) and scattered post-collisional volcanic centres; vi) magmatic hiatus after ca. 370 Ma, until the resumption of Palaeo-Tethyan subduction at ca. 290 Ma (Fig. 16h).

The Mesozoic-Cenozoic geology of western North America provides a partial analogue for the subduction and eventual closure of Proto-Tethys. At the North American margin, oblique subduction of the Pacific and related oceanic plates has caused dextral transport of elongate terranes northwards towards Alaska, where the continental margin curves to the west (e.g., Coney et al., 1980; Clennett et al., 2020). The North American terranes are more discontinuous and variable than the Proto-Tethyan equivalents, although this difference may relate to different degrees of mapping and classification. A similar kinematic model has been proposed for the assembly of the basement of the Turan and Scythian platforms to the west, later in the Palaeozoic (Natal'in and Şengör, 2005). There are also similarities in style with the unifying model proposed for the Altaids (Central Asia Orogenic Belt) by Şengör and Natal'in (1996), which also involves the strike-slip repetition of elongate terranes.

### 5.5. Wider correlations

Proto-Tethyan subduction also took west of China, in regions now coalesced within central and southwest Asia and Europe (Fig. 4). Global-scale reconstructions show a southwards-dipping subduction zone under the northern margin of Gondwana (Meert, 2003), which led to back-arc spreading and the separation of continental slivers away from the main Gondwanan margin (Fig. 4; Linnemann et al., 2008; Moghadam et al., 2015; Nouri et al., 2021). This scenario is broadly consistent with the southwards subduction of Proto-Tethys under the K-Qubed continent, although on present data it seems like K-Qubed initially rifted from South China before subduction began under its northern margin (Fig. 16a).

The Avalonian ribbon continent (Linnemann et al., 2008) is roughly equivalent to K-Qubed, in being an elongate chain of continental slivers derived from a larger continent mass – the western part of Gondwana. The Rheic Ocean that opened to the south of Avalonia during back-arc spreading is likewise equivalent to Palaeo-Tethys as developed in central China. The exact connections between Avalonia and K-Qubed, and between the Rheic and Palaeo-Tethys Oceans, remain to be determined.

Convergence across the western side of Gondwana involved a component of margin-parallel dextral shear (e.g., Linnemann et al., 2008). We therefore speculate that oblique closure of Proto-Tethys took place for over 10,000 km length of subduction zone in the early Palaeozoic, along the entire northern margin of Gondwana.

There is increasing evidence for early Palaeozoic magmatism within Asian terranes to the south of the main Proto-Tethyan units, within crust that remained part of Gondwana until later in the Phanerozoic, such as the Lhasa Block and the Himalaya (e.g., Zhu et al., 2012b; Zhang et al., 2019e). This magmatism can be reconciled with our reconstructions for Proto-Tethys to the north, given that we derive the crust within K-Qubed

from South China, rather than the main part of Gondwana, but it marks an apparent difference between the east and west ends of Gondwana.

## 6. Conclusions

We have presented a new tectonic model for the evolution of the CCOB in the Palaeozoic, accounting for the creation and destruction of the oceanic systems known as Proto-Tethys and Palaeo-Tethys.

Our model proposes that the Precambrian basement of the Kunlun, Qilian and Qinling ranges originated the South China Block. Rifting took place in the Late Neoproterozoic and generated an oceanic basin, the Proto-Tethys Ocean, which continued to spread in the Cambrian (Fig. 16a). We suggest that there was an elongate ribbon continent involved: the Kunlun-Qaidam-Qilian-Qinling (K-Qubed) continent. Subduction of Proto-Tethys under K-Qubed began in the Early Cambrian, or slightly earlier, and was accompanied by the generation of plutons and volcanic rocks with a broad range of arc signatures. Arc magmatism affected both the pre-existing continental basement, and subduction-accretion complexes that built outboard of it (Fig. 16b). Subduction polarity was initially mainly southwards (present coordinates) (Fig. 16b), with localised northwards subduction in the north Qilian region. There was a flip in polarity to northwards subduction under K-Qubed, possibly after the initial collision of the northern side of the ribbon continent with the southern side of the Tarim and North China blocks (Fig. 16c), at ca. 490–480 Ma. This northwards subduction and southwards continental accretion represent destruction of a different oceanic plate to the Proto-Tethyan closure on the north side of K-Qubed; it was subduction of an ocean normally regarded as Palaeo-Tethys, but at an earlier time than in existing models for Palaeo-Tethys.

A key element of the model is that subduction of Proto-Tethys and Palaeo-Tethys was oblique, and created dextral shear within and at the margins of all the main tectonic units. Shearing was sub-parallel to block boundaries, and led to the stacking of basement units and accretionary crust in much their present configuration within the Kunlun, Qilian and Qinling ranges. By the Early Silurian, the slivers had collided with each other and the southern margin of the North China Block. Their north-western terminations were at the southern side of the Tarim Block. Collision was accompanied by UHP metamorphism, with ages of ca. 440–420 Ma in separate localities.

Devonian terrestrial sedimentation and basic magmatism marked the terminal stage of the orogeny. Tectonic extension is typically claimed from the within-plate chemistry of magmatic rocks, rather than documented from structural or stratigraphic evidence. Nevertheless, thermochronology data for significant exhumation at this time is consistent with extension.

A different style of tectonics is preserved in the West Kunlun Orogen, as the repetitions of continental basement did not reach this far west. In this region, subduction-accretion was more continuous against the southwest margin of the Tarim Block through the early Palaeozoic, without the interleaving of terranes of Precambrian basement and younger rocks. However, Proterozoic Nd model ages of early Palaeozoic granulites indicate the presence of ancient crust beneath the West Kunlun Orogen (Yuan et al., 2003).

Magmatism largely ceased for a long interval from 370–290 Ma (e.g., Zhang et al., 2009a, 2009b, 2009c; Fig. 7), which we attribute to a pause in subduction of Palaeo-Tethys, or highly oblique subduction under the newly-accreted continental margin at the south side of Eurasia. Resumption of subduction and arc magmatism led to the destruction of Palaeo-Tethys in the Triassic, and the accretion of the Qiangtang and South China blocks along the south side of the Central Asian Orogenic Belt. These collisions sandwiched the vast Songpan Ganzi Accretionary Complex within the embayment between the colliding plates, and sealed off the crust to the north from the influence of subduction and oceanic plate tectonics.

The hybrid style of orogeny preserved in the CCOB (Fig. 13) is a

consequence of two main factors: oblique subduction and collision (which created the ability to slice and replicate crust across the strike of the orogeny) and the existence of the ribbon continent, K-Qubed, which was narrow enough to be completely dissected and reassembled. It may be that the operation of both conditions is relatively rare in orogeny (Fig. 3), but there are similarities in the architecture of the CCOB and the assembly of both the Central Asia Orogenic Belt and the basement to the Turan and Scythian platforms.

Correlations with Proto-Tethys evolution in western Gondwana remain to be resolved, but there is a similarity between the dextral shear reported within the K-Qubed collage and the Avalonian crust at the other end of Proto-Tethys (Fig. 4), ~7000 km to the west (Linnemann et al., 2008). These examples of strike-slip displacement may be a fragmentary record of oblique subduction along the entire northern margin of Gondwana.

### Declaration of Competing Interest

The authors declare that they have no known competing financial interests or personal relationships that could have appeared to influence the work reported in this paper.

### Data availability

Published data are compiled in a supplementary file

### Acknowledgements

We thank Wenjiao Xiao and Peter Cawood for their helpful reviews, and editor Yildirim Dilek for his guidance. Fatemeh Nouri provided Fig. 4. This work was supported by the National Natural Science Foundation of China (grant 91955202). MBA acknowledges John Allen for his support: “Do not go gentle into that good night”.

### Appendix A. Supplementary data

Supplementary data to this article can be found online at <https://doi.org/10.1016/j.earscirev.2023.104385>.

### References

- Abdallsamed, M.I.M., Wu, Y.-B., Zhang, W., Zhou, G., Wang, H., Yang, S., 2017. Early Paleozoic high-Mg granodiorite from the Erlangping unit, North Qinling orogen, central China, Partial melting of metasomatic mantle during the initial back-arc opening. *Lithos* 288, 282–294.
- Agard, P., Yamato, P., Jolivet, L., Burov, E., 2009. Exhumation of oceanic blueschists and eclogites in subduction zones: timing and mechanisms. *Earth Sci. Rev.* 92, 53–79.
- Allen, M.B., Walters, R.J., Song, S.G., Saville, C., De Paola, N., Ford, J., Hu, Z.X., Sun, W. L., 2017. Partitioning of oblique convergence coupled to the fault locking behavior of fold-and-thrust belts, Evidence from the Qilian Shan, northeastern Tibetan Plateau. *Tectonics* 36, 1679–1698.
- Bader, T., Franz, L., Ratschbacher, L., de Capitani, C., Webb, A.A.G., Yang, Z., Pfaender, J.A., Hofmann, M., Linnemann, U., 2013. The Heart of China revisited, II Early Paleozoic (ultra)high-pressure and (ultra)high-temperature metamorphic Qinling orogenic collage. *Tectonics* 32, 922–947.
- Bi, H., Song, S., Dong, J., Yang, L., Qi, S., Allen, M.B., 2018. First discovery of coesite in eclogite from East Kunlun, northwest China. *Sci. Bull.* 63, 1536–1538.
- Bi, H., Song, S., Yang, L., Allen, M.B., Qi, S., Su, L., 2020. UHP metamorphism recorded by coesite-bearing metapelite in the East Kunlun Orogen (NW China). *Geol. Mag.* 157, 160–172.
- Bi, H., Song, S., Whitney, D.L., Wang, C., Su, L., 2021. HP-UHT granulites in the East Kunlun Orogen, NW China, Constraints on the transition from compression to extension in an arc setting of the Proto-Tethys Ocean. *J. Metamorph. Geol.* 39, 1071–1095.
- Bian, Q.T., Gao, S.L., Li, D.H., Ye, Z.G., Chang, C.F., Luo, X.Q., 2001. A study of the Kunlun-Qilian-Qinling suture system. *Acta Geol. Sin. Engl. Ed.* 75, 364–374.
- Bian, Q.T., Li, D.H., Pospelov, I., Yin, L.M., Li, H.S., Zhao, D.S., Chang, C.F., Luo, X.Q., Gao, S.L., Astrakhantsev, O., Chamov, N., 2004. Age, geochemistry and tectonic setting of Buqingshan ophiolites, North Qinghai-Tibet Plateau, China. *J. Asian Earth Sci.* 23, 577–596.
- Cai, H., Zhang, H., Xu, W., 2009. U-Pb zircon ages, geochemical and Sr-Nd-Hf isotopic compositions of granitoids in western Songpan-Garze fold belt: Petrogenesis and implication for tectonic evolution. *J. Earth Sci.* 20, 681–698.

- Cawood, P.A., Johnson, M.R.W., Nemchin, A.A., 2007. Early Palaeozoic orogenesis along the Indian margin of Gondwana: tectonic response to Gondwana assembly. *Earth Planet. Sci. Lett.* 255, 70–84.
- Cawood, P.A., Wang, W., Zhao, T., Xu, Y., Mulder, J.A., Pisarevsky, S.A., Zhang, L., Gan, C., He, H., Liu, H., Qi, L., 2020. Deconstructing South China and consequences for reconstructing Nuna and Rodinia. *Earth Sci. Rev.* 204, 103169.
- Cawood, P.A., Martin, E.L., Murphy, J.B., Pisarevsky, S.A., 2021. Gondwana's interlinked peripheral orogens. *Earth Planet. Sci. Lett.* 568, 117057.
- Chen, N.S., Sun, M., He, L., Zhang, K.X., Wang, G.C., 2002. Precise timing of the Early Paleozoic metamorphism and thrust deformation in the Eastern Kunlun Orogen. *Chin. Sci. Bull.* 47, 1130–1133.
- Chen, N., Sun, M., Wang, Q., Zhang, K., Wan, Y., Chen, H., 2008. U-Pb dating of zircon from the Central Zone of the East Kunlun Orogen and its implications for tectonic evolution. *Sci. China Ser. D Earth Sci.* 51, 929–938.
- Chen, N., Gong, S., Sun, M., Li, X., Xia, X., Wang, Q., Wu, F., Xu, P., 2009. Precambrian evolution of the Quanji Block, northeastern margin of Tibet, Insights from zircon U-Pb and Lu-Hf isotope compositions. *J. Asian Earth Sci.* 35, 367–376.
- Chen, Y., Xia, X., Song, S., 2012a. Petrogenesis of Aoyougou high-silica adakite in the North Qilian orogen, NW China, Evidence for decompression melting of oceanic slab. *Chin. Sci. Bull.* 57, 2289–2301.
- Chen, X., Gehrels, G., Yin, A., Li, L., Jiang, R., 2012b. Paleozoic and Mesozoic basement magmatism of eastern Qaidam Basin, Northern Qinghai-Tibet Plateau, LA-ICP-MS Zircon U-Pb geochronology and its geological significance. *Acta Geol. Sin. Engl. Ed.* 86, 350–369.
- Chen, Y., Song, S., Niu, Y., Wei, C., 2014. Melting of continental crust during subduction initiation, A case study from the Chaidanuo peraluminous granite in the North Qilian suture zone. *Geochim. Cosmochim. Acta* 132, 311–336.
- Chen, X., Gehrels, G., Yin, A., Zhou, Q., Huang, P., 2015. Geochemical and Nd-Sr-Pb-O isotopic constrains on Permo-Triassic magmatism in eastern Qaidam Basin, northern Qinghai-Tibetan plateau, Implications for the evolution of the Paleo-Tethys. *J. Asian Earth Sci.* 114, 674–692.
- Chen, Y.X., Cui, Y., Song, S.G., Fu, S.M., Zhang, L.P., Sun, W.D., Xiao, T.F., 2020a. Late Cambrian tonalite-trondhjemite association in the eastern segment of North Qilian suture zone, petrogenesis and geodynamic implications. *Int. Geol. Rev.* 64, 1431–1449.
- Chen, Y.X., Cui, Y., Song, S.G., Wu, K., Sun, W.D., Xiao, T.F., 2020b. Petrogenesis and tectonic implications of Cambrian Nb-enriched I- and aluminous A-type granites in the North Qilian suture zone. *Int. Geol. Rev.* 63, 1090–1109.
- Chen, J., Fu, L., Wei, J., Selby, D., Zhang, D., Zhou, H., Zhao, X., Liu, Y., 2020c. Proto-Tethys magmatic evolution along northern Gondwana, Insights from Late Silurian-Middle Devonian A-type magmatism, East Kunlun Orogen, Northern Tibetan Plateau, China. *Lithos* 356, 105034.
- Cheng, F., Jolivet, M., Hallot, E., Zhang, D., Zhang, C., Guo, Z., 2017. Tectono-magmatic rejuvenation of the Qaidam craton, northern Tibet. *Gondwana Res.* 49, 248–263.
- Clennett, E.J., Sigloch, K., Mihalyuk, M.G., Seton, M., Henderson, M.A., Hosseini, K., Mohammadzahari, A., Johnston, S.T., Mueller, R.D., 2020. A Quantitative Tomotectonic Plate Reconstruction of Western North America and the Eastern Pacific Basin. *Geochim. Geophys. Geosyst.* 21 <https://doi.org/10.1029/2020GC009117>.
- Coney, P.J., Jones, D.L., Monger, J.W.H., 1980. Cordilleran suspect terranes. *Nature* 288, 329–333.
- Cowgill, E., Yin, A., Harrison, T.M., Wang, X.F., 2003. Reconstruction of the Altyn Tagh fault based on U-Pb geochronology, Role of back thrusts, mantle sutures, and heterogeneous crustal strength in forming the Tibetan Plateau. *Journal of Geophysical Research-Solid Earth* 108. <https://doi.org/10.1029/2002JB002080>.
- Cui, M.H., Meng, F.C., Wu, X.K., 2011. Early Ordovician island arc of Qimantag Mountain, eastern Kunlun, Evidences from geochemistry. Sm-Nd isotope and geochronology of intermediate-basic igneous rocks. *Acta Petrol. Sin.* 27, 3365–3379.
- Dai, J., Wang, C., Hourigan, J., Santosh, M., 2013. Multi-stage tectono-magmatic events of the Eastern Kunlun Range, northern Tibet, Insights from U-Pb geochronology and (U-Th)/He thermochronology. *Tectonophysics* 599, 97–106.
- Dan, W., Li, X.-H., Wang, Q., Wang, X.-C., Liu, Y., 2014. Neoproterozoic S-type granites in the Alxa Block, westernmost North China and tectonic implications, in situ zircon U-Pb-Hf-O isotopic and geochemical constraints. *Am. J. Sci.* 314, 110–153.
- Dan, W., Li, X.-H., Wang, Q., Wang, X.-C., Wyman, D.A., Liu, Y., 2016. Phanerozoic amalgamation of the Alxa Block and North China Craton, Evidence from Paleozoic granitoids, U-Pb geochronology and Sr-Nd-Pb-Hf-O isotope geochemistry. *Gondwana Res.* 32, 105–121.
- Diwu, C., Sun, Y., Zhang, H., Wang, Q., Guo, A., Fan, L., 2012. Episodic tectonothermal events of the western North China Craton and North Qinling Orogenic Belt in central China, Constraints from detrital zircon U-Pb ages. *J. Asian Earth Sci.* 47, 107–122.
- Diwu, C., Sun, Y., Zhao, Y., Liu, B., Lai, S., 2014. Geochronological, geochemical, and Nd-Hf isotopic studies of the Qinling Complex, central China, Implications for the evolutionary history of the North Qinling Orogenic Belt. *Geosci. Front.* 5, 499–513.
- Dong, Y., Santosh, M., 2016. Tectonic architecture and multiple orogeny of the Qinling Orogenic Belt, Central China. *Gondwana Res.* 29, 1–40.
- Dong, Y., Zhang, G., Yang, Z., Zhao, X., Ma, H., Yao, A., 2007. Geochemistry of the E-MORB type ophiolite and related volcanic rocks from the Wushan area, West Qinling. *Sci. China. Ser. D Earth Sci.* 50, 234–245.
- Dong, Y.P., Zhang, G.W., Hauenberger, C., Neubauer, F., Yang, Z., Liu, X.M., 2011a. Paleozoic tectonics and evolutionary history of the Qinling orogen, Evidence from geochemistry and geochronology of ophiolite and related volcanic rocks. *Lithos* 122, 39–56.
- Dong, Y.P., Zhang, G.W., Neubauer, F., Liu, X.M., Genser, J., Hauenberger, C., 2011b. Tectonic evolution of the Qinling orogen, China, Review and synthesis. *J. Asian Earth Sci.* 41, 213–237.

- Dong, Y.P., Yang, Z., Liu, X., Zhang, X., He, D., Li, W., Zhang, F., Sun, S., Zhang, H., Zhang, G., 2014. Neoproterozoic amalgamation of the Northern Qinling terrain to the North China Craton: Constraints from geochronology and geochemistry of the Kuangping ophiolite. *Precambrian Res.* 255, 77–95.
- Dong, Y., Zhang, X., Liu, X., Li, W., Chen, Q., Zhang, G., Zhang, H., Yang, Z., Sun, S., Zhang, F., 2015. Propagation tectonics and multiple accretionary processes of the Qinling Orogen. *J. Asian Earth Sci.* 104, 84–98.
- Dong, Y., Sun, S., Yang, Z., Liu, X., Zhang, F., Li, W., Cheng, B., He, D., Zhang, G., 2017. Neoproterozoic subduction-accretionary tectonics of the South Qinling Belt, China. *Precambrian Res.* 293, 73–90.
- Dong, Y.P., He, D.F., Sun, S.S., Liu, X.M., Zhou, X.H., Zhang, F.F., Yang, Z., Cheng, B., Zhao, G.C., Li, J.H., 2018. Subduction and accretionary tectonics of the East Kunlun orogen, western segment of the Central China Orogenic System. *Earth Sci. Rev.* 186, 231–261.
- Dong, Y.P., Sun, S.S., Liu, X.M., He, D.F., Zhou, X.H., Zhang, F.F., Yang, Z., Zhou, D.W., 2019. Geochronology and geochemistry of the Yazidaban ophiolitic melange in Qimantagh, constraints on the Early Paleozoic backarc basin of the East Kunlun Orogen, northern Tibetan Plateau. *J. Geol. Soc.* 176, 306–322.
- Dong, J., Song, S., Su, L., Allen, M.B., Li, Y., Wang, C., 2020. Early Devonian mafic igneous rocks in the East Kunlun Orogen, NW China, Implications for the transition from the Proto- to Paleo-Tethys oceans. *Lithos* 376, 105771.
- Dong, Y.P., Sun, S.S., Santosh, M., Zhao, J., Sun, J.P., He, D.F., Shi, X.H., Hui, B., Cheng, C., Zhang, G.W., 2021. Central China Orogenic Belt and amalgamation of East Asian continents. *Gondwana Res.* 100, 131–194.
- Du, Y.S., Zhu, J., Han, X., Gu, S.Z., 2004. From the back-arc basin to foreland basin—Ordovician–Devonian sedimentary basin and tectonic evolution in the North Qilian orogenic belt. *Geol. Bull. China* 23, 911–917.
- Du, Y., Zhu, J., Gu, S., Xu, Y., Yang, J., 2007. Sedimentary geochemistry of the Cambrian–Ordovician cherts, Implication on archipelagic ocean of North Qilian orogenic belt. *Sci. China. Ser. D Earth Sci.* 50, 1628–1644.
- Du, W., Jiang, C., Xia, M., Xia, Z., Zhou, W., Ling, J., Wang, B., 2017. A newly discovered Early Paleozoic ophiolite in Dagele, Eastern Kunlun, China, and its geological significance. *Geol. J.* 52, 425–435.
- Feng, Q., Yang, Z., Li, X., Crasquin, S., 2009. Middle and Late Triassic radiolarians from northern Tibet, Implications for the Bayan Har Basin evolution. *Geobios* 42, 581–601.
- Feng, C.Y., Li, G.C., Li, D.X., Zhou, A.S., Li, H.M., 2013. Ore-controlling structure and (40)Ar–(39)Ar geochronology of Kekekaerde tungsten-tin deposit in Qimantage area, Xinjiang. *Mineral Deposits* 32, 207–216.
- Feng, D., Wang, C., Song, S., Xiong, L., Zhang, G., Allen, M.B., Dong, J., Wen, T., Su, L., 2023. Tracing tectonic processes from Proto- to Paleo-Tethys in the East Kunlun Orogen by detrital zircons. *Gondwana Res.* 115, 1–16.
- Fu, J., Liang, X., Zhou, Y., Wang, C., Jiang, Y., Zhong, Y., 2015. Geochemistry, zircon U–Pb geochronology and Hf isotopes of granitic rocks in the Xitieshan area, North Qaidam, Northwest China, Implications for Neoproterozoic geodynamic evolutions of North Qaidam. *Precambrian Res.* 264, 11–29.
- Fu, C., Yan, Z., Wang, Z., Buckman, S., Aitchison, J.C., Niu, M., Cao, B., Guo, X., Li, X., Li, Y., Li, J., 2018. Lajishankou Ophiolite Complex, Implications for Paleozoic Multiple Accretionary and Collisional Events in the South Qilian Belt. *Tectonics* 37, 1321–1346.
- Fu, D., Kusky, T., Wilde, S.A., Polat, A., Huang, B., Zhou, Z., 2019. Early Paleozoic collision-related magmatism in the eastern North Qilian orogen, northern Tibet, A linkage between accretionary and collisional orogenesis. *Geol. Soc. Am. Bull.* 131, 1031–1056.
- Fu, C., Yan, Z., Aitchison, J.C., Xiao, W., Buckman, S., Wang, B., Li, W., Li, Y., Ren, H., 2020a. Multiple subduction processes of the Proto-Tethyan Ocean, Implication from Cambrian intrusions along the North Qilian suture zone. *Gondwana Res.* 87, 207–223.
- Fu, D., Kusky, T.M., Wilde, S.A., Windley, B.F., Polat, A., Huang, B., Zhou, Z., 2020b. Structural anatomy of the early Paleozoic Laohushan ophiolite and subduction complex: Implications for accretionary tectonics of the Proto-Tethyan North Qilian orogenic belt, northeastern Tibet. *GSA Bull.* 132, 2175–2201.
- Fu, D., Huang, B., Johnson, T.E., Wilde, S.A., Jourdan, F., Polat, A., Windley, B.F., Hu, Z., Kusky, T., 2022. Boninitic blueschists record subduction initiation and subsequent accretion of an arc–forearc in the northeast Proto-Tethys Ocean. *Geology* 50, 10–15.
- Gan, B., Li, Z., Song, Z., Li, J., 2020. Middle Cambrian granites in the Dunhuang Block (NW China) mark the early subduction of the southernmost Paleo-Asian Ocean. *Lithos* 372, 105654.
- Gao, Y., Li, W., Li, Z., Wang, J., Hattori, K., Zhang, Z., Geng, J., 2014. Geology, geochemistry and genesis of tungsten-tin deposits in the Baiganhu district, northern Kunlun Belt, northwestern China. *Econ. Geol.* 109, 1787–1799.
- Gehrels, G.E., Yin, A., Wang, X.F., 2003a. Detrital-zircon geochronology of the northeastern Tibetan plateau. *Geol. Soc. Am. Bull.* 115, 881–896.
- Gehrels, G.E., Yin, A., Wang, X.F., 2003b. Magmatic history of the northeastern Tibetan Plateau. *J. Geophys. Res. Solid Earth* 108. <https://doi.org/10.1029/2002jb001876>.
- Gong, S., Chen, N., Wang, Q., Kusky, T.M., Wang, L., Zhang, L., Ba, J., Liao, F., 2012. Early Paleoproterozoic magmatism in the Quanji Massif, northeastern margin of the Qinghai-Tibet Plateau and its tectonic significance, LA-ICPMS U–Pb zircon geochronology and geochemistry. *Gondwana Res.* 21, 152–166.
- Gong, J., Zhang, J., Wang, Z., Yu, S., Li, H., Li, Y., 2016. Origin of the Alxa Block, western China: New evidence from zircon U–Pb geochronology and Hf isotopes of the Longshoushan Complex. *Gondwana Res.* 36, 359–375.
- Guo, Z.J., Yin, A., Robinson, A., Jia, C.Z., 2005. Geochronology and geochemistry of deep-drill-core samples from the basement of the central Tarim basin. *J. Asian Earth Sci.* 25, 45–56.
- Guo, C.L., Chen, D.L., Fan, W., Qiang, A.G., 2010. Geochemical and zircon U–Pb chronological studies of the Manziyong granite in Erlangping area, western Henan Province. *Acta Petrol. Mineral.* 29, 15–22.
- Guo, T., Liu, R., Chen, F., Bai, X., Li, H., 2011. LA-MC-ICPMS zircon U–Pb dating of Wulanwuzhuer porphyritic syenite granite in the North Qimantagh belt mountain of Qinghai and its geological significance. *Geol. Bull. China* 30, 1203–1211.
- Hall, R., 2017. Southeast Asia: New views of the geology of the Malay Archipelago. *Annu. Rev. Earth Planet. Sci.* 45, 331–358.
- Han, Y., Zhao, G., Cawood, P.A., Sun, M., Eizenhöfer, P.R., Hou, W., Zhang, X., Liu, Q., 2016. Tarim and North China cratons linked to northern Gondwana through switching accretionary tectonics and collisional orogenesis. *Geology* 44, 95–98.
- He, F., Song, S., 2020. The Grenvillian-aged UHT granulite in Jinshuikou region, East Kunlun Orogenic Belt. *Acta Petrol. Sin.* 36, 1030–1040.
- He, D., Dong, Y., Liu, X., Yang, Z., Sun, S., Cheng, B., Li, W., 2016a. Tectono-thermal events in East Kunlun, Northern Tibetan Plateau, Evidence from zircon U–Pb geochronology. *Gondwana Res.* 30, 179–190.
- He, D., Dong, Y., Zhang, F., Yang, Z., Sun, S., Cheng, B., Zhou, B., Liu, X., 2016b. The 1.0 Ga S-type granite in the East Kunlun Orogen, Northern Tibetan Plateau, Implications for the Meso- to Neoproterozoic tectonic evolution. *J. Asian Earth Sci.* 130, 46–59.
- He, D., Dong, Y., Liu, X., Zhou, X., Zhang, F., Sun, S., 2018. Zircon U–Pb geochronology and Hf isotope of granitoids in East Kunlun: implications for the Neoproterozoic magmatism of Qaidam Block, Northern Tibetan Plateau. *Precambrian Res.* 314, 377–393.
- He, B., Jiao, C., Liu, R., Huang, T., Cai, Z., Cao, Z., Yun, X., Mingjie, L., Jiang, Z., Zhu, D., Yang, Y., Cui, J., Hao, G., 2020. Formation of the Neoproterozoic Rifting Depression Groups of the Tarim Basin and its Hydrocarbon Potential, Responded to the Initial Opening of the Proto-Tethy Ocean. *Acta Geol. Sin. Engl. Ed.* 94, 16.
- Hou, Q., Mou, C., Wang, Q., Tan, Z., 2018. Provenance and tectonic setting of the early and middle Devonian Xueshan formation, the north Qilian Belt, China. *Geol. J.* 53, 1404–1422.
- Hu, J., Wang, H., Huang, C., Tong, L., Mu, S., Qiu, Z., 2016a. Geological characteristics and age of the Dahongliutan Fe-ore deposit in the Western Kunlun orogenic belt, Xinjiang, northwestern China. *J. Asian Earth Sci.* 116, 1–25.
- Hu, F., Liu, S., Santosh, M., Deng, Z., Wang, W., Zhang, W., Yan, M., 2016b. Chronology and tectonic implications of Neoproterozoic blocks in the South Qinling Orogenic Belt, Central China. *Gondwana Res.* 30, 24–47.
- Hu, P., Wu, Y., Zhang, W., He, Y., 2019. Timing of the Erlangping back-arc basin in the Qinling orogen, central China and its tectonic significance. *Terra Nova* 31, 458–464.
- Hu, R.G., Wijbrans, J.R., Brouwer, F.M., Bai, X.J., Qiu, H.N., 2020. Constraints on retrograde metamorphism of UHP eclogites in North Qinling, Central China, from <sup>40</sup>Ar/<sup>39</sup>Ar dating of amphibole and phengite. *Gondwana Res.* 87, 83–106.
- Huang, Z.B., Zheng, J.P., Li, B.H., Wei, Z.J., Qi, W., Xu, Y.L., 2014. The discovery of Late Cambrian adakite in the western Central Qilian Mountain and its geological implications. *Acta Petrol. Mineral.* 33, 1008–1018.
- Huang, Z.B., Zheng, J.P., Li, B.H., Wei, Z.J., Qi, W., Chen, X., 2015. Geochronology and geochemistry of Yemashan batholiths in western Central Qilian and its tectonic implications. *Geol. China* 42, 406–420.
- Ji, W., Li, R., Chen, S., He, S., Zhao, Z., Ban, X., Zhu, H., Cui, J., Ren, J., 2011. The discovery of Palaeoproterozoic volcanic rocks in the Bulunkuoer Group from the Tianshuihai Massif in Xinjiang of Northwest China and its geological significance. *Sci. China Earth Sci.* 54, 61–72.
- Jia, R.Y., Jiang, Y.H., Liu, Z., Zhao, P., Zhou, Q., 2013. Petrogenesis and tectonic implications of early Silurian high-K calc-alkaline granites and their potassic microgranular enclaves, western Kunlun orogen, NW Tibetan Plateau. *Int. Geol. Rev.* 55, 958–975.
- Jia, L., Meng, F., Feng, H., 2018. The Wenquan ultramafic rocks in the Central East Kunlun Fault zone, Qinghai-Tibet Plateau—crustal relics of the Paleo-Tethys ocean. *Mineral. Petrol.* 112, 317–339.
- Jian, X., Weislogel, A., Pullen, A., Shang, F., 2020. Formation and evolution of the Eastern Kunlun Range, northern Tibet, Evidence from detrital zircon U–Pb geochronology and Hf isotopes. *Gondwana Res.* 83, 63–79.
- Jiang, Y.H., Jia, R.Y., Liu, Z., Liao, S.Y., Zhao, P., Zhou, Q., 2013. Origin of Middle Triassic high-K calc-alkaline granitoids and their potassic microgranular enclaves from the western Kunlun orogen, northwest China: A record of the closure of Paleo-Tethys. *Lithos* 156, 13–30.
- Kaislaniemi, L., van Hunen, J., Allen, M.B., Neill, I., 2014. Sublithospheric small-scale convection—A mechanism for collision zone magmatism. *Geology* 42, 291–294.
- Kang, Y.Z., Kang, Z.H., 1996. Tectonic evolution and oil and gas of Tarim basin. *J. SE Asian Earth Sci.* 13, 317–325.
- Kusky, T.M., Polat, A., Windley, B.F., Burke, K.C., Dewey, J.F., Kidd, W.S.F., Maruyama, S., Wang, J.P., Deng, H., Wang, Z.S., Wang, C., Fu, D., Li, X.W., Peng, H. T., 2016. Insights into the tectonic evolution of the North China Craton through comparative tectonic analysis, A record of outward growth of Precambrian continents. *Earth Sci. Rev.* 162, 387–432.
- Lai, S.C., Zhang, G.W., Dong, Y.P., Pei, X.Z., Chen, L., 2004. Geochemistry and regional distribution of ophiolites and associated volcanics in Mianlue suture, Qinling-Dabie Mountains. *Sci. China. Ser. D Earth Sci.* 47, 289–299.
- Li, W., Li, S., Guo, A., Sun, Y., Zhang, G., 2007a. Zircon SHRIMP U–Pb ages and trace element geochemistry of the Kuhai gabbro and the Dur'ngoi diorite in the southern east Kunlun tectonic belt, Qinghai, Western China and their geological implications. *Sci. China. Ser. D Earth Sci.* 50, 331–338.
- Li, S., Kusky, T.M., Wang, L., Zhang, G., Lai, S., Liu, X., Dong, S., Zhao, G., 2007b. Collision leading to multiple-stage large-scale extrusion in the Qinling orogen, Insights from the Mianlue suture. *Gondwana Res.* 12, 121–143.

- Li, R.B., Pei, X.Z., Li, Z.C., Sun, Y., Feng, J.Y., Pei, L., Chen, G.C., Liu, C.J., Chen, Y.X., 2013a. Geochemical features, age, and tectonic significance of the Kekekete mafic-ultramafic rocks, East Kunlun Orogen, China. *Acta Geol. Sin.* 87, 1319–1333.
- Li, W., Neubauer, F., Liu, Y., Genser, J., Ren, S., Han, G., Liang, C., 2013b. Paleozoic evolution of the Qimantagh magmatic arcs, Eastern Kunlun Mountains, Constraints from zircon dating of granitoids and modern river sands. *J. Asian Earth Sci.* 77, 183–202.
- Li, L., Meng, Q., Pullen, A., Garzzone, C.N., Wu, G., Wang, Y., Ma, S., Duan, L., 2014a. Late Permian-early Middle Triassic back-arc basin development in West Qinling, China. *J. Asian Earth Sci.* 87, 116–129.
- Li, X.B., Pei, X.Z., Liu, C.J., Chen, Y.X., Li, R.B., Li, Z.C., Chen, G.C., Wei, G.F., 2014b. Ductile shearing in the eastern segment of Central Kunlun tectonic belt and its geological significance. *Geol. China* 41, 419–436.
- Li, X.C., Niu, M.L., Yan, Z., Da, L.C., Han, Y., Wang, Y.S., 2015a. LP/HT metamorphic rocks in Wulan County, Qinghai Province, An Early Paleozoic paired metamorphic belt on the northern Qaidam Basin. *Chin. Sci. Bull.* 60, 3501–3513.
- Li, Y., Yang, J., Dilek, Y., Zhang, J., Pei, X., Chen, S., Xu, X., Li, J., 2015b. Crustal architecture of the Shangdan suture zone in the early Paleozoic Qinling orogenic belt, China, Record of subduction initiation and backarc basin development. *Gondwana Res.* 27, 733–744.
- Li, Z., Pei, X., Li, R., Pei, L., Liu, C., Chen, Y., Zhang, Y., Wang, M., Xu, T., 2017. Early Ordovician island-arc-type Manite granodiorite pluton from the Buqingshan Tectonic Mélange Belt in the southern margin of the East Kunlun Orogen: constraints on subduction of the Proto-Tethyan Ocean. *Geol. J.* 52, 510–528.
- Li, S., Zhao, S., Liu, X., Cao, H., Yu, S., Li, X., Somerville, I., Yu, S., Suo, Y., 2018a. Closure of the Proto-Tethys Ocean and Early Paleozoic amalgamation of microcontinental blocks in East Asia. *Earth Sci. Rev.* 186, 37–75.
- Li, Y., Tong, X., Zhu, Y., Lin, J., Zheng, J., Brouwer, F.M., 2018b. Tectonic affinity and evolution of the Precambrian Qilian block, Insights from petrology, geochemistry and geochronology of the Hualong Group in the Qilian Orogen, NW China. *Precambrian Res.* 315, 179–200.
- Li, R., Pei, X., Li, Z., Pei, L., Chen, G., Wei, B., Chen, Y., Liu, C., Wang, M., 2018c. Cambrian (similar to 510 Ma) ophiolites of the East Kunlun orogen, China, A case study from the Acite ophiolitic tectonic melange. *Int. Geol. Rev.* 60, 2063–2083.
- Li, R., Pei, X., Pei, L., Li, Z., Chen, G., Chen, Y., Liu, C., Wang, M., 2018d. The Early Triassic Andean-type Halagatu granitoids pluton in the East Kunlun orogen, northern Tibet Plateau, Response to the northward subduction of the Paleo-Tethys Ocean. *Gondwana Res.* 62, 212–226.
- Li, Y., Liang, W., Zhang, G., Ran, Y., Shen, Q., Wang, J., Jin, C., 2018e. Granitoid emplacement during syn-convergent transtension, an example from the Huamenlou pluton in North Qinling, central China. *Geosci. Front.* 9, 191–205.
- Li, H., Sun, F., Li, L., Yan, J., 2019a. The Hudeshe mafic-ultramafic intrusions in the Oulongbuluke Block, Qinghai Province, NW China, chronology, geochemistry, isotopic systematics and tectonic implications. *Geol. Mag.* 156, 1527–1546.
- Li, Y., Xiao, W., Tian, Z., 2019b. Early Paleozoic accretionary tectonics of West Kunlun Orogen, Insights from Datong granitoids, mafic-ultramafic complexes, and Silurian-Devonian sandstones, Xinjiang, NW China. *Geol. J.* 54, 1505–1517.
- Li, J., Qian, Y., Li, H., Sun, J., Yang, X., Chen, B., Fan, X., Sun, F., 2020a. The Late Ordovician granitoids in the East Kunlun Orogenic Belt, Northwestern China, petrogenesis and constraints for tectonic evolution of the Proto-Tethys Ocean. *Int. J. Earth Sci.* 109, 1439–1461.
- Li, R., Pei, X., Li, Z., Patias, D., Su, Z., Pei, L., Chen, G., Chen, Y., Liu, C., 2020b. Late Silurian to Early Devonian volcanics in the East Kunlun orogen, northern Tibetan Plateau, Record of postcollisional magmatism related to the evolution of the Proto-Tethys Ocean. *J. Geodyn.* 140, 101780.
- Li, R., Pei, X., Wei, B., Li, Z., Pei, L., Chen, G., Chen, Y., Liu, C., 2021a. Middle Cambrian-Early Ordovician ophiolites in the central fault of the East Kunlun Orogen: Implications for an epicontinental setting related to Proto-Tethyan Ocean subduction. *Gondwana Res.* 94, 243–258.
- Li, B., Zuzza, A.V., Chen, X., Wang, Z.Z., Shao, Z., Levy, D.A., Wu, C., Xu, S., Sun, Y., 2021b. Pre-Cenozoic evolution of the northern Qilian Orogen from zircon geochronology: framework for early growth of the northern Tibetan Plateau. *Palaeogeogr. Palaeoclimatol. Palaeoecol.* 562, 110091.
- Li, X.Y., Li, S., Yu, S., Liu, Y., Guo, X.Y., Huang, Z.B., Zhao, S., Cao, H., 2022a. Cambrian-Silurian sediments in the southeastern Qilian Orogen, NE Tibetan Plateau: Constraints on crustal and tectonic evolution of microcontinents in the northern Proto-Tethys Ocean. *J. Asian Earth Sci.* 232, 105122.
- Li, Y., Xiao, W., Zheng, J., Brouwer, F.M., 2022b. Northward subduction of the South Qilian ocean: Insights from early Paleozoic magmatism in the South-Central Qilian belts. *Geosyst. Geoenviron.* 1, 100013.
- Liang, X., Sun, S., Dong, Y., Yang, Z., Liu, X., He, D., 2017. Fabrics and geochronology of the Wushan ductile shear zone, Tectonic implications for the Shangdan suture zone in the Qinling orogen, Central China. *J. Asian Earth Sci.* 139, 71–82.
- Lin, Y., Zhang, L., Ji, J., Wang, Q., Song, S., 2010. Ar-40/Ar-39 isochron ages of lawsonite blueschists from Jiuquan in the northern Qilian Mountain, NW China, and their tectonic implications. *Chin. Sci. Bull.* 55, 2021–2027.
- Linnemann, U., Pereira, F., Jeffries, T.E., Drost, K., Gerdes, A., 2008. The Cadomian Orogeny and the opening of the Rheic Ocean, The diachrony of geotectonic processes constrained by LA-ICP-MS U-Pb zircon dating (Ossa-Morena and Saxo-Thuringian Zones, Iberian and Bohemian Massifs). *Tectonophysics* 461, 21–43.
- Liu, Y.J., Neubauer, F., Genser, J., Takasu, A., Ge, X.H., Handler, R., 2006a. Ar-40/Ar-39 ages of blueschist facies pelitic schists from Qingshuigou in the Northern Qilian Mountains, western China. *Island Arc* 15, 187–198.
- Liu, R., Fang, Q.X., Ma, Y.Z., 2006b. Formation time, petrology, geochemistry and tectonic setting of peraluminous granites in the Yunwurdige area, Xinjiang. *Xinjiang Geol.* 24, 223–228.
- Liu, L., Zhang, J., Green II, H.W., Jin, Z., Bozhilov, K.N., 2007. Evidence of former stishovite in metamorphosed sediments, implying subduction to > 350 km. *Earth Planet. Sci. Lett.* 263, 180–191.
- Liu, L., Wang, C., Chen, D., Zhang, A., Liou, J.G., 2009. Petrology and geochronology of HP-UHP rocks from the South Altyn Tagh, northwestern China. *J. Asian Earth Sci.* 35, 232–244.
- Liu, Z., Jiang, Y.H., Jia, R.Y., Zhao, P., Zhou, Q., Wang, G.-C., Ni, C.-Y., 2014. Origin of Middle Cambrian and Late Silurian potassic granitoids from the western Kunlun orogen, northwest China, a magmatic response to the Proto-Tethys evolution. *Mineral. Petrol.* 108, 91–110.
- Liu, S., Qian, T., Li, W., Dou, G., Wu, P., 2015. Oblique closure of the northeastern Paleo-Tethys in central China. *Tectonics* 34, 413–434.
- Liu, L., Liao, X., Wang, Y., Wang, C., Santosh, M., Yang, M., Zhang, C., Chen, D., 2016. Early Paleozoic tectonic evolution of the North Qinling Orogenic Belt in Central China, Insights on continental deep subduction and multiphase exhumation. *Earth Sci. Rev.* 159, 58–81.
- Liu, Q., Zhao, G., Sun, M., Han, Y., Eizenhofer, P.R., Hou, W., Zhang, X., Zhu, Y., Wang, B., Liu, D., Xu, B., 2017a. Early Paleozoic subduction processes of the Paleo-Asian Ocean, Insights from geochronology and geochemistry of Paleozoic plutons in the Alxa Terrane. *Lithosphere* 9, 665–680.
- Liu, Q., Zhao, G., Sun, M., Han, Y., Eizenhofer, P.R., Hou, W., Zhang, X., Zhu, Y., Wang, B., Liu, D., Xu, B., 2017b. Timing of the final closure of the Paleo-Asian Ocean in the Alxa Terrane: constraints from geochronology and geochemistry of Late Carboniferous to Permian gabbros and diorites. *Lithos* 275–275, 19–30.
- Liu, Q., Zhao, G., Han, Y., Li, X., Zhu, Y., Eizenhofer, P.R., Zhang, X., Wang, B., Tsui, R. W., 2018a. Geochronology and Geochemistry of Paleozoic to Mesozoic Granitoids in Western Inner Mongolia, China, Implications for the Tectonic Evolution of the Southern Central Asian Orogenic Belt. *J. Geol.* 126, 451–471.
- Liu, C., Wu, C., Zhou, Z., Yan, Z., Jiang, T., Song, Z., Liu, W., Yang, X., Zhang, H., 2018b. U-Pb detrital zircon geochronology from the basement of the Central Qilian Terrane, implications for tectonic evolution of northeastern Tibetan Plateau. *Int. J. Earth Sci.* 107, 673–686.
- Liu, X.Q., Zhang, C.L., Ye, X.T., Zou, H., Hao, X.S., 2019. Cambrian mafic and granitic intrusions in the Mazar-Tianshuihai terrane, West Kunlun Orogenic Belt, Constraints on the subduction orientation of the Proto-Tethys Ocean. *Lithos* 350, 105226.
- Liu, S., Feng, C., Fan, Y., Chen, X., Yang, Y., Zhao, H., Coulson, I.M., 2020. Zircon U-Pb dating, geochemical, and Sr-Nd-Pb-Hf isotopic constraints on the age and origin of intermediate to felsic igneous rocks at South Altyn, Xinjiang, China. *Acta Geochim.* 39, 698–716.
- Liu, Q., Zhao, G., Li, J., Yao, J., Han, Y., Wang, P., Tsunogae, T., 2021. Provenance of early Paleozoic sedimentary rocks in the Altyn Tagh orogen, Insights into the paleo-position of the Tarim craton in northern Gondwana associated with final closure of the Proto-Tethys Ocean. *Geol. Soc. Am. Bull.* 133, 505–522.
- Lo, C.-H., Yang, H.-Y., Yang, J., Knittel, U., 2006. Special issue on, Tectonic evolution of the Central Mountain Belt, China - Preface. *J. Asian Earth Sci.* 28, 117–118.
- Lü, J.G., Wang, J.C., Chu, C.H., Li, L.Q., Liu, R., Lei, H.M., 2006. Zircon SHRIMP U-Pb dating of the Wolonggang Monzogranite porphyry in the western segment of the Hoh Xil belt, Qinghai-Tibet Plateau and its geological significance. *Geol. Bull. China* 26, 721–724.
- Lu, Z., Zhang, J., Mattinson, C., 2018. Tectonic erosion related to continental subduction, An example from the eastern North Qaidam Mountains, NW China. *J. Metamorph. Geol.* 36, 653–666.
- Luo, Z., Zhang, Z., Li, J., Feng, Z., Tang, W., 2015. Geochronology of two kinds of Paleozoic granitic plutons from Sangawatang in Subei, the western margin of Central-South Qilian and their geological implications. *Acta Petrol. Sin.* 31, 176–188.
- Ma, Z., Wang, J.R., Zhang, L.L., Liu, Y.X., Gao, Y.Y., Zhang, X., Yu, S., Zhang, C., 2020. Petrogenesis and tectonic significance of the early Paleozoic Delenuoer ophiolite in the Central Qilian Shan, northeastern Tibetan Plateau. *Geosci. Front.* 11, 2017–2029.
- Magni, V., Allen, M.B., van Hunen, J., Bouilhol, P., 2017. Continental underplating after slab break-off. *Earth Planet. Sci. Lett.* 474, 59–67.
- Mao, X., Zhang, J., Lu, Z., Zhou, G., Teng, X., 2020. Structural style and geochronology of ductile shear zones in the western north Qinling orogenic belt, Central China, Implications for Paleozoic orogeny in the Central China orogeny. *J. Asian Earth Sci.* 201, 104498.
- Mattauer, M., Matte, P., Malavieille, J., Tapponnier, P., Maluski, H., Xu, Z.Q., Lu, Y.L., Tang, Y.Q., 1985. Tectonics of the Qinling Belt - Buildup and evolution of eastern Asia. *Nature* 317, 496–500.
- Mattern, F., Schneider, W., 2000. Suturing of the Proto- and Paleo-Tethys oceans in the western Kunlun (Xinjiang, China). *J. Asian Earth Sci.* 18, 637–650.
- Mattern, F., Schneider, W., Li, Y., Li, X., 1996. A traverse through the western Kunlun (Xinjiang, China), Tentative geodynamic implications for the Paleozoic and Mesozoic. *Geol. Rundsch.* 85, 705–722.
- Meert, J.G., 2003. A synopsis of events related to the assembly of eastern Gondwana. *Tectonophysics* 362, 1–40.
- Meng, Q.R., Zhang, G.W., 2000. Geologic framework and tectonic evolution of the Qinling orogen, central China. *Tectonophysics* 323, 183–196.
- Meng, F.C., Zhang, J.X., Cui, M.H., 2013. Discovery of Early Paleozoic eclogite from the East Kunlun, Western China and its tectonic significance. *Gondwana Res.* 23, 825–836.
- Meng, F.C., Cui, M.H., Wu, X.K., Ren, Y.F., 2015. Heishan mafic-ultramafic rocks in the Qimantag area of Eastern Kunlun, NW China, Remnants of an early Paleozoic incipient island arc. *Gondwana Res.* 27, 745–759.
- Metcalfe, I., 2013. Gondwana dispersion and Asian accretion, Tectonic and palaeogeographic evolution of eastern Tethys. *J. Asian Earth Sci.* 66, 1–33.

- Metcalf, I., 2021. Multiple Tethyan ocean basins and orogenic belts in Asia. *Gondwana Res.* 100, 87–130.
- Moghadam, H.S., Khademi, M., Hu, Z.C., Stern, R.J., Santos, J.F., Wu, Y.B., 2015. Cadomian (Ediacaran-Cambrian) arc magmatism in the ChahJam-Biarjmand metamorphic complex (Iran), Magmatism along the northern active margin of Gondwana. *Gondwana Res.* 27, 439–452.
- Natal'in, B.A., Şengör, A.M.C., 2005. Late Palaeozoic to Triassic evolution of the Turan and Scythian platforms, The pre-history of the Palaeo-Tethyan closure. *Tectonophysics* 404, 175–202.
- Nie, H., Yao, J., Wan, X., Zhu, X.Y., Siebel, W., Chen, F., 2016. Precambrian tectonothermal evolution of South Qinling and its affinity to the Yangtze Block: Evidence from zircon ages and Hf-Nd isotopic compositions of basement rocks. *Precambrian Res.* 286, 167–179.
- Nouri, F., Davoudian, A.R., Allen, M.B., Azizi, H., Asahara, Y., Shabanian, N., Anma, R., Tsuboi, M., Khodami, M., 2021. Early Cambrian highly fractionated granite, Central Iran, evidence for drifting of Northern Gondwana and the evolution of the Proto-Tethys Ocean. *Precambrian Res.* 362, 106291.
- Pan, F., Dong, Y.P., Li, X.M., Huang, B.T., Zhang, Y., Wang, G.Q., Yu, J.Y., Gao, Y.W., Zhao, X.M., 2020. Petrogenesis and tectonic setting of Early Paleozoic granites and high-Mg diorites in the Northern Qilian Orogen, China. *J. Asian Earth Sci.* 191, 104250.
- Peng, Y., Yu, S., Li, S., Zhang, J., Liu, Y., Li, Y., Santosh, M., 2019. Early Neoproterozoic magmatic imprints in the Altun-Qilian-Kunlun region of the Qinghai-Tibet Plateau: Response to the assembly and breakup of Rodinia supercontinent. *Earth Sci. Rev.* 199, 102954.
- Peng, Y., Yu, S., Zhang, J., Li, Y., Li, S., Lv, P., 2022. Building a continental arc section: Constraints from Paleozoic granulite-facies metamorphism, anatexis, and magmatism in the northern margin of the Qilian Block, northern Tibet Plateau. *Geol. Soc. Am. Bull.* 134, 1301–1318.
- Qi, X., Zhang, J., Li, H., 2004. Geochronology of the dextral strike ductile shear zone in south margin of the Northern Qilian Mountains and its geological significance. *Earth Sci. Front.* 11, 469–479.
- Qi, S.S., Song, S.G., Shi, L.C., Cai, H.J., Hu, J.C., 2014. Discovery and its geological significance of Early Paleozoic eclogite in Xiarihamu-Suhaitu area, western part of the East Kunlun. *Acta Petrol. Sin.* 30, 3345–3356.
- Qi, X.P., Yang, J., Fan, X.G., Cui, J.T., Cai, Z.F., Zeng, X.W., Qu, X.X., Zhai, L.M., 2016. Age, geochemical characteristics and tectonic significance of Changshishan ophiolite in central East Kunlun tectonic mélange belt along the east section of East Kunlun Mountains. *Geol. China* 43, 797–816.
- Qin, H.P., Wu, C.L., Wang, C.S., Li, X., Lei, M., Liu, C.H., Li, M.Z., 2014a. LA-ICP-MS zircon U-Pb characteristic of Xiagucheng granite in North Qilian. *Acta Geol. Sin.* 88, 1832–1842.
- Qin, Z.W., Wu, Y.B., Wang, H., Gao, S., Zhu, L.Q., Zhou, L., Yang, S.H., 2014b. Geochronology, geochemistry, and isotope compositions of Paochi S-type granitic intrusion in the Qinling orogen, central China, Petrogenesis and tectonic significance. *Lithos* 202, 347–362.
- Qin, Z.W., Wu, Y.B., Siebel, W., Gao, S., Wang, H., Abdallsamed, M.I.M., Zhang, W.X., Yang, S.H., 2015. Genesis of adakitic granitoids by partial melting of thickened lower crust and its implications for early crustal growth, A case study from the Huichizi pluton, Qinling orogen, central China. *Lithos* 238, 1–12.
- Qin, J.F., Lai, S.C., Long, X.P., Zhang, Z.Z., Ju, Y.J., Zhu, R.Z., Wang, X.Y., Li, Y.F., Wang, J.B., Li, T., 2021. Thermotectonic evolution of the Paleozoic granites along the Shangdan suture zone (central China). Crustal growth and differentiation by magma underplating in an orogenic belt. *Geol. Soc. Am. Bull.* 133, 523–528.
- Ratschbacher, L., Hacker, B.R., Calvert, A., Webb, L.E., Grimmer, J.C., McWilliams, M.O., Ireland, T., Dong, S., Hu, J., 2003. Tectonics of the Qinling (Central China): tectonostratigraphy, geochronology, and deformation history. *Tectonophysics* 366, 1–53.
- Ren, L., Liang, H., Bao, Z., Zhang, J., Li, K., Huang, W., 2018. The petrogenesis of early Paleozoic high-Ba-Sr intrusions in the North Qinling terrane, China, and tectonic implications. *Lithos* 314, 534–550.
- Ren, Y., Chen, D., Wang, H., Zhu, X., Bai, B., 2021. Grenvillian and early Paleozoic polyphase metamorphism recorded by eclogite and host garnet mica schist in the North Qaidam orogenic belt. *Geosci. Front.* 12, 101170.
- Robinson, A.C., Ducea, M., Lapen, T.J., 2012. Detrital zircon and isotopic constraints on the crustal architecture and tectonic evolution of the northeastern Pamir. *Tectonics* 31. <https://doi.org/10.1029/2011tc003013>.
- Roger, F., Arnaud, N., Gilder, S., Tapponnier, P., Jolivet, M., Brunel, M., Malavieille, J., Xu, Z.Q., Yang, J.S., 2003. Geochronological and geochemical constraints on Mesozoic suturing in east central Tibet. *Tectonics* 22. <https://doi.org/10.1029/2002tc001466>.
- Roger, F., Jolivet, M., Malavieille, J., 2008. Tectonic evolution of the Triassic fold belts of Tibet. *Compt. Rendus Geosci.* 340, 180–189.
- Schliffke, N., van Hunen, J., Gueydan, F., Magni, V., Allen, M.B., 2021. Curved orogenic belts, back-arc basins, and obduction as consequences of collision at irregular continental margins. *Geology* 49, 1436–1440.
- Şengör, A.M.C., 1987. Tectonics of the Tethysides - Orogenic collage development in a collisional setting. *Annu. Rev. Earth Planet. Sci.* 15, 213–244.
- Şengör, A.M.C., Natal'in, B.A., 1996. Paleotectonics of Asia, fragments of a synthesis. In: Yin, A., H. M. (Eds.), *The Tectonic Evolution of Asia*. Cambridge University Press, New York, pp. 486–640.
- Şengör, A.M.C., Okurogullari, A.H., 1991. The role of accretionary wedges in the growth of continents - Asiatic examples from Argand to plate tectonics. *Eclogae Geol. Helv.* 84, 535–597.
- Şengör, A.M.C., Natal'in, B.A., Sunal, G., van der Voo, R., 2018. The Tectonics of the Altaids, Crustal Growth During the Construction of the Continental Lithosphere of Central Asia Between similar to 750 and similar to 130 Ma Ago. In: Jeanloz, R., Freeman, K.H. (Eds.), *Annual Review of Earth and Planetary Sciences, Annual Review of Earth and Planetary Sciences*, vol 46, pp. 439–494.
- Shao, F., Niu, Y., Liu, Y., Chen, S., Kong, J., Duan, M., 2017. Petrogenesis of Triassic granitoids in the East Kunlun Orogenic Belt, northern Tibetan Plateau and their tectonic implications. *Lithos* 282, 33–44.
- Shi, R.D., Yang, J.S., Wu, C.L., 2004. First SHRIMP dating for the formation of the Late Sinian Yushigou Ophiolite North Qilian Mountains. *Acta Geol. Sin.* 78, 649–657.
- Shi, R., Yang, J., Wu, C., Iizuka, T., Hirata, T., 2006. Island arc volcanic rocks in the north Qaidam UHP belt, northern Tibet plateau, Evidence for ocean-continent subduction preceding continent-continent subduction. *J. Asian Earth Sci.* 28, 151–159.
- Shi, Y., Yu, J.-H., Santosh, M., 2013. Tectonic evolution of the Qinling orogenic belt, Central China. New evidence from geochemical, zircon U-Pb geochronology and Hf isotopes. *Precambrian Res.* 231, 19–60.
- Shi, Y., Huang, Q., Liu, X., Krapež, B., Yu, J., Bai, Z., 2018. Provenance and tectonic setting of the supra-crustal succession of the Qinling Complex: Implications for the tectonic affinity of the North Qinling Belt, Central China. *J. Asian Earth Sci.* 158, 112–139.
- Smith, A.D., 2006. The geochemistry and age of ophiolitic strata of the Xinglongshan Group, Implications for the amalgamation of the Central Qilian belt. *J. Asian Earth Sci.* 28, 133–142.
- Sobel, E.R., Arnaud, N., 1999. A possible middle Paleozoic suture in the Altyn Tagh, NW China. *Tectonics* 18, 64–74.
- Song, S., Li, X.H., 2019. A positive test for the Greater Tarim Block at the heart of Rodinia: Mega-dextral suturing of supercontinent assembly: COMMENT. *Geology* 47, e453.
- Song, S.G., Yang, J.S., Liou, J.G., Wu, C.L., Shi, R.D., Xu, Z.Q., 2003. Petrology, geochemistry and isotopic ages of eclogites from the Dulan UHPM Terrane, the North Qaidam, NW China. *Lithos* 70, 195–211.
- Song, S.G., Zhang, L.F., Niu, Y.L., Song, B., Zhang, G.B., Wang, Q.J., 2004. Zircon U-Pb SHRIMP ages of eclogites from the North Qilian Mountains in NW China and their tectonic implication. *Chin. Sci. Bull.* 49, 848–852.
- Song, S.G., Zhang, L.F., Niu, Y.L., Su, L., Jian, P., Liu, D.Y., 2005. Geochronology of diamond-bearing zircons from garnet peridotite in the North Qaidam UHPM belt, Northern Tibetan Plateau, A record of complex histories from oceanic lithosphere subduction to continental collision. *Earth Planet. Sci. Lett.* 234, 99–118.
- Song, S.G., Zhang, L.F., Niu, Y.L., Su, L., Song, B.A., Liu, D.Y., 2006. Evolution from oceanic subduction to continental collision, a case study from the Northern Tibetan Plateau based on geochemical and geochronological data. *J. Petrol.* 47, 435–455.
- Song, S.G., Zhang, L.F., Niu, Y., Wie, C.J., Liou, J.G., Shu, G.M., 2007. Eclogite and carpholite-bearing metasedimentary rocks in the North Qilian suture zone, NW China, implications for early Paleozoic cold oceanic subduction and water transport into mantle. *J. Metamorph. Geol.* 25, 547–563.
- Song, S., Niu, Y., Wei, C., Liou, J.G., Su, L., 2009a. Tectonic evolution of early Paleozoic HP metamorphic rocks in the North Qilian Mountains, NW China: New perspectives. *J. Asian Earth Sci.* 35, 334–353.
- Song, S., Su, L., Niu, Y., Zhang, G., Zhang, L., 2009b. Two types of peridotite in North Qaidam UHPM belt and their tectonic implications for oceanic and continental subduction. A review. *J. Asian Earth Sci.* 35, 285–297.
- Song, S., Su, L., Li, X.-H., Zhang, G., Niu, Y., Zhang, L., 2010. Tracing the 850-Ma continental flood basalts from a piece of subducted continental crust in the North Qaidam UHPM belt, NW China. *Precambrian Res.* 183, 805–816.
- Song, S., Su, L., Li, X.-H., Niu, Y., Zhang, L., 2012. Grenville-age orogenesis in the Qaidam-Qilian block, The link between South China and Tarim. *Precambrian Res.* 220, 9–22.
- Song, S., Niu, Y., Su, L., Xia, X., 2013. Tectonics of the North Qilian orogen, NW China. *Gondwana Res.* 23, 1378–1401.
- Song, S., Niu, Y., Su, L., Zhang, C., Zhang, L., 2014a. Continental orogenesis from ocean subduction, continent collision/subduction, to orogen collapse, and orogen recycling. The example of the North Qaidam UHPM belt, NW China. *Earth Sci. Rev.* 129, 59–84.
- Song, S., Niu, Y., Su, L., Wei, C., Zhang, L., 2014b. Adakitic (tonalitic-trondhjemitic) magmas resulting from eclogite decompression and dehydration melting during exhumation in response to continental collision. *Geochim. Cosmochim. Acta* 130, 42–62.
- Song, D., Xiao, W., Collins, A.S., Glorie, S., Han, C., Li, Y., 2017a. New chronological constrains on the tectonic affinity of the Alxa Block, NW China. *Precambrian Res.* 299, 230–243.
- Song, S., Yang, L., Zhang, Y., Niu, Y., Wang, C., Su, L., Gao, Y., 2017b. Qi-Qin Accretionary Belt in Central China Orogen, accretion by trench jam of oceanic plateau and formation of intra-oceanic arc in the Early Paleozoic Qin-Qi-Kun Ocean. *Sci. Bull.* 62, 1035–1038.
- Song, S., Bi, H., Qi, S., Yang, L., Allen, M.B., Niu, Y., Su, L., Li, W., 2018. HP-UHP Metamorphic Belt in the East Kunlun Orogen, Final Closure of the Proto-Tethys Ocean and Formation of the Pan-North-China Continent. *J. Petrol.* 59, 2043–2060.
- Song, S., Niu, Y., Zhang, G., Zhang, L., 2019a. Two epochs of eclogite metamorphism link 'cold' oceanic subduction and 'hot' continental subduction, the North Qaidam UHP belt, NW China. In: Zhang, L., Zhang, Z., Schertl, H.P., Wei, C. (Eds.), *Hp-Uhp Metamorphism and Tectonic Evolution of Orogenic Belts*. Geological Society Special Publication, pp. 275–289.
- Song, S.G., Wu, Z.Z., Yang, L.M., Su, L., Xia, X.H., Wang, C., Dong, J.L., Zhou, C.A., Bi, H. Z., 2019b. Ophiolite belts and evolution of the Proto-Tethys Ocean in the Qilian Orogen. *Acta Petrol. Sin.* 35, 2948–2970.
- Stern, R.J., 1994. Arc assembly and continental collision in the Neoproterozoic East African Orogen. *Annu. Rev. Earth Planet. Sci.* 22, 319–351.

- Su, L., Song, S.G., Song, B., Zhou, D.W., Hao, J.R., 2004. SHRIMP zircon U-Pb ages of garnet pyroxenite and Fushui gabbroic complex in Song-shugou region and constraints on tectonic evolution of Qinling Orogenic belt. *Chin. Sci. Bull.* 49, 1307–1310.
- Sui, Q.L., Chen, D.H., Zhao, X.J., Zha, X.F., Sun, J.M., Zhang, L.P., Gao, X.F., Sun, W.D., 2021. Diachronous subduction of the Proto-Tethys Ocean along the northern margin of East Gondwana. Insights from SHRIMP and LA-ICP-MS zircon geochronology in the West Kunlun Orogenic Belt, Northwestern China. *Int. Geol. Rev.* <https://doi.org/10.1080/00206814.2021.1885505>.
- Sun, H.S., Li, H., Algeo, T.J., Gabo-Ratio, J.A.S., Yang, H., Wu, J.H., Wu, P., Liu, Y., 2019. Geochronology and geochemistry of volcanic rocks from the Tanjianshan Group, NW China, Implications for the early Palaeozoic tectonic evolution of the North Qaidam Orogen. *Geol. J.* 54, 1769–1796.
- Sun, Y., Niu, M., Yan, Z., Palin, R.M., Li, C., Li, X., Yuan, X., 2022. Late early Palaeozoic continental collision on the northern margin of the Central Qilian Block, NE Tibetan Plateau: Evidence from a two-stage tectono-metamorphic event. *J. Asian Earth Sci.* 105121.
- Tao, L., Zhang, H., Yang, H., Gao, Z., Pan, F., Luo, B., 2018. Initial back-arc extension, Evidence from petrogenesis of early Palaeozoic MORB-like gabbro at the southern Central Qilian block, NW China. *Lithos* 322, 166–178.
- Teng, X., Zhang, J.X., Mao, X.H., Lu, Z.L., Zhou, G.S., 2020. The earliest Cambrian UHT metamorphism in the Qaidam block, western China, A record of the final assembly of Greater Gondwana? *Gondwana Res.* 87, 118–137.
- Tseng, C.Y., Yang, H.J., Yang, H.Y., Liu, D.Y., Tsai, C.L., Wu, H.Q., Zuo, G.C., 2007. The Dongcaohé ophiolite from the North Qilian Mountains, A fossil oceanic crust of the Paleo-Qilian ocean. *Chin. Sci. Bull.* 52, 2390–2401.
- Tseng, C.-Y., Yang, H.-J., Yang, H.-Y., Liu, D., Wu, C., Cheng, C.-K., Chen, C.-H., Ker, C.-M., 2009. Continuity of the North Qilian and North Qinling orogenic belts, Central Orogenic System of China, Evidence from newly discovered Palaeozoic adakitic rocks. *Gondwana Res.* 16, 285–293.
- Tung, K., Yang, H.J., Yang, H.Y., Liu, D.Y., Zhang, J.X., Wan, Y.S., Tseng, C.Y., 2007. SHRIMP U-Pb geochronology of the zircons from the Precambrian basement of the Qilian Block and its geological significances. *Chin. Sci. Bull.* 52, 2687–2701.
- Tung, K.A., Yang, H.Y., Liu, D.Y., Zhang, J.X., Yang, H.J., Shau, Y.H., Tseng, C.Y., 2013. The Neoproterozoic granitoids from the Qilian block, NW China, Evidence for a link between the Qilian and South China blocks. *Precambrian Res.* 235, 163–189.
- Tung, K.A., Yang, H.Y., Yang, H.J., Smith, A., Liu, D., Zhang, J., Wu, C., Shau, Y.H., Weng, D.J., Tseng, C.Y., 2016. Magma sources and petrogenesis of the early-middle Palaeozoic backarc granitoids from the central part of the Qilian block, NW China. *Gondwana Res.* 38, 197–219.
- Wan, Y.S., Xu, Z.Q., Yang, J.S., Zhang, J.X., 2001. Ages and compositions of the Precambrian high-grade basement of the Qilian terrane and its adjacent areas. *Acta Geol. Sin. Engl. Ed.* 75, 375–384.
- Wang, Z.H., 2004. Tectonic evolution of the western Kunlun orogenic belt, western China. *J. Asian Earth Sci.* 24, 153–161.
- Wang, X.R., Hua, H., Sun, Y., 1995. A study on microfossils of the Erlangping Group in Wantan area, Xixia county, Henan province. *J. Northwest Univ.* 25, 353–358.
- Wang, C.Y., Zhang, Q., Qian, Q., Zhou, M.F., 2005a. Geochemistry of the Early Palaeozoic Baiyin volcanic rocks (NW China), Implications for the tectonic evolution of the North Qilian Orogenic Belt. *J. Geol.* 113, 83–94.
- Wang, T., Pei, X.Z., Wang, X.X., Hu, N.G., Li, W.P., Zhang, G.W., 2005b. Orogen-parallel westward oblique uplift of the Qinling basement complex in the core of the Qinling orogen (China), An example of oblique extrusion of deep-seated metamorphic rocks in a collisional orogen. *J. Geol.* 113, 181–200.
- Wang, T., Wang, X., Tian, W., Zhang, C., Li, W., Li, S., 2009. North Qinling Palaeozoic granite associations and their variation in space and time, Implications for orogenic processes in the orogens of central China. *Sci. China. Ser. D Earth Sci.* 52, 1359–1384.
- Wang, H., Wu, Y.B., Gao, S., Liu, X.C., Gong, H.J., Li, Q.L., Li, X.H., Yuan, H.L., 2011. Eclogite origin and timings in the North Qinling terrane, and their bearing on the amalgamation of the South and North China Blocks. *J. Metamorph. Geol.* 29, 1019–1031.
- Wang, L.J., Yu, J.H., Griffin, W.L., O'Reilly, S.Y., 2012. Early crustal evolution in the western Yangtze Block, Evidence from U-Pb and Lu-Hf isotopes on detrital zircons from sedimentary rocks. *Precambrian Res.* 222, 368–385.
- Wang, H., Wu, Y.B., Gao, S., Liu, X.C., Liu, Q., Qin, Z.W., Xie, S.W., Zhou, L., Yang, S.H., 2013. Continental origin of eclogites in the North Qinling terrane and its tectonic implications. *Precambrian Res.* 230, 13–30.
- Wang, M., Song, S., Niu, Y., Su, L., 2014a. Post-collisional magmatism: Consequences of UHPM terrane exhumation and orogen collapse, N. Qaidam UHPM belt, NW China. *Lithos* 210, 181–198.
- Wang, C., Liu, L., Xiao, P.X., Cao, Y.T., Yu, H.Y., Meert, J.G., Liang, W.T., 2014b. Geochemical and geochronologic constraints for Palaeozoic magmatism related to the orogenic collapse in the Qimantagh-South Altyn region, northwestern China. *Lithos* 202, 1–20.
- Wang, C., Li, R.-S., Li, M., Meert, J.G., Peng, Y., 2015. Palaeoproterozoic magmatic-metamorphic history of the Qunaji Massif, Northwest China, implications for a single North China-Qunaji-Tarim craton within the Columbia supercontinent? *Int. Geol. Rev.* 57, 1772–1790.
- Wang, H., Wu, Y.-B., Gao, S., Qin, Z.W., Hu, Z.C., Zheng, J.P., Yang, S.H., 2016. Continental growth through accreted oceanic arc, Zircon Hf-O isotope evidence for granitoids from the Qinling orogen. *Geochim. Cosmochim. Acta* 182, 109–130.
- Wang, C., Li, R.S., Smithies, R.H., Li, M., Peng, Y., Chen, F.N., He, S.P., 2017a. Early Palaeozoic felsic magmatic evolution of the western Central Qilian belt, Northwestern China, and constraints on convergent margin processes. *Gondwana Res.* 41, 301–324.
- Wang, J., Hattori, K., Liu, J., Song, Y., Gao, Y., Zhang, H., 2017b. Shoshonitic-and adakitic magmatism of the Early Palaeozoic age in the Western Kunlun orogenic belt, NW China: Implications for the early evolution of the northwestern Tibetan plateau. *Lithos* 286, 345–362.
- Wang, K.X., Yu, C.D., Yan, J., Liu, X.D., Liu, W.H., Pan, J.Y., 2019. Petrogenesis of Early Silurian granitoids in the Longshouan area and their implications for the extensional environment of the North Qilian Orogenic Belt, China. *Lithos* 342, 152–174.
- Wang, B.Z., Pan, T., Ren, H.D., Wang, T., Zhao, Z.Y., Feng, J.P., Zhang, J.M., 2021. Cambrian Qimantagh island arc in the East Kunlun orogen, Evidences from zircon U-Pb ages, litho-geochemistry and Hf isotopes of high-Mg andesite/diorite from the Lalinggaolihe area. *Earth Sci. Front.* 28, 318–333.
- Wang, H., Xiao, W., Windley, B.F., Zhang, Q.W., Tan, Z., Wu, C., Shi, M., 2022. Diverse P-T-t Paths Reveal High-Grade Metamorphosed Forearc Complexes in NW China. *J. Geophys. Res. Solid Earth* 127, e2022JB024309.
- Wang, P., Zhao, G., Liu, Q., Yao, J., Han, Y., 2022a. Evolution of the Paleo-Tethys Ocean in Eastern Kunlun, North Tibetan Plateau: From continental rift-drift to final closure. *Lithos* 422, 106717.
- Wang, Q., Zhao, J., Zhang, C., Yu, S., Ye, X., Liu, X., 2022b. Palaeozoic post-collisional magmatism and high-temperature granulite-facies metamorphism coupling with lithospheric delamination of the East Kunlun Orogenic Belt, NW China. *Geosci. Front.* 13, 101271.
- Wang, C., Song, S.G., Zhao, G.C., Allen, M.B., Su, L., Gao, T.Y., Wen, T., Feng, D., 2023. Calc-alkaline plutons in a Proto-Tethyan intra-oceanic arc (Qilian Orogen, NW China): implications for the construction of arc crust. *J. Petrol.* 64, 1–29.
- Wen, T., Song, S.G., Wang, C., Allen, M.B., Dong, J., Feng, D., Li, S., 2022a. IBM-type forearc magmatism in the Qilian Orogen records evolution from a continental to an intra-oceanic arc system in the Proto-Tethyan Ocean. *Gondwana Res.* 110, 197–213.
- Wen, T., Dong, J., Wang, C., Song, S., 2022b. Two ophiolite belts in the East Kunlun Orogenic Belt record evolution from the Proto-Tethys to Paleo-Tethys Oceans. *Int. Geol. Rev.* <https://doi.org/10.1080/00206814.2022.2116605>, 1–20.
- Wu, H.Q., Feng, Y.M., Song, S.G., 1993. Metamorphism and deformation of blueschist belts and their tectonic implications, North Qilian Mountains, China. *J. Metamorph. Geol.* 11, 523–536.
- Wu, C., Gao, Y., Wu, S., Chen, Q., Wooden, J.L., Mazadab, F.K., Mattinson, C., 2007. Zircon SHRIMP U-Pb dating of granites from the Da Qaidam area in the north margin of Qaidam basin, NW China. *Acta Petrol. Sin.* 23, 1861–1875.
- Wu, C., Wooden, J.L., Robinson, P.T., Gao, Y., Wu, S., Chen, Q., Mazdab, F.K., Mattinson, C., 2009a. Geochemistry and zircon SHRIMP U-Pb dating of granitoids from the west segment of the North Qaidam. *Sci. China. Ser. D Earth Sci.* 52, 1771–1790.
- Wu, C., Yang, J., Robinson, P.T., Wooden, J.L., Mazdab, F.K., Gao, Y., Wu, S., Chen, Q., 2009b. Geochemistry, age and tectonic significance of granitic rocks in north Altun, northwest China. *Lithos* 113, 423–436.
- Wu, C., Gao, Y., Frost, B.R., Robinson, P.T., Wooden, J.L., Wu, S., Chen, Q., Lei, M., 2011. An early Palaeozoic double-subduction model for the North Qilian oceanic plate, evidence from zircon SHRIMP dating of granites. *Int. Geol. Rev.* 53, 157–181.
- Wu, C., Gao, Y., Li, Z., Lei, M., Qin, H., Li, M., Liu, C., Frost, R.B., Robinson, P.T., Wooden, J.L., 2014a. Zircon SHRIMP U-Pb dating of granites from Dulan and the chronological framework of the North Qaidam UHP belt, NW China. *Sci. China Earth Sci.* 57, 2945–2965.
- Wu, C., Gao, Y., Lei, M., Qin, H., Liu, C., Li, M., Frost, B.R., Wooden, J.L., 2014b. Zircon SHRIMP U-Pb dating, Lu-Hf isotopic characteristics and petrogenesis of the Palaeozoic granites in Mangya area, southern Altun, NW China. *Acta Petrol. Sin.* 30, 2297–2323.
- Wu, C., Yin, A., Zuzza, A.V., Zhang, J., Liu, W., Ding, L., 2016. Pre-Cenozoic geologic history of the central and northern Tibetan Plateau and the role of Wilson cycles in constructing the Tethyan orogenic system. *Lithosphere* 8, 254–292.
- Wu, C., Zuzza, A.V., Yin, A., Liu, C., Reith, R.C., Zhang, J., Liu, W., Zhou, Z., 2017. Geochronology and geochemistry of Neoproterozoic granitoids in the central Qilian Shan of northern Tibet, Reconstructing the amalgamation processes and tectonic history of Asia. *Lithosphere* 9, 609–636.
- Wu, C., Chen, H., Wu, D., Ernst, W.G., 2018. Palaeozoic granitic magmatism and tectonic evolution of the South Altun block, NW China, Constraints from zircon U-Pb dating and Lu-Hf isotope geochemistry. *J. Asian Earth Sci.* 160, 168–199.
- Wu, C., Zuzza, A.V., Chen, X., Ding, L., Levy, D.A., Liu, C., Liu, W., Jiang, T., Stockli, D.F., 2019a. Tectonics of the Eastern Kunlun Range, Cenozoic reactivation of a Palaeozoic-Early Mesozoic Orogen. *Tectonics* 38, 1609–1650.
- Wu, C.L., Wu, D., Mattinson, C., Lei, M., Chen, H.J., 2019b. Petrogenesis of granitoids in the Wulan area, Magmatic activity and tectonic evolution in the North Qaidam, NW China. *Gondwana Res.* 67, 147–171.
- Wu, S., Qin, J.F., Lai, S.C., Long, X.P., Ju, Y.J., Zhang, Z.Z., Wang, J.B., Li, C., 2020. Early-Palaeozoic mafic intrusion in North Qinling (Central China), Implication for the initiation back-arc system along the Shanggan suture zone. *Geol. J.* 55, 4733–4747.
- Wu, C., Zuzza, A.V., Yin, A., Chen, X., Haproff, P.J., Li, J., Li, B., Ding, L., 2021. Punctuated orogeny during the assembly of Asia, Tectonostratigraphic Evolution of the North China Craton and the Qilian Shan from the Palaeoproterozoic to Early Palaeozoic. *Tectonics* 40, e2020TC006503.
- Wu, C., Li, J., Zuzza, A.V., Haproff, P.J., Chen, X., Ding, L., 2022a. Proterozoic-Phanerozoic tectonic evolution of the Qilian Shan and Eastern Kunlun Range, northern Tibet. *Geol. Soc. Am. Bull.* 134, 2179–2205. <https://doi.org/10.1130/B36306.1>.
- Wu, C., Li, J., Zuzza, A.V., Haproff, P.J., Yin, A., Ding, L., 2022b. Palaeoproterozoic-Palaeozoic tectonic evolution of the Longshou Shan, western North China craton. *Geosphere* 18, 1177–1193.

- Xia, L.Q., Xia, Z.C., Xu, X.Y., 2003. Magmatism in the Ordovician backarc basins of the Northern Qilian Mountains, China. *Geol. Soc. Am. Bull.* 115, 1510–1522.
- Xia, X., Song, S., Niu, Y., 2012. Tholeiite-Boninite terrane in the North Qilian suture zone, Implications for subduction initiation and back-arc basin development. *Chem. Geol.* 328, 259–277.
- Xia, R., Wang, C., Deng, J., Carranza, E.J.M., Li, W., Qing, M., 2014. Crustal thickening prior to 220 Ma in the East Kunlun Orogenic Belt, Insights from the Late Triassic granitoids in the Xiao-Nuomuhong pluton. *J. Asian Earth Sci.* 93, 193–210.
- Xiao, W.J., Windley, B.F., Hao, J., Li, J.L., 2002a. Arc-ophiolite obduction in the Western Kunlun Range (China), implications for the Palaeozoic evolution of central Asia. *J. Geol. Soc.* 159, 517–528.
- Xiao, W.J., Windley, B.F., Chen, H.L., Zhang, G.C., Li, J.L., 2002b. Carboniferous-Triassic subduction and accretion in the western Kunlun, China, Implications for the collisional and accretionary tectonics of the northern Tibetan Plateau. *Geology* 30, 295–298.
- Xiao, X.C., Wang, J., Su, L., Song, S.G., 2003. A further discussion of the Kuda ophiolite, West Kunlun, and its tectonic significance. *Geol. Bull. China* 22, 745–750.
- Xiao, W.J., Windley, B.F., Liu, D.Y., Jian, P., Liu, C.Z., Yuan, C., Sun, M., 2005. Accretionary tectonics of the Western Kunlun Orogen, China, A Palaeozoic-early Mesozoic, long-lived active continental margin with implications for the growth of southern Eurasia. *J. Geol.* 113, 687–705.
- Xiao, W., Windley, B.F., Yong, Y., Yan, Z., Yuan, C., Liu, C., Li, J., 2009a. Early Paleozoic to Devonian multiple-accretionary model for the Qilian Shan, NW China. *J. Asian Earth Sci.* 35, 323–333.
- Xiao, W., Windley, B.F., Han, C., Liu, W., Wan, B., Zhang, J.E., Ao, S., Zhang, Z., Song, D., 2018. Late Paleozoic to early Triassic multiple roll-back and oroclinal bending of the Mongolia collage in Central Asia. *Earth Sci. Rev.* 186, 94–128.
- Xin, W., Sun, F.-Y., Li, L., Yan, J.-M., Zhang, Y.-T., Wang, Y.-C., Shen, T.-S., Yang, Y.-J., 2018. The Wulonggou metaluminous A(2)-type granites in the Eastern Kunlun Orogenic Belt, NW China, Rejuvenation of subduction-related felsic crust and implications for post-collision extension. *Lithos* 312, 108–127.
- Xiong, Q., Zheng, J.-P., Griffin, W.L., O'Reilly, S.Y., Pearson, N.J., 2014a. Pyroxenite Dykes in Orogenic Peridotite from North Qaidam (NE Tibet, China) Track Metasomatism and Segregation in the Mantle Wedge. *J. Petrol.* 55, 2347–2376.
- Xiong, F., Ma, C., Zhang, J., Liu, B., Jiang, H.A., 2014b. Reworking of old continental lithosphere, an important crustal evolution mechanism in orogenic belts, as evidenced by Triassic I-type granitoids in the East Kunlun orogen, Northern Tibetan Plateau. *J. Geol. Soc.* 171, 847–863.
- Xiong, L., Song, S., Su, L., Zhang, G., Allen, M.B., Feng, D., Yang, S., 2023. Detrital zircons from high-pressure trench sediments (Qilian Orogen): Constraints on continental-arc accretion, subduction initiation and polarity of the Proto-Tethys Ocean. *Gondwana Res.* 113, 194–209.
- Xu, Z., Yang, J., Wu, C., Li, H., Zhang, J., Qi, X., Song, S., Qiu, H., 2006. Timing and mechanism of formation and exhumation of the Northern Qaidam ultrahigh-pressure metamorphic belt. *J. Asian Earth Sci.* 28, 160–173.
- Xu, Y.J., Du, Y.S., Cawood, P.A., Yang, J., 2010a. Provenance record of a foreland basin, Detrital zircon U-Pb ages from Devonian strata in the North Qilian Orogenic Belt, China. *Tectonophysics* 495, 337–347.
- Xu, Y.J., Du, Y.S., Cawood, P.A., Guo, H., Huang, H., An, Z.H., 2010b. Detrital zircon record of continental collision: assembly of the Qilian Orogen, China. *Sediment. Geol.* 230, 35–45.
- Xu, Z.Q., He, B.Z., Zhang, C.L., Zhang, J.X., Wang, Z.M., Cai, Z.H., 2013. Tectonic framework and crustal evolution of the Precambrian basement of the Tarim Block in NW China, New geochronological evidence from deep drilling samples. *Precambrian Res.* 235, 150–162.
- Xu, X., Song, S.G., Su, L., Li, Z.X., Niu, Y.L., Allen, M.B., 2015. The 600–580 Ma continental rift basalts in North Qilian Shan, northwest China: Links between the Qilian-Qaidam block and SE Australia, and the reconstruction of East Gondwana. *Precambrian Res.* 257, 47–64.
- Xu, X., Song, S., Allen, M.B., Ernst, R.E., Niu, Y., Su, L., 2016. An 850–820 Ma LIP dismembered during breakup of the Rodinia supercontinent and destroyed by Early Paleozoic continental subduction in the northern Tibetan Plateau, NW China. *Precambrian Res.* 282, 52–73.
- Xu, N., Wu, C.-L., Gao, Y.-H., Lei, M., Zheng, K., Gao, D., 2020. Tectonic evolution of the South Altyn, NW China, constraints by geochemical, zircon U-Pb and Lu-Hf isotopic analysis of the Palaeozoic granitic plutons in the Mangya area. *Geol. Mag.* 157, 1121–1143.
- Xu, C., Sun, F., Fan, X., Yu, L., Yang, D., Bakht, S., Wu, D., 2022. Composition, Age, and Origin of Ordovician-Devonian Tanjianshan granitoids in the North Qaidam Orogenic Belt of northern Tibet: Implications for Tectonic Evolution. *Int. Geol. Rev.* <https://doi.org/10.1080/00206814.2022.2032415>.
- Yan, Z., Xiao, W.J., Windley, B.F., Wang, Z.Q., Li, J.L., 2010. Silurian clastic sediments in the North Qilian Shan, NW China Chemical and isotopic constraints on their forearc provenance with implications for the Paleozoic evolution of the Tibetan Plateau. *Sediment. Geol.* 231, 98–114.
- Yan, Z., Aitchison, J., Fu, C., Guo, X., Niu, M., Xia, W., Li, J., 2015. Hualong Complex, South Qilian terrane, U-Pb and Lu-Hf constraints on Neoproterozoic micro-continental fragments accreted to the northern Proto-Tethyan margin. *Precambrian Res.* 266, 65–85.
- Yan, Z., Fu, C., Wang, Z., Yan, Q., Chen, L., Chen, J., 2016. Late Paleozoic subduction-accretion along the southern margin of the North Qinling terrane, central China, Evidence from zircon U-Pb dating and geochemistry of the Wuguan Complex. *Gondwana Res.* 30, 97–111.
- Yan, Z., Fu, C.L., Aitchison, J.C., Niu, M.L., Buckman, S., Cao, B., 2019a. Early Cambrian Muli arc-ophiolite complex, a relic of the Proto-Tethys oceanic lithosphere in the Qilian Orogen, NW China. *Int. J. Earth Sci.* 108, 1147–1164.
- Yan, Z., Fu, C., Aitchison, J.C., Buckman, S., Niu, M., Cao, B., Sun, Y., Guo, X., Wang, Z., Zhou, R., 2019b. Retro-foreland basin development in response to Proto-Tethyan ocean closure, NE Tibet Plateau. *Tectonics* 38, 4229–4248.
- Yan, J.M., Sun, F.Y., Li, L., Yang, Y.Q., Zhang, D.X., 2019c. A slab break-off model for mafic-ultramafic igneous complexes in the East Kunlun Orogenic Belt, northern Tibet, insights from early Palaeozoic accretion related to post-collisional magmatism. *Int. Geol. Rev.* 61, 1171–1188.
- Yan, Z., Fu, C.L., Aitchison, J.C., Zhou, R.J., Buckman, S., Chen, L., 2020. Silurian sedimentation in the South Qilian Belt: Arc-Continent collision-related deposition in the NE Tibet Plateau? *Acta Geol. Sin.* 94, 901–913.
- Yan, Z., Xiao, W., Aitchison, J.C., Yuan, C., Liu, C., Fu, C., 2021. Age and origin of accreted ocean plate stratigraphy in the North Qilian belt, NE Tibet Plateau: evidence from microfossils and geochemistry of cherts and siltstones. *J. Geol. Soc.* 178.
- Yan, Z., Fu, C., Aitchison, J.C., Niu, M., Buckman, S., Xiao, W., Zhou, R., Chen, L., Li, J., 2022. Arc-continent collision during culmination of Proto-Tethyan Ocean closure in the Central Qilian belt, NE Tibetan Plateau. *GSA Bull.* <https://doi.org/10.1130/B36328.1>.
- Yang, J.S., Robinson, P.T., Jiang, C.F., Xu, Z.Q., 1996. Ophiolites of the Kunlun mountains, China and their tectonic implications. *Tectonophysics* 258, 215–231.
- Yang, J.S., Xu, Z.Q., Zhang, J.X., Chu, C.Y., Zhang, R.Y., Liou, J.G., 2001. Tectonic significance of early Paleozoic high-pressure rocks in Altun-Qaidam-Qilian Mountains, northwest China. In: *Paleozoic and Mesozoic Tectonic Evolution of Central Asia, From Continental Assembly to Intracontinental Deformation*, 194, pp. 151–170.
- Yang, J.S., Xu, Z.Q., Zhang, J.X., Song, S.G., Wu, C.L., Shi, R.D., Li, H.B., Brunel, M., 2002. Early Palaeozoic North Qaidam UHP metamorphic belt on the north-eastern Tibetan plateau and a paired subduction model. *Terra Nova* 14, 397–404.
- Yang, J.H., Du, Y.S., Cawood, P.A., Xu, Y.J., 2009. Silurian collisional suturing onto the southern margin of the North China craton, Detrital zircon geochronology constraints from the Qilian Orogen. *Sediment. Geol.* 220, 95–104.
- Yang, W., Liu, L., Cao, Y., Wang, C., He, S., Li, R., Zhu, X., 2010. Geochronological evidence of Indosinian (high-pressure) metamorphic event and its tectonic significance in Taxkorgan area of the Western Kunlun Mountains, NW China. *Sci. China Earth Sci.* 53, 1445–1459.
- Yang, L.Q., Deng, J., Dilek, Y., Qiu, K.F., Ji, X.Z., Li, N., Taylor, R.D., Yu, J.Y., 2015. Structure, geochronology, and petrogenesis of the Late Triassic Puziba granitoid dikes in the Mianlue suture zone, Qinling orogen, China. *Geol. Soc. Am. Bull.* 127, 1831–1854.
- Yang, L., Song, S., Allen, M.B., Su, L., Dong, J., Wang, C., 2018. Oceanic accretionary belt in the West Qinling Orogen, Links between the Qinling and Qilian orogens, China. *Gondwana Res.* 64, 137–162.
- Yang, L., Song, S., Su, L., Allen, M.B., Niu, Y., Zhang, G., Zhang, Y., 2019a. Heterogeneous oceanic arc volcanic rocks in the South Qilian accretionary belt (Qilian Orogen, NW China). *J. Petrol.* 60, 85–116.
- Yang, L., Su, L., Song, S., Allen, M.B., Bi, H., Feng, D., Li, W., Li, Y., 2019b. Interaction between oceanic slab and metasomatized mantle wedge: Constraints from sodic lavas from the Qilian Orogen, NW China. *Lithos* 348, 105182.
- Yang, H., Zhang, H.F., Xiao, W.J., Luo, B.J., Gao, Z., Tao, L., Zhang, L.Q., Guo, L., 2020a. Petrogenesis of Early Paleozoic high Sr/Y intrusive rocks from the North Qilian orogen: implication for diachronous continental collision. *Lithosphere* 12, 53–73.
- Yang, S., Su, L., Song, S., Allen, M.B., Feng, D., Wang, M., Wang, C., Zhang, H., 2020b. Melting of subducted continental crust during collision and exhumation: Insights from granitic rocks from the North Qaidam UHP metamorphic belt, NW China. *Lithos* 378–379, 105794.
- Yao, W.H., Li, Z.X., Li, W.X., Li, X.H., Yang, J.H., 2014. From Rodinia to Gondwanaland: A tale of detrital zircon provenance analyses from the southern Nanhua Basin, South China. *Am. J. Sci.* 314, 278–313.
- Yao, J., Cawood, P.A., Zhao, G., Han, Y., Xia, X., Liu, Q., Wang, P., 2021. Mariana-type ophiolites constrain the establishment of modern plate tectonic regime during Gondwana assembly. *Nat. Commun.* 12, 1–10.
- Ye, H.M., Li, X.H., Li, Z.X., Zhang, C.L., 2008. Age and origin of high Ba-Sr apatite-granites at the northwestern margin of the Tibet Plateau: implications for early Paleozoic tectonic evolution of the Western Kunlun orogenic belt. *Gondwana Res.* 13, 126–138.
- Ye, X.T., Zhang, C.L., Wang, Q., Wang, G.D., 2020. Subduction initiation of Proto-Tethys Ocean and back-arc extension in the northern Altun Mountains, northwestern China: Evidence from high-Mg diorites and A-type rhyolites. *Lithos* 376, 105748.
- Yin, A., Nie, S.Y., 1996. A Phanerozoic palinspastic reconstruction of China and its neighboring regions. In: Yin, A., H. M. (Eds.), *The Tectonic Evolution of Asia*. Cambridge University Press, New York, pp. 442–485.
- Yin, A., Manning, C.E., Lovera, O., Menold, C.A., Chen, X., Gehrels, G.E., 2007. Early Paleozoic tectonic and thermomechanical evolution of ultrahigh-pressure (UHP) metamorphic rocks in the northern Tibetan Plateau, northwest China. *Int. Geol. Rev.* 49, 681–716.
- Yin, A., Dang, Y.Q., Zhang, M., Chen, X.H., McRivette, M.W., 2008. Cenozoic tectonic evolution of the Qaidam basin and its surrounding regions (Part 3): Structural geology, sedimentation, and regional tectonic reconstruction. *Geol. Soc. Am. Bull.* 120, 847–876.
- Yin, J., Xiao, W., Sun, M., Chen, W., Yuan, C., Zhang, Y., Wang, T., Du, Q., Wang, X., Xia, X., 2020. Petrogenesis of Early Cambrian granitoids in the western Kunlun orogenic belt, Northwest Tibet: Insight into early stage subduction of the Proto-Tethys Ocean. *Geol. Soc. Am. Bull.* 132, 2221–2240.
- Yu, S.G., Zhang, J.X., Li, H.K., Hou, K.J., Mattinson, C.G., Gong, J.H., 2013. Geochemistry, zircon U-Pb geochronology and Lu-Hf isotopic composition of

- eclogites and their host gneisses in the Dulan area, North Qaidam UHP terrane, New evidence for deep continental subduction. *Gondwana Res.* 23, 901–919.
- Yu, S., Zhang, J., Qin, H., Sun, D., Zhao, X., Cong, F., Li, Y., 2015a. Petrogenesis of the early Paleozoic low-Mg and high-Mg adakitic rocks in the North Qilian orogenic belt, NW China, Implications for transition from crustal thickening to extension thinning. *J. Asian Earth Sci.* 107, 122–139.
- Yu, S.G., Zhang, J.X., Sun, D.Y., Del Real, P.G., Li, Y.S., Zhao, X.L., Hou, K.J., 2015b. Petrology, geochemistry, zircon U–Pb dating and Lu–Hf isotope of granitic leucosomes within felsic gneiss from the North Qaidam UHP terrane, Constraints on the timing and nature of partial melting. *Lithos* 218–219, 1–21.
- Yu, H., Zhang, H.-F., Li, X.-H., Zhang, J., Santosh, M., Yang, Y.-H., Zhou, D.-W., 2016. Tectonic evolution of the North Qinling Orogen from subduction to collision and exhumation, Evidence from zircons in metamorphic rocks of the Qinling Group. *Gondwana Res.* 30, 65–78.
- Yu, S., Zhang, J., Li, S., Sun, D., Li, Y., Liu, X., Guo, L., Suo, Y., Peng, Y., Zhao, X., 2017a. Paleoproterozoic granulite-facies metamorphism and anatexis in the Oulongbuluke Block, NW China, Respond to assembly of the Columbia supercontinent. *Precambrian Res.* 291, 42–62.
- Yu, M., Feng, C.Y., Santosh, M., Mao, J.W., Zhu, Y.F., Zhao, Y.M., Li, D.X., Li, B., 2017b. The Qiman Tagh Orogen as a window to the crustal evolution in northern Qinghai-Tibet Plateau. *Earth Sci. Rev.* 167, 103–123.
- Yu, S., Li, S., Zhang, J., Peng, Y., Somerville, I., Liu, Y., Wang, Z., Li, Z., Yao, Y., Li, Y., 2019. Multistage anatexis during tectonic evolution from oceanic subduction to continental collision: A review of the North Qaidam UHP Belt, NW China. *Earth Sci. Rev.* 191, 190–211.
- Yu, M., Dick, J.M., Feng, C.Y., Li, B., Wang, H., 2020. The tectonic evolution of the East Kunlun Orogen, northern Tibetan Plateau: A critical review with an integrated geodynamic model. *J. Asian Earth Sci.* 191, 104168.
- Yu, S., Peng, Y., Zhang, J., Li, S., Santosh, M., Li, Y., Liu, Y., Gao, X., Ji, W., Lv, P., Li, C., 2021. Tectono-thermal evolution of the Qilian orogenic system: Tracing the subduction, accretion and closure of the Proto-Tethys Ocean. *Earth Sci. Rev.* 215, 103547.
- Yuan, W., Yang, Z., 2015a. The Alashan Terrane did not amalgamate with North China block by the Late Permian, Evidence from Carboniferous and Permian paleomagnetic results. *J. Asian Earth Sci.* 104, 145–159.
- Yuan, W., Yang, Z., 2015b. The Alashan Terrane was not part of North China by the Late Devonian, Evidence from detrital zircon U–Pb geochronology and Hf isotopes. *Gondwana Res.* 27, 1270–1282.
- Yuan, C., Sun, M., Zhou, M.F., 2002. Tectonic evolution of the West Kunlun, Geochronologic and geochemical constraints from Kudi granitoids. *Int. Geol. Rev.* 44, 653–669.
- Yuan, C., Sun, M., Xiao, W.J., Zhou, H., Hou, Q.L., Li, J.L., 2003. Subduction polarity of the protoliths, insights from the Yirba pluton of the western Kunlun range, NW China. *Acta Petrol. Sin.* 19, 399–408.
- Yuan, C., Sun, M., Yang, J.S., Zhou, H., Zhou, M.F., 2004. Nb-depleted, continental rift-related Akaz metavolcanic rocks (West Kunlun), implication for the rifting of the Tarim Craton from Gondwana. In: Malpas, J., Fletcher, C.J.N., Ali, J.R., Aitchison, J. C. (Eds.), *Aspects of the Tectonic Evolution of China*. Geological Society Special Publication, pp. 131–143.
- Yuan, D.Y., Champagnac, J.-D., Ge, W.P., Molnar, P., Zhang, P.Z., Zheng, W.J., Zhang, H. P., Liu, X.W., 2011. Late Quaternary right-lateral slip rates of faults adjacent to the lake Qinghai, northeastern margin of the Tibetan Plateau. *Bull. Geol. Soc. Am.* 123, 2016–2030.
- Zeng, R.Y., Lai, J.Q., Mao, X.C., Yan, J., Zhang, C.G., Xiao, W.Z., 2021. Geochemistry and zircon ages of the Yushigou diabase in the Longshoushan area, Alxa Block, implications for crust–mantle interaction and tectonic evolution. *Geol. J.* 158, 685–700.
- Zhai, Q.G., Jahn, B.M., Wang, J., Hu, P.Y., Chung, S.L., Lee, H.Y., Tang, S.H., Tang, Y., 2016. Oldest paleo-Tethyan ophiolitic mélange in the Tibetan Plateau. *Geol. Soc. Am. Bull.* 128, 355–373.
- Zhang, G.W., Zhang, B.R., Yuan, X.C., Xiao, Q.H., 2001. Qinling Orogenic Belt and Continental Dynamics. Science Press, Beijing.
- Zhang, K., Lin, Q., Zhu, Y., Yin, H., Luo, M., Chen, N., Wang, G., 2004a. New paleontological evidence on time determination of the east part of the Eastern Kunlun Mélange and its tectonic significance. *Sci. China Ser. D Earth Sci.* 47, 865–873.
- Zhang, C.L., Yu, H.F., Shen, J.L., Dong, J.G., Ye, H.M., Guo, K.Y., 2004b. Zircon SHRIMP age determination of the giant-crystal gabbro and basalt in Kuda, west Kunlun, dismembering of the Kuda ophiolite. *Geol. Rev.* 50, 639–643.
- Zhang, G.W., Dong, Y.P., Lai, S.C., Guo, A.L., Meng, Q.R., Liu, S.F., Cheng, S.Y., Yao, A.P., Zhang, Z.Q., Pei, X.Z., Li, S.Z., 2004c. Mianlue tectonic zone and Mianlue suture zone on southern margin of Qinling-Dabie orogenic belt. *Sci. China. Ser. D Earth Sci.* 47, 300–316.
- Zhang, J.X., Meng, F.C., Yang, J.S., 2005. A new HP/LT metamorphic terrane in the northern Altyn Tagh, Western China. *Int. Geol. Rev.* 47, 371–386.
- Zhang, J., Yang, J., Meng, F., Wan, Y., Li, H., Wu, C., 2006. U–Pb isotopic studies of eclogites and their host gneisses in the Xitieshan area of the North Qaidam mountains, western China, New evidence for an early Paleozoic HP-UHP metamorphic belt. *J. Asian Earth Sci.* 28, 143–150.
- Zhang, J.X., Meng, F.C., Wan, Y.S., 2007a. A cold Early Palaeozoic subduction zone in the North Qilian Mountains, NW China, Petrological and U–Pb geochronological constraints. *J. Metamorph. Geol.* 25, 285–304.
- Zhang, J.X., Meng, F.C., Yu, S.Y., Chen, W., Chen, S.Y., 2007b. Ar–Ar geochronology of blueschist and eclogite in the north Altyn Tagh HP/LT metamorphic belt and their regional tectonic implication. *Geol. China* 34, 558–564.
- Zhang, C., Lu, S., Yu, H., Ye, H., 2007c. Tectonic evolution of the Western Kunlun orogenic belt in northern Qinghai-Tibet Plateau: Evidence from zircon SHRIMP and LA-ICP-MS U–Pb geochronology. *Sci. China Ser. D Earth Sci.* 50, 825–835.
- Zhang, G.B., Song, S.G., Zhang, L.F., Niu, Y.L., 2008. The subducted oceanic crust within continental-type UHP metamorphic belt in the North Qaidam, NW China, Evidence from petrology, geochemistry and geochronology. *Lithos* 104, 99–118.
- Zhang, G., Zhang, L., Song, S., Niu, Y., 2009a. UHP metamorphic evolution and SHRIMP geochronology of a coesite-bearing meta-ophiolitic gabbro in the North Qaidam, NW China. *J. Asian Earth Sci.* 35, 310–322.
- Zhang, X.X., Chen, B.H., Ma, B.J., 2009b. Geological and geochemical characteristics of the Kezhitage ophiolitic mélange in the Eastern Kunlun. *Geotecton. Metallog.* 33, 313–319.
- Zhang, D.Q., She, H.Q., Feng, C.Y., Li, D.X., Li, J.W., 2009c. Geology, age, and fluid inclusions of the Tanjianshan gold deposit, western China: Two orogenies and two gold mineralizing events. *Ore Geol. Rev.* 36, 250–263.
- Zhang, J.X., Mattinson, C.G., Yu, S.Y., Li, J.P., Meng, F.C., 2010. U–Pb zircon geochronology of coesite-bearing eclogites from the southern Dulan area of the North Qaidam UHP terrane, northwestern China, spatially and temporally extensive UHP metamorphism during continental subduction. *J. Metamorph. Geol.* 28, 955–978.
- Zhang, C., Zhang, L., Van Roermund, H., Song, S., Zhang, G., 2011. Petrology and SHRIMP U–Pb dating of Xitieshan eclogite, North Qaidam UHP metamorphic belt, NW China. *J. Asian Earth Sci.* 42, 752–767.
- Zhang, J.X., Gong, J.H., Yu, S.Y., Li, H.K., Hou, J.K., 2013a. Neoproterozoic–Paleoproterozoic multiple tectonothermal events in the western Alxa block, North China Craton and their geological implication: Evidence from zircon U–Pb ages and Hf isotopic composition. *Precambrian Res.* 235, 36–57.
- Zhang, C., Liu, L., Wang, T., Wang, X., Li, L., Gong, Q., Li, X., 2013b. Granitic magmatism related to early Paleozoic continental collision in North Qinling. *Chin. Sci. Bull.* 58, 4405–4410.
- Zhang, L.Y., Ding, L., Pullen, A., Xu, Q., Liu, D.L., Cai, F.L., Yue, Y.H., Lai, Q.Z., Shi, R.D., Ducea, M.N., Kapp, P., 2014. Age and geochemistry of western Hoh-Xil–Songpan-Ganzi granitoids, northern Tibet: Implications for the Mesozoic closure of the Paleo-Tethys Ocean. *Lithos* 190, 328–348.
- Zhang, G., Niu, Y., Song, S., Zhang, L., Tian, Z., Christy, A.G., Han, L., 2015a. Trace element behavior and P–T–t evolution during partial melting of exhumed eclogite in the North Qaidam UHPM belt (NW China): Implications for adakite genesis. *Lithos* 226, 65–80.
- Zhang, Z., Li, S., Cao, H., Somerville, I.D., Zhao, S., Yu, S., 2015b. Origin of the North Qinling microcontinent and Proterozoic geotectonic evolution of the Kuanping Ocean, Central China. *Precambrian Res.* 266, 179–193.
- Zhang, J., Zhang, B., Zhao, H., 2016. Timing of amalgamation of the Alxa Block and the North China Block, Constraints based on detrital zircon U–Pb ages and sedimentologic and structural evidence. *Tectonophysics* 668, 65–81.
- Zhang, L., Zhang, H., Zhang, S., Xiong, Z., Luo, B., Yang, H., Pan, F., Zhou, X., Xu, W., Guo, L., 2017a. Lithospheric delamination in post-collisional setting, Evidence from intrusive magmatism from the North Qilian orogen to southern margin of the Alxa block, NW China. *Lithos* 288, 20–34.
- Zhang, Y.Q., Song, S.G., Yang, L.M., Su, L., Niu, Y.L., Allen, M.B., Xu, X., 2017b. Basalts and picrites from a plume-type ophiolite in the South Qilian Accretionary Belt, Qilian Orogen, Accretion of a Cambrian Oceanic Plateau? *Lithos* 278, 97–110.
- Zhang, J., Yu, S., Mattinson, C.G., 2017c. Early Paleozoic polyphase metamorphism in northern Tibet, China. *Gondwana Res.* 41, 267–289.
- Zhang, C.L., Zou, H.B., Ye, X.T., Chen, X.Y., 2018a. A newly identified Precambrian terrane at the Pamir Plateau, The Archean basement and Neoproterozoic granitic intrusions. *Precambrian Res.* 304, 73–87.
- Zhang, C.L., Zou, H.B., Ye, X.-T., Chen, X.-Y., 2018b. Timing of subduction initiation in the Proto-Tethys Ocean, Evidence from the Cambrian gabbros from the NE Pamir Plateau. *Lithos* 314, 40–51.
- Zhang, C.L., Zou, H.B., Ye, X.-T., Chen, X.Y., 2018c. Tectonic evolution of the NE section of the Pamir Plateau, New evidence from field observations and zircon U–Pb geochronology. *Tectonophysics* 723, 27–40.
- Zhang, J., Mattinson, C., Yu, S., Li, Y., Yu, X., Mao, X., Lu, Z., Peng, Y., 2019a. Two contrasting accretion v. collision orogenies, insights from Early Paleozoic polyphase metamorphism in the Altyn-Qilian-North Qaidam orogenic system, NW China. In: Zhang, L., Zhang, Z., Schertl, H.P., Wei, C. (Eds.), *Hp-Uhp Metamorphism and Tectonic Evolution of Orogenic Belts*. Geological Society Special Publication, pp. 153–181.
- Zhang, C.L., Zou, H.B., Ye, X.-T., Chen, X.Y., 2019b. Tectonic evolution of the West Kunlun Orogenic Belt along the northern margin of the Tibetan Plateau, Implications for the assembly of the Tarim terrane to Gondwana. *Geosci. Front.* 10, 973–988.
- Zhang, Q.C., Wu, Z.H., Li, S., Li, K.X., Liu, Z.W., Zhou, Q., 2019c. Ordovician granitoids and Silurian mafic dikes in the Western Kunlun Orogen, Northwest China, Implications for evolution of the Proto-Tethys. *Acta Geol. Sin.* 93, 30–49.
- Zhang, Q., Wu, Z., Chen, X., Zhou, Q., Shen, N., 2019d. Proto-Tethys oceanic slab break-off, Insights from early Paleozoic magmatic diversity in the West Kunlun Orogen, NW Tibetan Plateau. *Lithos* 346, 105147.
- Zhang, L.K., Li, G.M., Santosh, M., Cao, H.W., Dong, S.L., Zhang, Z., Fu, J.G., Xia, X.B., Huang, Y., Liang, W., Zhang, S.T., 2019e. Cambrian magmatism in the Tethys Himalaya and implications for the evolution of the Proto-Tethys along the northern Gondwana margin: A case study and overview. *Geol. J.* 54, 2545–2565.
- Zhang, L.Q., Zhang, H.F., Hawkesworth, C., Luo, B.J., Yang, H., 2021. Mafic rocks from the southern Alxa block of Northwest China and its geodynamic evolution in the Paleozoic. *J. Geol. Soc.* 178 <https://doi.org/10.1144/jgs2020-038>.
- Zhao, G.C., Cawood, P.A., 2012. Precambrian geology of China. *Precambrian Res.* 222, 13–54.

- Zhao, G.C., Sun, M., Wilde, S.A., Li, S.Z., 2005. Late Archean to Paleoproterozoic evolution of the North China Craton: key issues revisited. *Precambrian Res.* 136, 177–202.
- Zhao, G.C., Wang, C., Zhu, X., Hao, J., Li, H., Meert, J.G., Gai, Y., Long, X.M., Ma, T., 2020. Intraoceanic back-arc magma diversity: Insights from a relic of the Proto-Tethys oceanic lithosphere in the western Qilian Orogen, NW China. *Chem. Geol.* 550, 119756.
- Zhao, S.J., Li, S.Z., Liu, X., Santosh, M., Somerville, I.D., Cao, H.H., Yu, S., Zhang, Z., Guo, L.L., 2015. The northern boundary of the Proto-Tethys Ocean, Constraints from structural analysis and U-Pb zircon geochronology of the North Qinling Terrane. *J. Asian Earth Sci.* 113, 560–574.
- Zhao, F., Sun, F., Liu, J., 2017a. Zircon U-Pb Geochronology and Geochemistry of the Gneissic Granodiorite in Manite Area from East Kunlun, with Implications for Geodynamic Setting. *Earth Sci.* 42, 927–940.
- Zhao, S.J., Li, S.Z., Li, X.Y., Somerville, I., Cao, H.H., Liu, X., Wang, P.C., 2017b. Structural analysis of ductile shear zones in the North Qinling Orogen and its implications for the evolution of the Proto-Tethys Ocean. *Geol. J.* 52, 202–214.
- Zhao, G.C., Wang, Y.J., Huang, B.C., Dong, Y.P., Li, S.Z., Zhang, G.W., Yu, S., 2018a. Geological reconstructions of the East Asian blocks, From the breakup of Rodinia to the assembly of Pangea. *Earth Sci. Rev.* 186, 262–286.
- Zhao, Z., Wei, J., Santosh, M., 2018b. Late Devonian postcollisional magmatism in the ultrahigh-pressure metamorphic belt, Xitieshan terrane, NW China. *Geol. Soc. Am. Bull.* 130, 999–1016.
- Zhao, J., Long, X., Dong, Y., Li, J., Gao, Y., Zhao, B., 2019. Petrogenesis, tectonic setting and formation age of the metaperidotites in the Lajishan ophiolite, Central Qilian Block, NW China. *J. Asian Earth Sci.* 186, 104076.
- Zheng, R.G., Wu, T.R., Zhang, W., Xu, C., Meng, Q.P., Zhang, Z.Y., 2014. Late Paleozoic subduction system in the northern margin of the Alxa block, Altaids, Geochronological and geochemical evidences from ophiolites. *Gondwana Res.* 25, 842–858.
- Zheng, Z., Chen, Y.J., Deng, X.H., Yue, S.W., Chen, H.J., Wang, Q.F., 2018. Origin of the Bashierxi monzogranite, Qiman Tagh, East Kunlun Orogen, NW China, A magmatic response to the evolution of the Proto-Tethys Ocean. *Lithos* 296, 181–194.
- Zheng, K., Wu, C.L., Lei, M., Zhang, X., Chen, H.J., Wu, D., Gao, D., 2019. Petrogenesis and tectonic implications of granitoids from western North Altun, Northwest China. *Lithos* 340, 255–269.
- Zhong, S.H., Feng, C.Y., Seltmann, R., Li, D.X., 2017. Middle Devonian volcanic rocks in the Weibao Cu-Pb-Zn deposit, East Kunlun Mountains, NW China, Zircon chronology and tectonic implications. *Ore Geol. Rev.* 84, 309–327.
- Zhou, X.C., Zhang, H.F., Luo, B.J., Pan, F.B., Zhang, S.S., Guo, L., 2016a. Origin of high Sr/Y-type granitic magmatism in the southwestern of the Alxa Block, Northwest China. *Lithos* 256–257, 211–227.
- Zhou, B., Dong, Y.P., Zhang, F.F., Yang, Z., Sun, S.S., He, D.F., 2016b. Geochemistry and zircon U-Pb geochronology of granitoids in the East Kunlun Orogenic Belt, northern Tibetan Plateau, origin and tectonic implications. *J. Asian Earth Sci.* 130, 265–281.
- Zhou, W.X., Li, H.Q., Chang, F., Lv, X.B., 2020. The Early Silurian gabbro in the Eastern Kunlun Orogenic Belt, Northeast Tibet, Constraints on the Proto-Tethyan Ocean closure. *Minerals* 10. <https://doi.org/10.3390/min10090794>.
- Zhou, C.A., Song, S.G., Allen, M.B., Wang, C., Su, L., Wang, M., 2021. Post-collisional mafic magmatism, Insights into orogenic collapse and mantle modification from North Qaidam collisional belt, NW China. *Lithos* 398–399, 106311.
- Zhu, X., Chen, D., Liu, L., Li, D., 2010. Zircon LA-ICP-MS U-Pb dating of the Wanggaxiu gabbro complex in the Dulan area, northern margin of Qaidam Basin, China and its geological significance. *Geol. Bull. China* 29, 227–236.
- Zhu, X., Chen, D., Liu, L., Wang, C., Yang, W., Cao, Y., Kang, L., 2012a. Chronology and geochemistry of the mafic rocks in Xitieshan area, North Qaidam. *Geol. Bull. China* 31, 2079–2089.
- Zhu, D.C., Zhao, Z.D., Niu, Y.L., Dilek, Y., Wang, Q., Ji, W.H., Dong, G.C., Sui, Q.L., Liu, Y.S., Yuan, H.L., Mo, X.X., 2012b. Cambrian bimodal volcanism in the Lhasa Terrane, southern Tibet, Record of an early Paleozoic Andean-type magmatic arc in the Australian proto-Tethyan margin. *Chem. Geol.* 328, 290–308.
- Zhu, J., Li, Q.G., Wang, Z.Q., Tang, H.S., Chen, X., Xiao, B., 2016. Magmatism and tectonic implication of Early Cambrian granitoid plutons in Tianshuhai Terrane of the Western Kunlun Orogenic Belt, Northwest China. *Northwest. Geol.* 49, 1–18.
- Zuza, A.V., Yin, A., 2017. Balkatach hypothesis, A new model for the evolution of the Pacific, Tethyan, and Paleo-Asian oceanic domains. *Geosphere* 13, 1664–1712.
- Zuza, A.V., Wu, C., Reith, R.C., Yin, A., Li, J.H., Zhang, J.Y., Zhang, Y.X., Wu, L., Liu, W. C., 2018. Tectonic evolution of the Qilian Shan, an early Paleozoic orogen reactivated in the Cenozoic. *Geol. Soc. Am. Bull.* 130, 881–925.